2018

Protective Role of Kallistatin in Vascular Injury, Senescence and Aging

Youming Guo
Medical University of South Carolina

Protective Role of Kallistatin in Vascular Injury, Senescence and Aging

by

Youming Guo

A dissertation submitted to the faculty of the Medical University of South Carolina in partial fulfillment of the requirements for the degree of Doctor of Philosophy in the College of Graduate Studies.

Department of Biochemistry and Molecular Biology

2018

Approved by:

Chairman, Advisory Committee

Julie Chao

Lee Chao

Robin Muise-Helmericks

Yi-Te Hsu

Hongkuan Fan

ACKNOWLEDGEMENTS

It is with deep respect that I offer my gratitude to my mentor Dr. Julie Chao for the training, guidance and support. Her continual encouragement has enriched my graduate training and made it an excellent experience. I would also thank my advisory committee members, Drs. Lee Chao, Robin Muise-Helmericks, Yi-Te Hsu and Hongkuan Fan, for their valuable advice, wisdom and assistance on my research project. Meanwhile, I would like to thank my workmates who have aided me in experimental design, laboratory techniques and result interpretation, particularly Drs. Pengfei Li and Zhirong Yang. Finally, I am forever indebted to my family for their understanding, support and encouragement during my four years' graduate training.

TABLE OF CONTENTS

LIST OF FIGURES

Page

YOUMING GUO. Protective Role of Kallistatin in Vascular Injury, Senescence and Aging (Under the direction of JULIE CHAO)

Kallistatin, a plasma protein, consists of two essential structural elements, an active site and a heparin-binding domain. Kallistatin exerts pleiotropic effects on angiogenesis, inflammation, fibrosis and tumor growth. This study aims to decipher the role and mechanism of kallistatin in vascular injury, senescence and aging. First, we determined the effect of kallistatin on endothelial-mesenchymal transition (EndMT), a process mediating vascular injury, organ fibrosis and cancer progression. Recombinant human kallistatin via its heparin-binding site blocked TGF-β-induced EndMT, associated with downregulated microRNA (miR)-21-Akt signaling and oxidative stress in human endothelial cells. Kallistatin's active site is essential for stimulating antioxidant genes, endothelial nitric oxide synthase (eNOS) and sirtuin 1 (SIRT1) by interacting with a tyrosine kinase. These findings indicate that kallistatin suppresses EndMT by inhibiting miR-21-Akt signaling and oxidative stress. Secondly, we determined the role and mechanism of kallistatin in vascular senescence and aging. Kallistatin antagonized TNF-α-induced senescence and oxidative stress, and inhibited miR-34a, a senescence inducer, leading to elevated SIRT1/eNOS synthesis in human endothelial progenitor cells. Kallistatin administration in streptozotocin (STZ)-induced diabetic mice attenuated aortic senescence associated with reduced miR-34a and elevated SIRT1/eNOS levels. Consistently, kallistatin delayed stress-induced organismal aging in *Caenorhabditis elegans* by inhibiting miR-34 and elevating the longevity gene, sir-2.1 (SIRT1 homolog) synthesis. Therefore, kallistatin reduces vascular senescence and aging by inhibiting miR-34a-SIRT1/eNOS pathway. Thirdly, we determined the role of endogenous kallistatin in endothelial senescence, oxidative stress and inflammation by generating

two strains of kallistatin knockout mice, endothelial cell-specific and general kallistatin knockout mice. Kallistatin via inducing an endo-protective miRNA Let-7g antagonized miR-34a-SIRT1-eNOS pathway and inhibited senescence, oxidative stress and inflammation in human endothelial cells. Conversely, kallistatin deficiency in mouse lung endothelial cells aggravated H_2O_2-induced senescence, oxidative stress and inflammation associated with downregulated Let-7g and antioxidant genes and upregulated miR-34a synthesis, indicating that kallistatin protects against endothelial senescence by modulating Let-7g mediated miR-34a-SIRT1-eNOS pathway. Moreover, systemic depletion of kallistatin exacerbated aortic oxidative stress and renal fibrosis in STZ-induced diabetic mice. These studies indicate that kallistatin plays a novel role in protection against vascular injury, senescence and aging by regulating Let-7g, miR-34a and miR-21 synthesis, and antioxidant gene expression.

ABBREVIATIONS

α-SMA	α-smooth muscle actin
BUN	blood urea nitrogen
C. elegans	*Caenorhabditis elegans*
CLP	caecal ligation and puncture
DCFH-DA	2', 7'-dichlorodihydrofluorescein diacetate
DHE	dihydroethidium
DOCA	deoxycorticosterone acetate
EndMT	endothelial–mesenchymal transition
eNOS	endothelial nitric oxide synthase
EPC	endothelial progenitor cell
FoxO1	forkhead box O1
HMGB-1	high-mobility group box-1
HUVECs	human umbilical vein endothelial cells
ICAM-1	intercellular adhesion molecule-1
IL-6	interleukin-6
KBP	tissue kallikrein-binding protein
KLF4	kruppel like factor 4
KS	kallistatin
$KS^{endo-/-}$	endothelium-specific kallistatin-deficient
$KS^{-/-}$	general kallistatin knockout
L-NAME	Nω-nitro-L-arginine methyl ester hydrochloride
LPS	lipopolysaccharide
MACS	magnetic-activated cell sorting system
miRNA	microRNA
MMP	matrix metalloproteinase
NAM	nicotinamide
NF-κB	nuclear factor-κB
PAI-1	plasminogen activator inhibitor-1
PBS	phosphate-buffered saline
PVDF	polyvinylidene difluoride
qRT-PCR	quantitative real-time polymerase chain reaction
ROS	reactive oxygen species
SA-β-gal	senescence-associated β-galactosidase
serpin	serine proteinase inhibitor
SIRT1	sirtuin 1
SOCS 3	suppressor of cytokine signaling-3
SOD	superoxide dismutase
STZ	streptozotocin
TGF-β	transforming growth factor-β
TNF-α	tumor necrosis factor-α
VCAM-1	vascular cell adhesion molecule-1
VE-cadherin	vascular endothelial-cadherin
VEGF	vascular endothelial growth factor

CHAPTER I

GENERAL INTRODUCTION

Biochemical and Molecular Properties of Kallistatin

Kallistatin was first identified in human plasma as a tissue kallikrein-binding protein (KBP) in 1986 (Chao *et al.*, 1986). Tissue kallikrein is a serine proteinase which cleaves low molecular weight kininogen to release vasoactive kinin peptide (Bhoola *et al.*, 1992). Intact kinin binds to kinin B2 receptors and induces vasodilation and a wide spectrum of biological effects (Regoli *et al.*, 1990). Purified and ^{125}I-labeled human tissue kallikrein and human serum rapidly forms a high molecular weight complex, which is resistant to SDS treatment and boiling, indicating a covalent linkage between tissue kallikrein and a serum protein (Chao *et al.*, 1986). Molecular cloning and sequence analyses indicate that KBP is a novel serine proteinase inhibitor (serpin) (Zhou *et al.*, 1992, Chai *et al.*, 1993). KBP was designated as kallistatin as it inhibited tissue kallikrein activity (Zhou *et al.*, 1992, Chai *et al.*, 1993, Chai *et al.*, 1994). Kallistatin is an acidic glycoprotein with a molecular mass of 58-60 kDa and isoelectric points of 4.6 to 5.2 (Chao *et al.*, 1990, Zhou *et al.*, 1992). The amino acid sequence derived from human kallistatin cDNA shares 44-46% homology with other human serpins (Chai *et al.*, 1993). Kallistatin belongs to the serpin superfamily including α1-antitrypsin, α1-antichymotrypsin, protein C inhibitor, plasminogen activator inhibitor, and heparin cofactor (Rosenberg & Damus, 1973, Baker *et al.*, 1980, Chao *et al.*, 1990, Ehrlich *et al.*, 1991). Human kallistatin gene is located on chromosome 14q31-32.1 within a serpin gene cluster (Billingsley *et al.*, 1993, Chai *et al.*, 1994). The kallistatin gene has a typical five exon-four intron gene structure. The full-length human kallistatin cDNA encodes 427 amino acid residues (Chai *et al.*, 1993, Chai *et al.*, 1994).

The three-dimensional structure of human kallistatin created by molecular modeling showed that kallistatin consists of three β-sheets and eight α-helices, a property similar to other serpins (Chen *et al.*, 2000, Chen *et al.*, 2001). Kallistatin

contains two structural elements: an active site and a heparin-binding domain (Chen *et al.*, 2000, 2000, Chen *et al.*, 2001). Human kallistatin is a unique serpin as it contains a reactive center sequence, Phe-Phe-Ser (P2-P1-P1'), for the cleavage site of tissue kallikrein (Chen *et al.*, 2000). Moreover, heparin prevents the formation of tissue kallikrein-kallistatin complex and inhibitory effect of kallistatin on tissue kalllikrein's enzymatic activity, leading to the identification of a major heparin-binding site in kallistatin (Chen *et al.*, 2001). The basic residues, particularly Lys312-Lys313, in the region between the H helix and C2 sheet of kallistatin, comprise a major heparin-binding site (Chen *et al.*, 2001). Kallistatin via its two structural domains regulates multiple signaling pathways and a wide spectrum of biological activities.

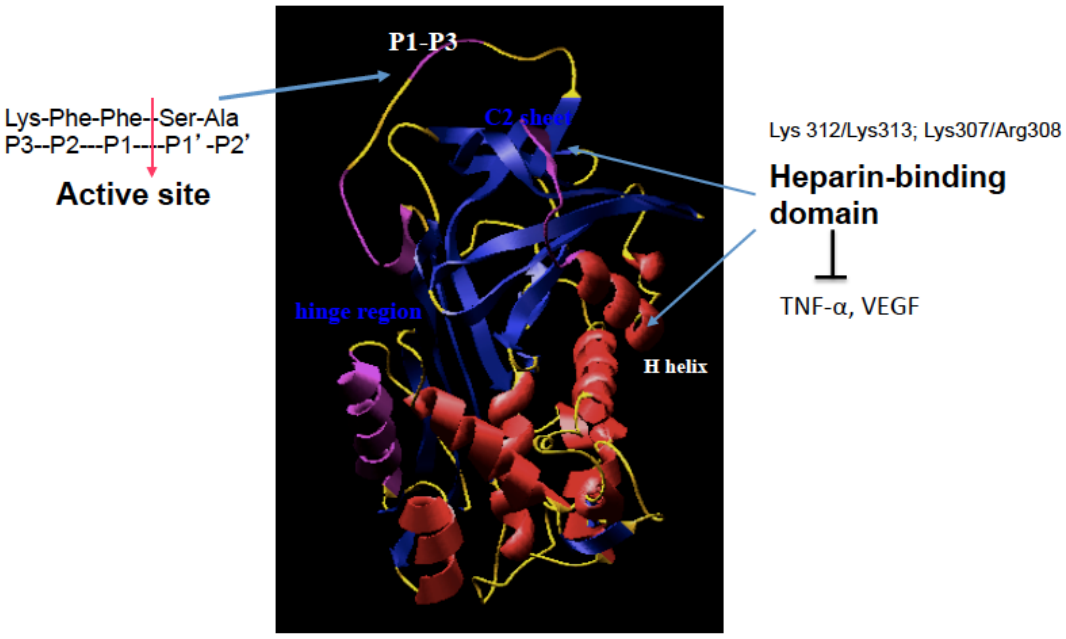

Figure 1-1. Molecular model of human kallistatin according to α1-antitrypsin. Active site is located in the reactive center loop, heparin-binding domain is located between C2 sheet and H helix as indicated by the arrows (Chen *et al*., 2000; Chen *et al*., 2001).

Kallistatin via Its Structural Elements Regulates Biological Functions

Kallistatin through its two functional domains regulates different signaling pathways independent of tissue kallikrein. On one hand, kallistatin via its active site inhibits tissue kallikrein's enzymatic activity, thus the biological function (Chen *et al.*, 2000). On the other hand, kallistatin via its heparin-binding site interacts with cellular surface heparan sulfate proteoglycans, thus antagonizing vascular endothelial growth factor (VEGF)-induced proliferation and migration of human endothelial cells (Miao *et al.*, 2003). Likewise, kallistatin's heparin-binding site is essential for competing with tumor necrosis factor (TNF)-α binding to heparan-sulfate proteoglycans, and thus blocking TNF-α–induced nuclear factor (NF)-κB activation and inflammatory gene expression in endothelial cells (Yin *et al.*, 2010). Similarly, kallistatin via the heparin-binding site antagonized high mobility group box-1 (HMGB1)-mediated inflammation, and EGF-mediated caner cell proliferation and invasion (Li *et al.*, 2014, Li P. *et al.*, 2016). Thus, through the active site and heparin-binding domain, kallistatin exerts pleiotropic functions, including inhibition of angiogenesis, inflammation and cancer development (Chen *et al*., 2000, Miao *et al*., 2003, Yin *et al*., 2010, Li *et al.*, 2014, Li *et al*., 2016).

Distribution and Expression of Kallistatin

Kallistatin is mainly synthesized in the liver, and is widely distributed in organs relevant to cardiovascular function (Chao & Chao, 1995). Human kallistatin transcripts and protein can be detected in the plasma, liver, heart, lung, kidney, prostate gland and aorta (Chai *et al.*, 1993, Chao & Chao, 1995, Chao *et al.*, 1996). Kallistatin is also localized in endothelial cells and smooth muscle cells of large, medium, and small blood vessels (Wolf *et al.*, 1999). Circulating kallistatin levels are markedly decreased in animal models of hypertension, streptozotocin (STZ)-induced diabetes mellitus, lipopolysaccharide (LPS)-induced endotoxemia, renal injury and hepatocellular

carcinoma (Chao *et al.*, 1990, Chao *et al.*, 1996, Chen *et al.*, 1997, Shen *et al.*, 2008, Zhi *et al.*, 2015). Importantly, kallistatin levels are significantly lower in patients with liver disease, septic syndrome, diabetic retinopathy, severe pneumonia, inflammatory bowel disease, and colon and prostate cancer (Chao *et al.*, 1996, Ma *et al.*, 1996, Stadnicki *et al.*, 2003, Lin *et al.*, 2013, Chao *et al.*, 2016). Moreover, reduced plasma kallistatin levels are associated with adiposity and cardiometabolic risk in apparently healthy African American youths (Zhu H. *et al.*, 2013). These findings indicate that kallistatin is reduced under various pathological conditions, implicating the involvement of kallistatin in cardiovascular damage.

Kallistatin Is A Vasodilator Independent of Tissue Kallikrein

The first pivotal finding regarding kallistatin's function in vascular biology is kallistatin-mediated reduction of blood pressure. The levels of kallistatin mRNA and protein in tissues and serum are significantly lower in spontaneously hypertensive rats compared with normotensive control rats (Chao & Chao, 1988). Moreover, the expression of the hepatic kallistatin is markedly reduced in N-nitroarginine methyl ester (L-NAME)-induced arterial hypertensive rats (Chao *et al.*, 1996). Overexpression of rat kallistatin in transgenic mice results in significant reduction in blood pressure compared with the control littermates (Chen *et al.*, 1996). These findings indicate a potential role of kallistatin in blood pressure regulation**.** Importantly, kallistatin was identified to be a potent vasodilator in 1997 (Chao *et al.*, 1997). Human kallistatin administration produced a rapid and transient reduction in mean arterial blood pressure in rats, and caused vasorelaxation in aortic rings and perfused rat kidney (Chao *et al.*, 1997). Additionally, the blood pressure-lowering effect induced by kallistatin is independent of its interaction with tissue kallikrein**,** as icatibant (Hoe 140), a bradykinin B2-receptor antagonist, had no effect on the hypotensive effect of kallistatin but abolished kallikrein/kinin-mediated blood

pressure reduction (Chao *et al.*, 1997). Moreover, the nitric oxide synthase inhibitor, L-NAME blocked kallistatin-mediated vasodilatory effect in rats (Chao *et al.*, 2016), indicating that kallistatin induces vasodilation, in part, through stimulation of NO production. Therefore, these findings indicate that kallistatin is a vasodilator and plays a role in maintaining normal blood pressure unrelated to the interaction with tissue kallikrein.

Kallistatin Inhibits Vascular Inflammation

TNF-α, a potent pro-inflammatory cytokine, activates the transcription factor NF-κB and promotes inflammatory gene expression, leading to increased oxidative stress, vascular inflammation and endothelial dysfunction (Lawrence, 2009). In cultured endothelial cells, kallistatin via the heparin-binding site inhibited TNF-α-induced NF-κB activation and monocyte adhesion to endothelial cells, as well as cell adhesion molecule and cytokine expression, including ICAM-1, VCAM-1 and MCP-1 (Shen *et al.*, 2009, Yin *et al.*, 2010). Moreover, kallistatin gene delivery attenuated mouse vascular leakage induced by complement factor C5a, and reduced VEGF-induced endothelial cell permeability (Yin *et al.*, 2010). Kallistatin gene or protein therapy alleviated joint swelling and inflammation in rats with joint arthritis, inhibited renal inflammation in diabetic db/db mice and caecal ligation and puncture (CLP)-induced septic mice, and ameliorated lung injury and inflammation in LPS-challenged mice (Yin *et al.*, 2010, Li *et al.*, 2014, Lin *et al.*, 2015, Yiu *et al.*, 2016). Kallistatin also antagonized the pro-inflammatory mediator HMGB1-induced inflammatory cytokine expression through its heparin-binding site in endothelial cells (Li *et al.*, 2014). Moreover, kallistatin via interaction with the transcription factor kruppel like factor (KLF) 4 induced eNOS expression, leading to the inhibition of vascular inflammation (Shen *et al.*, 2009). eNOS promotes bioavailable NO production. NO plays a critical role in inhibiting inflammatory gene expression by

preventing NF-κB activation (Matthews *et al.*, 1996). Overall, these findings indicate that kallistatin exhibits potent anti-inflammatory actions.

Kallistatin Inhibits Endothelial Apoptosis

Cell apoptosis, the programmed cell death, occurs in both physiological and pathological conditions in the cardiovascular system. The pathogenesis of cell apoptosis is commonly implicated in heart failure, myocardial infarction and other cardiovascular diseases (Bennett, 2002). The cardiomyocytes in cardiac tissue and endothelial cells in vascular wall are the typical cells afflicted by apoptosis. Kallistatin has been shown to attenuate cardiomyocyte apoptosis in rats at 1 day after acute myocardial ischemia-reperfusion (I/R) injury, and reduce renal tubular necrosis in mice with I/R (Chao *et al.*, 2006, Zhou *et al.*, 2015). Kallistatin-mediated anti-apoptotic actions in the kidney and heart suggest the potential protective role of kallistatin in vascular rarefaction. Indeed, kallistatin gene delivery prevented glomerular capillary loss in hypertensive rats (Shen *et al.*, 2010, Gao *et al.*, 2014). However, depletion of endogenous kallistatin augmented endothelial loss and aortic oxidative injury in deoxycorticosterone acetate (DOCA)-salt induced hypertensive rats (Liu Y. *et al.*, 2012, Gao *et al.*, 2014). These studies substantiate the role of kallistatin in vascular protection.

Endothelial cells line the blood vessel and compose the inner layer of blood vessel wall. Kallistatin has the ability to attenuate TNF-α-induced endothelial apoptosis through inhibition of reactive oxygen species (ROS) and activation of Akt-eNOS signaling (Shen *et al.*, 2010). Circulating endothelial progenitor cells (EPCs) are a subset of mononuclear cells derived from bone marrow that have regenerative capacity to differentiate into mature endothelial cells (Yoder, 2012). Reduced EPC number is associated with defective proliferation and mobility as well as accelerated apoptosis and

senescence (Imanishi *et al.*, 2008). Kallistatin gene transfer increased circulating EPC number in hypertensive rat model, and promoted EPC migration, adhesion and tube formation associated with NO stimulation *in vitro* (Gao *et al.*, 2014). In contrast, kallistatin depletion by kallistatin neutralized antibody injection decreased EPC levels and exacerbated vascular oxidative stress and endothelial rarefaction (Liu Y. *et al.*, 2012, Gao *et al.*, 2014). Collectively, kallistatin protects against vascular injury via attenuating endothelial cell apoptosis and enhancing EPC mobility and function.

Kallistatin Protects against Oxidative Organ Damage

Oxidative Stress plays a pivotal role in pathological events such as inflammation and organ injury. Inhibition of oxidative stress is crucial for alleviation of oxidative multi-organ damage. Time-dependent elevation of circulating ROS levels are associated with reduced kallistatin levels in animal models of hypertension and renal injury (Shen *et al.*, 2008, Shen *et al.*, 2010). Kallistatin's antioxidant activity has been exhibited in multiple animal models, including hypertension, myocardial infarction, sepsis and diabetes (Chao *et al.*, 2006, Shen *et al.*, 2008, Shen *et al.*, 2010, Li *et al.*, 2015, Yiu *et al.*, 2016). With its antioxidant activity, kallistatin administration reduced organ injury and improved survival in mice with CLP-induced polymicrobial sepsis, and alleviated LPS-induced acute lung injury in mice (Huang *et al.*, 2014, Li *et al.*, 2014, Lin *et al.*, 2015). Kallistatin gene transfer displayed a renoprotective effect partially by its antioxidant action in diabetic db/db mice (Yiu *et al.*, 2016). Moreover, kallistatin gene delivery attenuated organ damage in conjunction with decreased ROS formation and increased eNOS and NO levels in animal models of myocardial infarction and hypertension (Chao *et al.*, 2006, Shen *et al.*, 2008, Shen *et al.*, 2010). Conversely, endogenous kallistatin depletion by neutralizing antibody injection aggravated cardiovascular and renal lesions, accompanied by elevated oxidative stress, inflammation and hypertrophy in hypertensive

rats (Liu Y. *et al.*, 2012). NO is capable of inhibiting NADPH oxidase activity (Selemidis *et al.*, 2007), thus promoting NO bioavailability should lead to the attenuation of oxidative stress. Kallistatin increases NO formation by activating Akt-eNOS signaling pathway (Shen *et al.*, 2010, Gao *et al.*, 2014). Moreover, kallistatin via NO formation inhibits NADPH oxidase activity provoked by TNF-α, H_2O_2 or angiotensin II in cultured renal cells, cardiomyocytes, myofibroblasts, EPCs and endothelial cells (Gao *et al.*, 2008, Shen *et al.*, 2008, Shen *et al.*, 2009, Shen *et al.*, 2010, Yin *et al.*, 2010, Gao *et al.*, 2014). Taken together, these findings indicate that kallistatin through its antioxidant actions protects against multi-organ damage.

Kallistatin Inhibits Organ Fibrosis and Tumor Growth

Myofibroblast accumulation, aberrant angiogenesis and vascular remodeling are the common features of organ fibrosis and tumor growth (Wynn, 2008). Kallistatin administration attenuated salt-Induced renal fibrosis and collagen expression in hypertensive rats, and reduced carbon tetrachloride-induced liver fibrosis in rats, associated with decreased oxidative parameter including malondialdehyde level and superoxide dismutase activity (Huang *et al.*, 2014). Kallistatin overexpression in db/db diabetic mice allevated glomerulosclerosis and tubular interstitial injury and attenuated renal fibrosis by inhibiting TGF-β signaling (Yiu *et al.*, 2016). TGF-β is a central regulator of fibrosis. In contrast, kallistatin depletion by neutralizing antibody injection worsened renal fibrosis by elevating fibrotic gene expression and myofibroblast number (Liu Y. *et al.*, 2012). Moreover, adenovirus carrying the human kallistatin gene inhibited tumor growth in nude mice with human breast tumor xenografts (Miao *et al.*, 2002). Lentivirus-mediated kallistatin gene delivery dramatically decreased pulmonary tumor metastasis in association with reduced angiogenesis and inflammation in mice bearing pulmonary

tumor (Strait & Lakatta, 2012). Therefore, kallistatin administration displays potential application value for controlling fibrosis formation and tumor growth and metastasis.

Potential Role of Kallistatin in Vascular Injury, Senescence and Aging

Aging is one of the dominant risk factors for the development of cardiovascular disease (Lakatta, 2002). It is well known that aging is associated with a decreased capacity to repair and regenerate damaged blood vessels. Cellular senescence can acquire senescence-associated secretory phenotype (SASP) causes vascular rarefaction, inflammation and fibrosis (Clements *et al.*, 2013). Endothelial-mesenchymal transition (EndMT) remodels vascular structure by rarefaction of endothelial cells but thickening of smooth muscle layers. EndMT is a critical process mediating organ fibrosis and tumor progression. Kallistatin has been known to inhibit organ fibrosis and tumor growth in animal models. It is not yet known whether kallistatin through regulating EndMT to inhibit organ and vascular injury. Moreover, plasma kallistatin levels are decreased in multiple aging-associated vascular diseases, including hypertension, coronary artery disease and diabetes. Plasma kallistatin levels are recently reported to be positively associated with leukocyte telomere length in African Americans (Zhu *et al*. 2016). As leukocyte telomere length shortens with age and is a valuable biomarker for cellular senescence and organismal aging (Shammas, 2011), thus kallistatin may have a potential protective role in age-related vascular diseases. Oxidative stress is a particular important inducer of organ fibrosis and vascular senescence (Chen *et al.*, 2008, Erusalimsky, 2009). Therefore, enhancing cellular antioxidant defense is an effective means to alleviate vascular injury and aging.

At the molecular level, eNOS plays a crucial role in regulating vascular tone, proliferation and oxidative stress via NO production (Forstermann & Munzel, 2006).

SIRT1 as a longevity gene stimulates the expression eNOS and other antioxidant enzymes, such as manganese superoxide dismutase (MnSOD) and catalase, contributing to vascular endothelial homeostasis (Chen *et al.*, 2010, Olmos *et al.*, 2013, Xia *et al.*, 2013). Conversely, microRNA (miR)-34a and miR-21 have emerged as important regulators of cellular senescence and aging (Ito *et al.*, 2010, Zhu S. *et al.*, 2013). Let-7g as an endo-protective miRNA, has been shown to improve multiple endothelial functions by inhibiting senescence and inflammation (Liao *et al*., 2014). miR-21-Akt pathway is also involved in EndMT process (Kumarswamy *et al.*, 2012). Therefore, kallistatin may exert a novel function in inhibiting vascular injury, senescence and aging by regulating eNOS, SIRT1, miR-34a, miR-21 and Let-7g. Studying the role and mechanism of kallistatin in vascular injury, senescence and aging process will foster the development of kallistatin-based therapeutic strategies for aging-related vascular diseases.

Objective

The object of this research project is to determine the role and mechanism of kallistatin in vascular injury, senescence and aging. To achieve this goal, we generated two strains of kallistatin knockout mice, systemic kallistatin depletion and endothelial cell-specific kallistatin depletion. We hypothesized that kallistatin protects against vascular and organ injury, senescence and aging by downregulating miR-34a and miR-21, and upregulating Let-7g and antioxidant genes, SIRT1 and eNOS. We explored the role of kallistatin in regulating vascular injury and senescence using: 1) recombinant kallistatin protein administration, and 2) kallistatin deficiency in mouse lung endothelial cells, and systemic kallistatin deletion in general kallistatin knockout mice.

Specific Aims

I. To determine the role and mechanism of kallistatin in endothelial-mesenchymal transition.

II. To determine the role and mechanism of kallistatin in vascular senescence and aging.

III. To determine the role of endogenous kallistatin in endothelial senescence, vascular and organ injury.

CHAPTER II

TO DETERMINE THE ROLE AND MECHANISM OF KALLISTATIN IN ENDOTHELIAL-MESENCHYMAL TRANSITION

Summary

Kallistatin exhibits anti-tumor and anti-fibrotic activities in animal models. Endothelial-mesenchymal transition (EndMT) is one of the underlying mechanisms contributing to fibrosis and cancer. Endothelial transdifferentiation is also activated and contributes to the maladaptive remodeling of vasculature, leading to rarefaction of endothelium and thickening of smooth muscle layers. Transforming growth factor-β (TGF-β) is the most common inducer of EndMT. Recombinant human kallistatin treatment blocked TGF-β-induced EndMT in human endothelial cells, as evidenced by morphological changes as well as increased endothelial marker expression of VE-cadherin and CD31, and reduced mesenchymal marker α-SMA expression. Kallistatin inhibited TGF-β-mediated reactive oxygen species (ROS) formation and NADPH oxidase expression and activity. Kallistatin blocked TGF-β-induced miR-21-Akt survival pathway activation, including Akt phosphorylation, NF-κB activation, Snail1 synthesis, and matrix metalloproteinase 2 synthesis and activation. Kallistatin via its heparin-binding site blocked TGF-β-induced miR-21, Snail1 expression and ROS formation. Conversely, kallistatin through its active site stimulated the synthesis of endothelial nitric oxide synthase (eNOS), sirtuin 1 (SIRT1) and forkhead box O1 (FoxO1), via interacting with a tyrosine kinase. These combined findings reveal that kallistatin suppresses EndMT by inhibiting TGF-β-induced miR-21-Akt pathway and oxidative stress and stimulating the expression of antioxidant genes. The study may provide new insights into the role of kallistatin in vascular and organ injury.

Introduction

Endothelial–mesenchymal transition (EndMT) is a critical underlying mechanism for organ fibrosis and tumor metastasis (Lin *et al.*, 2012). In adults, abnormal differentiation of EndMT-derived fibroblast-like cells results in fibrosis in the heart, kidney and lung (Zeisberg *et al.*, 2008, Hashimoto *et al.*, 2010, Braitsch *et al.*, 2013). Moreover, in later stage of vascular disease EndMT is also activated and contribute to the maladaptive remodeling of vasculature, leading to vascular injury including rarefaction of endothelium and thickening of smooth muscle layers (Lin *et al.*, 2012, Nicolosi *et al.*, 2016). TGF-β signaling has been shown to be involved in controlling endothelial and epithelial plasticity by eliciting their transition to a mesenchymal state (Yoshimatsu & Watabe, 2011, van Meeteren & ten Dijke, 2012). The TGF-β-Akt-Snail axis is one of the important pathways in epithelial–mesenchymal transition (EMT) (Peinado *et al.*, 2003). TGF-β induces Akt activation and nuclear factor-κB (NF-κB) nuclear translocation (Huber *et al.*, 2004, Meadows *et al.*, 2009), leading to elevated expression of the Snail transcription factor and thus reduced epithelial (E)-cadherin expression (Julien *et al.*, 2007). Snail also mediates downregulation of vascular endothelial (VE)-cadherin expression (Cheng *et al.*, 2013). Typical morphology changes of EndMT include loss of cell–cell junctions, such as VE-cadherin and CD31, as well as gain of invasive and migratory properties characterized by mesenchymal markers, including α-smooth muscle actin (SMA), fibronection and N-cadherin. Additionally, aberrant expression of microRNAs (miRs) is implicated in EndMT-related diseases. One such miRNA, miR-21 is markedly upregulated during fibrosis and cancer (Kumarswamy *et al.*, 2012, Luo *et al.*, 2015). It has been reported that TGF-β-induced EndMT is partly regulated by miR-21-Akt pathway, as blockade of miR-21 was found to prevent EndMT and inhibit Akt activation (Kumarswamy *et al.*, 2012). Moreover, reactive oxygen species (ROS) production further stimulates miR-21 synthesis (Ling *et al.*, 2012), and oxidative stress

contributes to cell invasion and fibrogenesis. Therefore, miR-21 and ROS are the major mediators of EndMT, and thus EndMT-associated vascular and organ injury.

Kallistatin gene or protein delivery has been shown to improve cardiac and renal function, and decrease cardiac and renal fibrosis in conjunction with reduced superoxide formation and increased eNOS expression and NO production in animal models (Chao *et al.*, 2006, Gao *et al.*, 2008, Shen *et al.*, 2008). Specifically, kallistatin reduced collagen accumulation, collagen fraction volume and TGF-β1 expression in the myocardium of mice with myocardial infarction (Gao *et al.*, 2008). Kallistatin inhibited renal fibrosis and aortic injury in hypertensive rats (Shen *et al.*, 2008, Shen *et al.*, 2010). Liver fibrosis was also decreased upon kallistatin treatment via inhibition of oxidative stress (Huang *et al.*, 2014). Moreover, kallistatin has displayed inhibitory effect on tumor growth in mice with breast tumor xenografts (Miao *et al.*, 2002). These findings led us to investigate the role and mechanism of kallistatin in modulating EndMT, the process underlying vascular injury, fibrosis and cancer.

Materials and Methods

Cell Culture

Human umbilical vein endothelial cells (HUVECs) were kindly provided by Dr. Robin Muise-Helmericks (Medical University of South Carolina). HUVECs were cultured in endothelial cell basal medium (EBM)-2 supplemented with EGM-2 SingleQuots (Lonza), and maintained in a humidified atmosphere of 5% CO_2 in air at 37°C. HUVECs were incubated in the presence or absence of kallistatin (1 μM) for 30 min, followed by the addition of 10 ng/ml TGF-β1 (R&D Systems) for another 24 h (for gene analysis) or 72 h (activity assay or protein expression). Culture media containing TGF-β1 or kallistatin were replaced every 24 h. In another set of experiments, cells were pretreated with 5 μM genistein (Sigma) for 30 min, and then further incubated with 2 μM WT-KS, HM-KS or AM-KS in the presence of 10 μg/ml polymyxin B sulfate (Sigma) for 30 min followed by stimulation with TGF-β1 for another 24 h.

Purification and Characterization of Recombinant Human Kallistatins

Recombinant human kallistatin was secreted into the serum-free medium of cultured human embryonic kidney cells (HEK293T). Cultured medium was concentrated by ammonium sulfate precipitation followed by nickel-affinity chromatography as described (Chen *et al.*, 2000, Li *et al.*, 2014). Recombinant wild-type kallistatin (WT-KS), heparin-binding site mutant (K312A/K313A) kallistatin (HM-KS), and active-site mutant (A377T) kallistatin (AM-KS) were expressed in *E. coli* and purified as described (Chen *et al.*, 2000). The purity and identity of human kallistatin were verified by sodium dodecyl sulfate-poly-acrylamide gel electrophoresis (SDS-PAGE) and western blot using a specific monoclonal antibody (Chao *et al.*, 1996, Li *et al.*, 2014).

Detection of ROS Formation and NF-κB Activity Assay

Intracellular ROS generation was detected using the peroxide-sensitive fluorescent probe 2', 7'-dichlorofluorescin diacetate (DCFH-DA; Sigma) as described previously (Shen *et al.*, 2010). Phosphorylated NF-κB activities in nuclear lysates were determined using ELISA kit (Cell Signaling Technology) according to the manufacturer's instructions.

Quantitative Real-time Polymerase Chain Reaction (qRT-PCR)

RNA was isolated from cells using Trizol reagent (Invitrogen) per the manufacturer's instructions. Total RNA was reverse-transcribed using the High-Capacity cDNA Reverse Transcription Kit (Applied Biosystems) for messenger RNA, or microRNA Reverse Transcription Kit (Applied Biosystems) for microRNA. qRT-PCR was performed with Taqman Gene Expression Assay (Applied Biosystems). The following human primers were purchased from Applied Biosystems: 18S (Hs 99999901_sl), U6 (001973), hsa-miR-21-3p (002438), eNOS (Hs 01574659_ml), MMP2 (Hs 00234422_ml), Snail1 (Hs 00195591_ml), SIRT1 (Hs 01009006_ml), forkhead box O1 (FoxO1) (Hs 01054576_ml), and NADPH oxidase 4 (Nox4) (Hs 00418356_ml). Data were analyzed with $2^{-\Delta\Delta Ct}$ value calculation using 18S or U6 for normalization.

Measurement of NADPH Oxidase Activity

The enzymatic activity of NADPH oxidase in cell or aortic homogenates was assessed by lucigenin enhanced chemiluminescence (ECL) as previously described (Shen *et al.*, 2010). Protein concentrations were measured by Pierce BCA protein assay kit (Thermo Fisher Scientific). The chemiluminescence signal was corrected for by the protein concentration of each sample homogenate.

Gelatin Zymography

Conditioned HUVEC medium was collected and centrifuged for zymography. Briefly, the medium was mixed with non-reducing loading buffer and resolved at 125 V by 10% SDS-PAGE separating gels copolymerized with 1 mg/ml gelatin. The renaturing buffer (2.5% Triton X-100) was used to restore the enzyme activity. The gels were incubated in fresh developing buffer at 37°C for 16 h, followed by staining with Coomassie blue to visualize the proteolytic bands.

Western Blot Analysis

Cells were lysed in lysis buffer supplemented with a protease inhibitor cocktail (Thermo Fisher Scientific), and separated on a 10% polyacrylamide gel, and transferred on polyvinylidene difluoride (PVDF) membranes (Amersham Biosciences). After being blocked for 1 h in a buffer containing 5% nonfat milk, PVDF membranes were then probed with primary antibodies to phosphorylated Akt (S473), total Akt, CD31, VE-cadherin, α-SMA and α-tubulin (Cell Signaling Technology) overnight at 4°C. The respective horseradish peroxidase-labeled secondary antibodies were then added to the membrane for 1 h at room temperature. Chemiluminescence was detected by an ECL-plus kit (GE Healthcare).

Statistical Analysis

Data are expressed as means ± SE of three independent experiments. Statistical significance was determined by analysis of variance with Fisher's probability least-squares difference test or Student *t-test* using GRAPHPAD PRISM software. A value of $P < 0.05$ was considered statistically significant.

Results

Kallistatin Inhibits TGF-β-Induced EndMT and Conserves the Endothelial Phenotype

We first determined the effect of kallistatin on TGF-β1-mediated EndMT in cultured endothelial cells. Exposure of HUVECs to TGF-β1 for 3 days caused an obvious alteration in cellular morphology from a polygonal, cobblestone-like shape to a more spindle, fibroblast-like shape (Figure 2-1 A). In contrast, kallistatin treatment markedly suppressed the transition by conserving the endothelial phenotype. Cells undergoing EndMT were characterized with the expression of fibroblast marker α-SMA and endothelial markers VE-cadherin and CD31. Representative immunostaining showed that TGF-β1-induced EndMT was associated with reduced CD31 and VE-cadherin levels (Figure 2-1 B&C) and increased α-SMA levels (Figure 2-1 D). However, upon kallistatin treatment, most cells were positive for VE-cadherin and CD31, and negative for α-SMA. These observations were further confirmed by western blot analysis. In the presence of TGF-β1, VE-cadherin and CD31 protein levels were greatly reduced, and α-SMA protein levels were increased (Figure 2-1 E). However, kallistatin treatment reversed TGF-β1-mediated effects. Quantitative analysis of the western blots verified our results. These findings demonstrate that kallistatin suppresses EndMT induced by TGF-β.

Kallistatin Inhibits TGF-β-Induced ROS Formation and NADPH Oxidase Expression and Activity

We next determined the effect of kallistatin on ROS formation driven by TGF-β1 in endothelial cells. TGF-β1 significantly stimulated ROS formation compared to the control group, whereas kallistatin reversed TGF-β's effect by restoring ROS production to basal levels (Figure 2-2 A). We also evaluated the effect of kallistatin on the NADPH

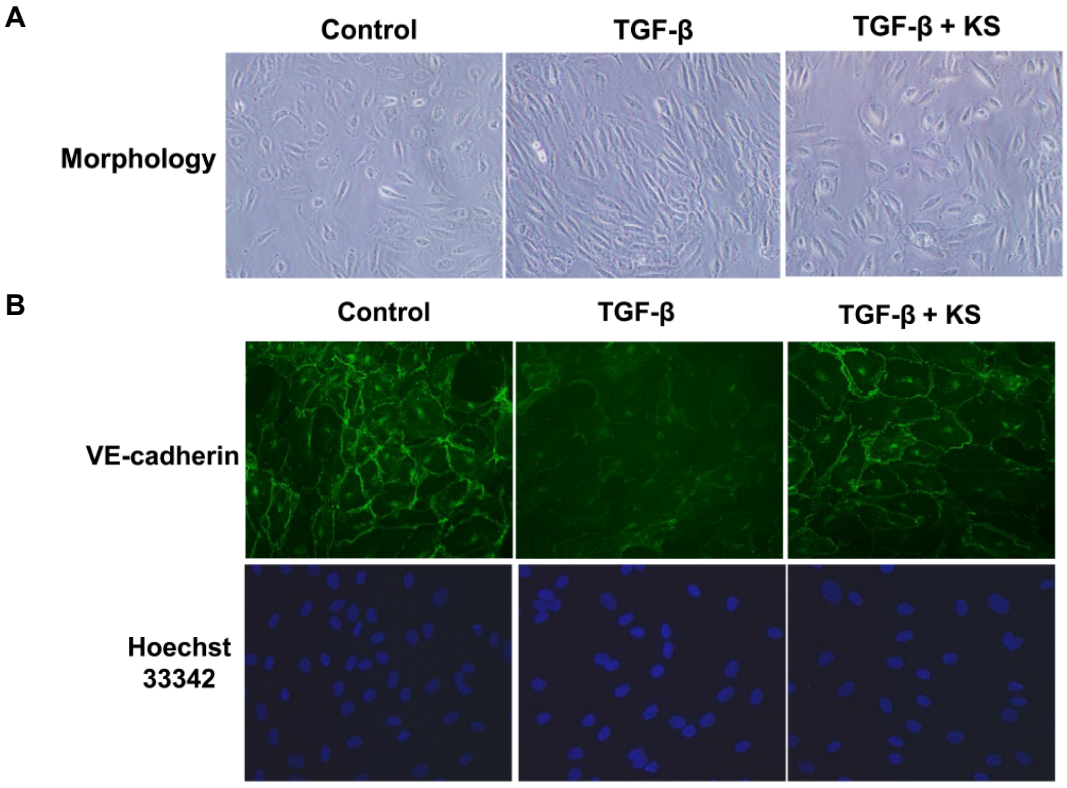

Figure 2-1 A&B. Kallistatin (KS) inhibits TGF-β-induced EndMT. (A) Representative images of endothelial morphology under light microscope. Original magnification 200×. (B) Representative immunofluorescent images of endothelial marker VE-cadherin expression in human endothelial cells.

C

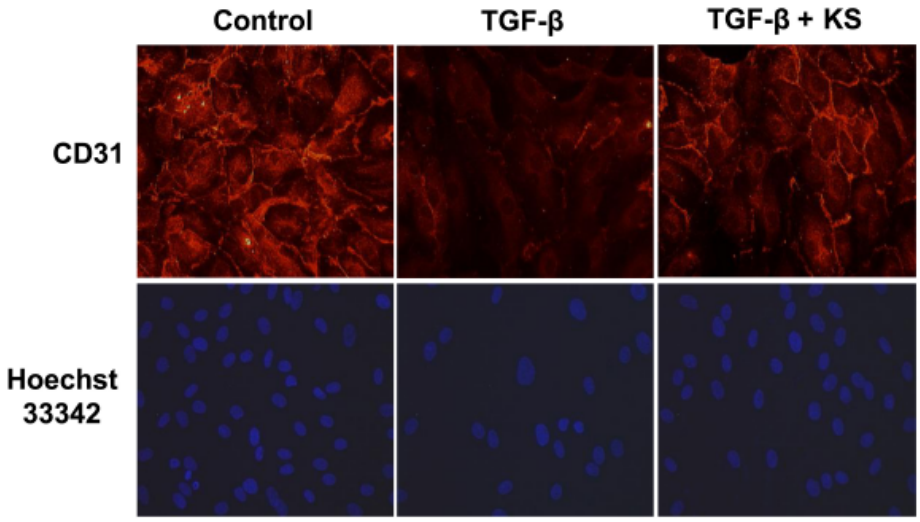

D

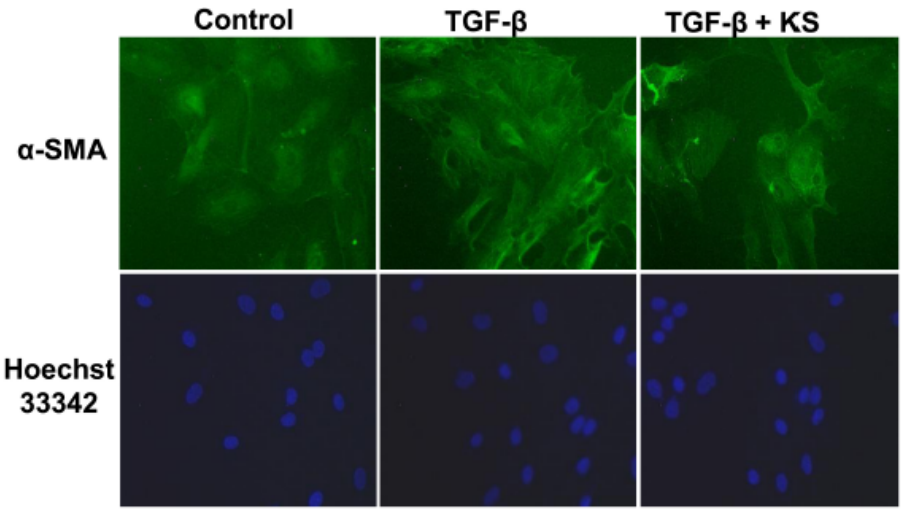

Figure 2-1 C&D. Kallistatin (KS) inhibits TGF-β-induced EndMT. (C) Representative immunofluorescent images of endothelial marker CD-31 and (D) mesenchymal marker α-SMA in human endothelial cells. Original magnification 200 ×. Nuclei are counterstained with Hoechst 33342.

E

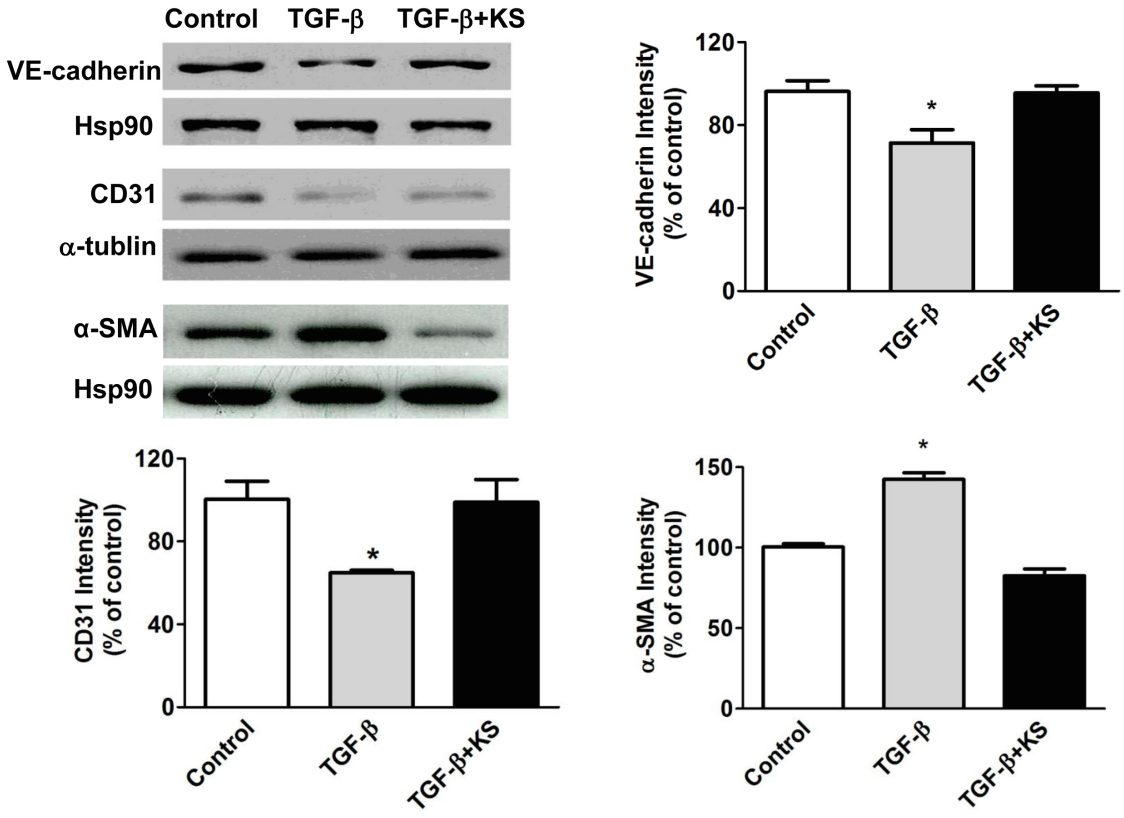

Figure 2-1 E. Kallistatin (KS) inhibits TGF-β-induced EndMT marker expression. Representative western blots of VE-cadherin, CD31 and α-SMA and quantification of these EndMT makers are shown. n=3. **P* <0.05 vs. control.

oxidase stimulates the production of ROS (Yan *et al.*, 2014). Kallistatin treatment completely antagonized TGF-β1-induced Nox4 mRNA levels and NADPH oxidase activity (Figure 2-2 B&C). Therefore, kallistatin can block TGF-β-induced oxidative stress in endothelial cells.

Kallistatin Prevents TGF-β-Induced miR-21 Synthesis, Akt and NF-κB Activation, Snail1 Expression, and MMP2 Synthesis and Activation

Since the miR-21-Akt signaling pathway plays an important role in EndMT, we tested whether kallistatin regulates TGF-β-induced EndMT through this pathway. Our results showed that TGF-β1 upregulated miR-21 synthesis, but the effect was prevented by kallistatin (Figure 2-3 A). Kallistatin also prevented TGF-β1-induced Akt phosphorylation (Figure 2-3 B). These results indicate that kallistatin blocks TGF-β-induced EndMT by inhibiting the miR-21-Akt pathway. Moreover, kallistatin treatment attenuated TGF-β1-mediated NF-κB activation (Figure 2-3 C). Since NF-κB leads to the activation of the Snail transcription factor, we measured Snail1 mRNA levels. TGF-β1 significantly induced Snail1 transcription, whereas kallistatin treatment prevented the effect (Figure 2-3 D). Furthermore, we analyzed MMP2 synthesis and activation by PCR and zymography, respectively. TGF-β1 increased MMP2 mRNA levels and activity, which were abolished by kallistatin (Figure 2-3E). These results indicate that kallistatin blocks TGF-β-mediated EndMT, in part, by inhibiting the miR-21-Akt-NF-κB pathway, Snail1 expression, and MMP2 synthesis and activity.

Kallistatin's Heparin-Binding Site Is Essential for Preventing TGF-β-Induced miR-21 Synthesis, Oxidative Stress and Snail1 Expression

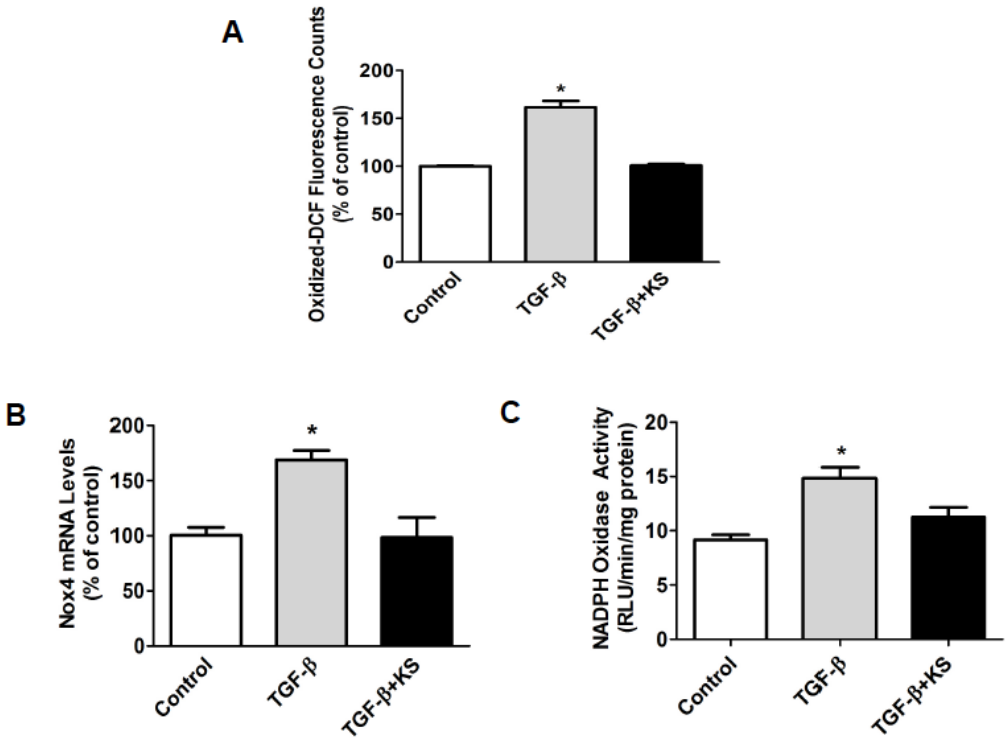

Figure 2-2. Kallistatin (KS) inhibits TGF-β-induced ROS formation and NADPH oxidase expression and activity in human endothelial cells. (A) Cellular ROS formation determined by measuring oxidized fluorescent dye DCF counts. (B) QPCR analysis of mRNA levels of NADPH oxidase 4 (Nox4). (C) NADPH oxidase activity determined by lucigenin-dependent chemiluminescence. n=3. *P <0.05 vs. other groups.

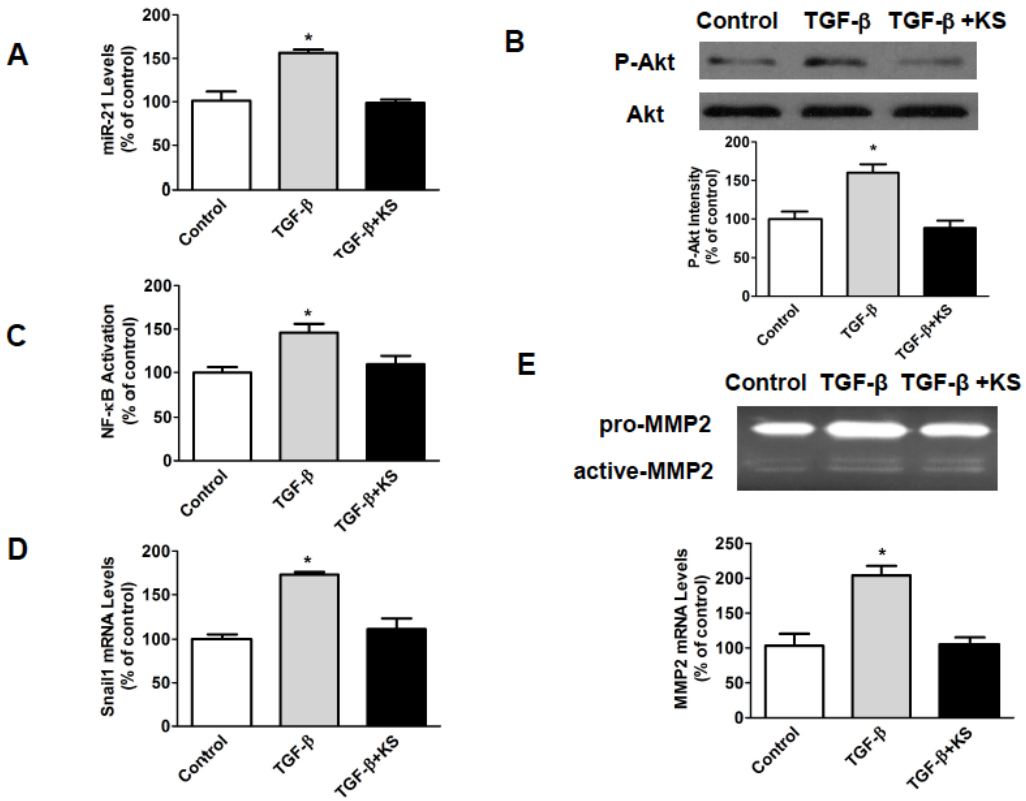

Figure 2-3. Kalistatin (KS) inhibits TGF-β-induced miR-21-Akt signaling in human endothelial cells. (A) QPCR analysis of miR-21. (B) Representative western blot of phospho-Akt and quantitative analysis. (C) NF-κB activity determined by ELISA. (D) QPCR analysis of Snail1 mRNA. (E) MMP2 activity was determined by zymography, and MMP2 mRNA expression was determined by QPCR. n=3. *P < 0.05 vs. other groups.

We analyzed the role of kallistatin's heparin-binding site in modulating TGF-β1-induced miR-21 synthesis and ROS generation. Wild-type kallistatin significantly reduced TGF-β1-driven miR-21 expression, whereas heparin-binding site mutant kallistatin had no effect (Figure 2-4 A). Likewise, wild-type kallistatin, but not heparin mutant kallistatin, inhibited TGF-β1-induced ROS formation (Figure 2-4 B). Moreover, kallistatin's heparin-binding site was found to be essential for abolishing TGF-β1-mediated Snail1 expression (Figure 2-4 C). Our results demonstrate that kallistatin competes with TGF-β1's ability to bind to heparan sulfate proteoglycans, thus preventing TGF-β1-mediated signaling. These new findings indicate that kallistatin's heparin-binding site plays an important role in antagonizing TGF-β-induced miR-21, ROS formation and Snail1 expression.

Kallistatin via Its Active Site Stimulates eNOS, SIRT1, and FoxO1 Expression

We next examined the role of kallistatin's structural elements on the expression of antioxidant genes in endothelial cells. Our results showed that wild-type kallistatin and heparin-binding site mutant kallistatin treatment led to a noticeable rise in eNOS, SIRT1 and FoxO1 mRNA levels, whereas active site-mutant kallistatin had no effect (Figure 2-5). This finding clearly indicates that the active site of kallistatin is crucial for mediating the expression of eNOS, SIRT1 and FoxO1. Moreover, treatment with genistein, a tyrosine kinase inhibitor, abolished kallistatin-induced eNOS, SIRT1 and FoxO1 expression (Figure 2-5). These new results show that kallistatin via its active site interacts with a cell surface tyrosine kinase, thus stimulating expression of the antioxidant genes eNOS, SIRT1 and FoxO1.

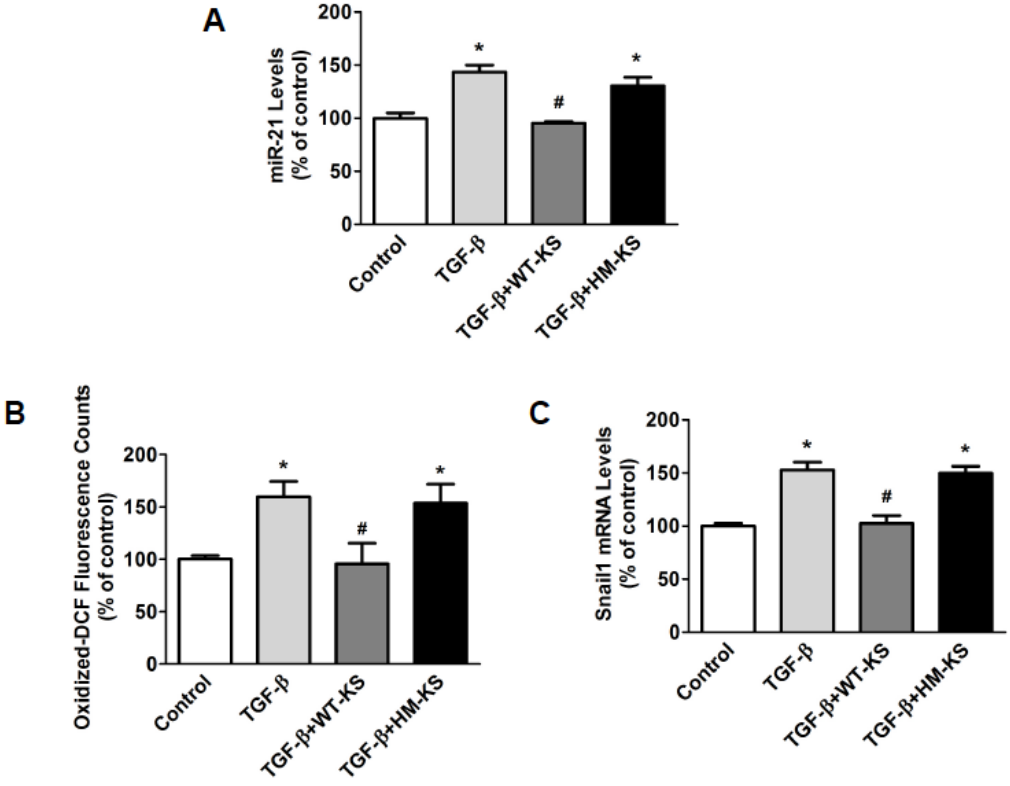

Figure 2-4. Kallistatin via heparin-binding site inhibits miR-21 synthesis, ROS formation and Snail 1 expression in human endothelial cells. (A) QPCR analysis of miR-21. (B) Cellular ROS formation determined by measuring oxidized fluorescent DCF counts. (C) QPCR analysis of Snail1 mRNA. WT-KS: wild-type kallistatin; HM-KS: heparin-binding site mutant kallistatin. n=3. $^{*}P$ <0.05 vs. control; $^{\#}P$ <0.05 vs. TGF-β.

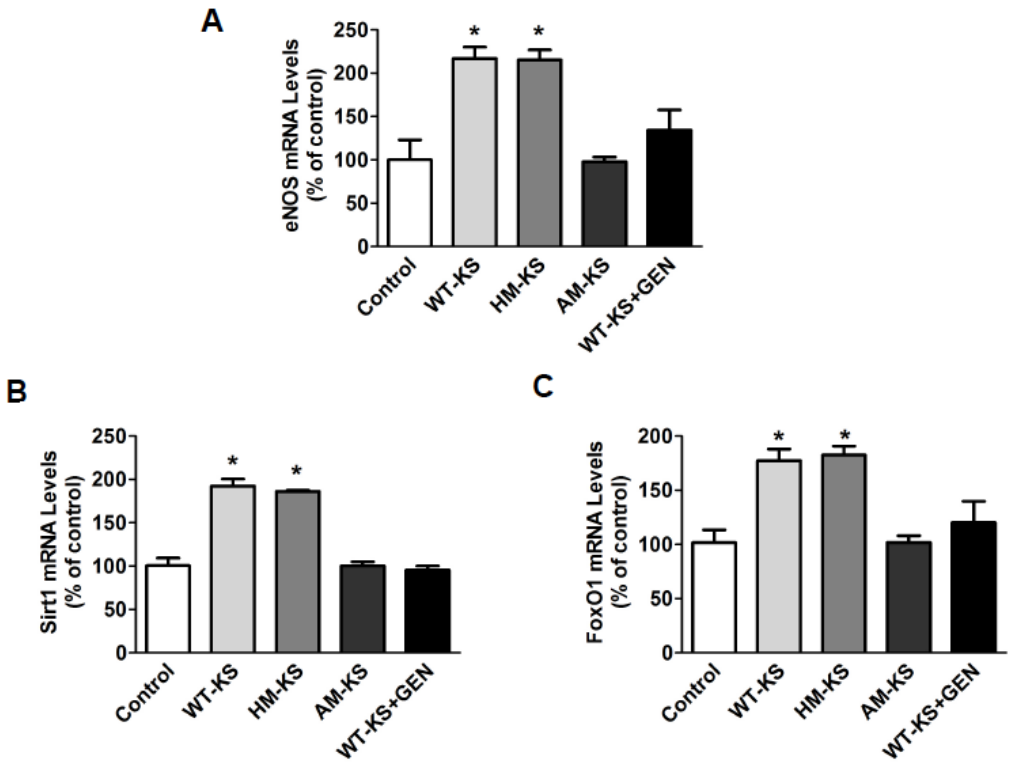

Figure 2-5. The active site of kallistatin is essential for increasing the expression of eNOS, SIRT1 and FoxO1 via a tyrosine kinase. QPCR analysis of mRNA levels of (A) eNOS, (B) SIRT1 and (C) FoxO1 in human endothelial cells. GEN, genistein, a tyrosine kinase inhibitor. WT-KS: wild-type kallistatin; HM-KS: heparin-binding site mutant kallistatin; AM-KS: active site mutant kallistatin. n=3. * *P* <0.05 vs. other groups.

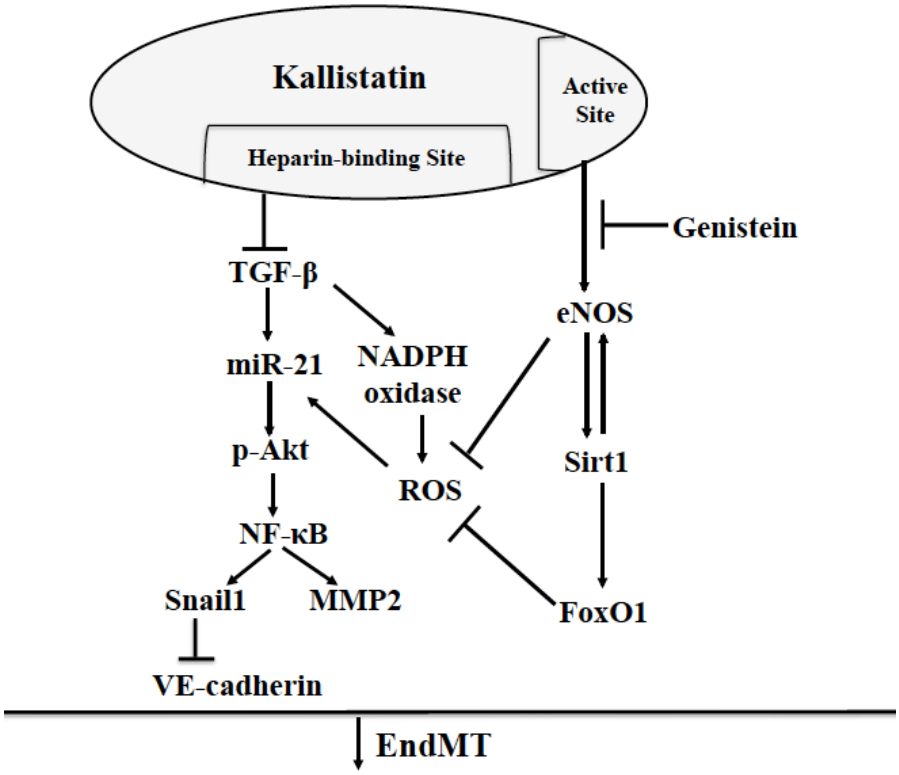

Figure 2-6. Signaling pathway by which kallistatin inhibits EndMT. Kallistatin's heparin-binding site is responsible for suppression of TGF-β-induced miR-21-Akt signaling and ROS formation, while its active site is key for stimulating the expression of eNOS, SIRT1 and FoxO1 through interacting with a tyrosine kinase. GEN: genistein, a tyrosine kinase inhibitor.

Discussion

This study provides new insights into the protective role of kallistatin in EndMT and EndMT-associated pathological processes, such as vascular injury and fibrosis. We showed that kallistatin prevented EndMT by blocking TGF-β1-induced miR-21 synthesis and oxidative stress, and also by directly stimulating the expression of the antioxidant genes eNOS, SIRT1 and FoxO1. Moreover, this is the first study to demonstrate that kallistatin's structural elements play crucial roles in the differential regulation of TGF-β signaling and eNOS/SIRT1 expression in human endothelial cells. We found that kallistatin via its heparin-binding site inhibited TGF-β1-induced miR-21 expression, ROS formation, and Snail1 synthesis. Conversely, kallistatin's active site was observed to be essential for stimulating the expression of eNOS, SIRT1 and FoxO1 (Figure 2-6). Both eNOS and SIRT1 are responsible for increasing NO production, and NO has been shown to be an antioxidant by decreasing ROS levels and NADPH oxidase activity (Clancy *et al.*, 1992). Our previous finding has shown that kallistatin administration attenuated vascular injury, and cardiac and renal fibrosis in conjunction with reduced oxidative stress and increased NO production in animal models with hypertension or myocardial infarction (Gao *et al.*, 2008, Shen *et al.*, 2008). Thus, our findings reveal a new mechanism that kallistatin, through its structural elements, inhibits vascular injury and organ fibrosis by antagonizing EndMT process.

miR-21 is an oncogenic microRNA that is overexpressed in most human tumors, and can thus promote tumor growth and progression by acting on multiple target genes (Kumarswamy *et al.*, 2011). Increased miR-21 leads to Akt activation, which in turn upregulates miR-21 in endothelial cells (Thum *et al.*, 2008). These studies are consistent with our findings that TGF-β1 stimulated miR-21 synthesis and Akt phosphorylation/activation; however, kallistatin efficiently blocked TGF-β1-mediated

effects. Oxidative stress also stimulates miR-21 expresson (Jiang *et al.*, 2014). The present study showed that kallistatin not only antagonized TGF-β1-mediated miR-21-Akt activation, but also blocked TGF-β1-induced oxidative stress. Therefore, kallistatin can attenuate TGF-β-induced EndMT by targeting the miR-21-Akt pathway and oxidative stress.

The role of TGF-β-induced Akt-NF-κB activation in the context of EndMT is not well understood. In the EMT process, Akt stimulates the nuclear translocation of the NF-κB complex. NF-κB acts as a transcriptional factor for Snail1 and MMP2 expression (Julien *et al.*, 2007, Yan & Boyd, 2007). During EndMT the basal lamina is degraded by matrix metalloproteinases, such as MMP2 (Potenta *et al.*, 2008). Snail factors are known to repress both VE-cadherin and E-cadherin transcription. Consequently, elevated Snail expression can stimulate the loss of endothelial cell–cell junctions. In the present study, our results showed that NF-κB was induced by TGF-β1 in endothelial cells undergoing EndMT, resulting in elevated Snail1 and MMP2 expression and loss of the endothelial marker VE-cadherin. In contrast, kallistatin treatment blocked TGF-β1-mediated miR-21-Akt activation, leading to suppression of TGF-β-induced NF-κB-Snail1/MMP2 signaling. Thus, these results indicate that kallistatin inhibits EndMT through blockade of TGF-β-induced Akt-NF-κB signaling pathway.

Heparan sulfate proteoglycans are present on the surface of vascular smooth muscle cells and endothelial cells (Adhikari *et al.*, 2010, Sarrazin *et al.*, 2011). TGF-β1 is a heparin-binding growth factor, and the ability of TGF-β1 to bind to heparan or related proteoglycans is the first step to initiate metabolic signals (Chen Q. *et al.*, 2007). Our previous studies showed that the heparin-binding site of kallistatin is essential for antagonizing signaling pathways mediated by other heparin-binding proteins, such as

VEGF, TNF-α, and HMGB1 (Miao *et al.*, 2003, Yin *et al.*, 2010, Li *et al.*, 2014). It is likely that kallistatin competes with TGF-β1 from binding to heparan sulfate proteoglycans on the endothelial cells. Indeed, we showed that kallistatin's heparin-binding site is essential for preventing TGF-β1-induced miR-21-Akt signaling and ROS formation in endothelial cells. Therefore, these results provide new information regarding the role of kallistatin's heparin-binding site in antagonizing TGF-β-induced signaling.

eNOS-derived NO is an antioxidant by inhibiting NADPH oxidase activity (Clancy *et al.*, 1992, Fujii *et al.*, 1997). In addition to eNOS/NO, both SIRT1 and FoxO1 are capable of suppressing ROS formation. SIRT1 can function to deacetylate and activate eNOS and FoxO1. FoxO1 is known to promote activation of the antioxidant enzyme manganese superoxide dismutase to scavenge ROS (Storz, 2011). Our present finding indicates that kallistatin's active site is responsible for stimulating the expression of the antioxidant genes eNOS, SIRT1 and FoxO1, and the effect was blocked by genistein, a tyrosine kinase inhibitor. Thus kallistatin's active site could interact with a tyrosine kinase to increase eNOS/SIRT1 expression. The identity of the putative kallistatin-binding protein or kallistatin receptor on the endothelial cell surface awaits further investigation.

Taken together, the present study indicates that kallistatin has a novel role in inhibiting EndMT, and new functions of kallistatin's functional domains have been identified. Mechanistically, kallistatin through its two structural elements differentially regulates miR-21, oxidative stress and eNOS expression. Kallistatin's heparin-binding site plays an important role in suppressing miR-21-Akt signaling and ROS formation, whereas its active site is key for stimulating the expression of eNOS, SIRT1 and FoxO1. Moreover, kallistatin via its active site interacts with a tyrosine kinase to stimulate eNOS synthesis, which can lead to NO formation and reduced oxidative stress. Thus, kallistatin

exerts potent antioxidant activity by dual mechanisms: (1) blocking TGF-β-induced oxidative stress, and (2) increasing eNOS/SIRT1/FoxO1 levels. These new findings shed light on the pleiotropic functions and mechanisms of kallistatin in the potential treatment of fibrosis-related vascular diseases.

CHAPTER III

TO DETERMINE THE ROLE AND MECHANISM OF KALLISTATIN IN VASCULAR SENESCENCE AND AGING

Summary

Kallistatin protects against vascular injury by inhibiting oxidative stress in hypertensive rats and enhancing the mobility and function of endothelial progenitor cells (EPCs). We further determined the role and mechanism of kallistatin in vascular senescence and aging using cultured EPCs, streptozotocin (STZ)-induced diabetic mice, and *Caenorhabditis elegans* (*C. elegans*). Human kallistatin significantly decreased TNF-α-induced EPC senescence, as indicated by reduced senescence-associated β-galactosidase activity, plasminogen activator inhibitor-1 expression, and elevated telomerase activity. Kallistatin blocked TNF-α-induced superoxide levels, NADPH oxidase activity, miR-21 expression and cell cycle inhibitor $p16^{INK4a}$ synthesis. The microRNA (miR)-34a-SIRT1 axis is an important signaling in regulating senescence. Kallistatin prevented TNF-α mediated inhibition of SIRT1, eNOS, and catalase, and directly stimulated the expression of these antioxidant enzymes. Importantly, kallistatin inhibited miR-34a synthesis, whereas miR-34a overexpression abolished kallistatin-induced SIRT1/eNOS expression and anti-senescence activity. Kallistatin via its active site inhibited miR-34a, and stimulated SIRT1 and eNOS synthesis in EPCs, which was abolished by genistein, indicating an event mediated by tyrosine kinase. Moreover, kallistatin administration attenuated aortic senescence, oxidative stress, associated with reduced miR-34a and miR-21 synthesis and increased SIRT1, eNOS, and catalase levels in STZ-induced diabetic mice. Furthermore, kallistatin treatment reduced superoxide formation and improved wild-type *C. elegans* survival under oxidative or heat stress, although kallistatin's protective effect was abolished in miR-34 or sir-2.1 (SIRT1 homolog) mutant *C. elegans*. Kallistatin inhibited miR-34, but stimulated sir-2.1 and sod-3 synthesis in *C. elegans*. These *in vitro* and *in vivo* studies provided significant insights into the role and mechanism of kallistatin in vascular senescence and aging by regulating miR-34a-SIRT1 pathway.

Introduction

EPCs are a major contributor to vascular repair, and can be derived from bone marrow, circulating mononuclear cells, and cord blood (Lin *et al.*, 2000, Reyes *et al.*, 2002). Circulating EPCs are the most important cell population for the replenishment of damaged or senescent endothelial cells. Advanced aging is a major risk factor for suppressed EPC function (Williamson *et al.*, 2012). Senescent or impaired EPCs contribute to endothelial dysfunction, which is a predictor of cardiovascular diseases(Heiss *et al.*, 2005). Type I diabetes is one of cardiovascular-associated diseases characterized by reduced EPC numbers and vascular repair (Loomans *et al.*, 2004). Moreover, the nematode *C. elegans* has a number of distinct advantages that are useful for understanding the molecular basis of organismal dysfunction underlying age-related diseases. Due to its short life cycle (3.5 days) and conserved longevity genes from worm to human (Zhou *et al.*, 2011). *C. elegans* is an ideal model for investigating the aging process. Consequently, EPCs, STZ-induced diabetic mice, and *C. elegans* are valuable models for examining the mechanisms of vascular senescence and aging.

Oxidative stress is a key inducer of endothelial senescence, with the inflammatory cytokine TNF-α being the main contributor to reactive oxygen species (ROS) production (Chen *et al.*, 2008). Upregulation of antioxidant proteins, such as endothelial nitric oxide synthase (eNOS), sirtuin 1 (SIRT1), catalase, and manganese superoxide dismutase (MnSOD), has been shown to protect against oxidative stress-mediated insults (Wassmann *et al.*, 2004, Ota *et al.*, 2010). eNOS maintains the redox state of endothelial cells and promotes vasorelaxation through NO production (Forstermann & Sessa, 2012). SIRT1 is a conservative longevity gene from yeast to human, and accounts for vascular homeostasis by activating many antioxidant enzymes, such as eNOS, catalase, and MnSOD, to diminish ROS (Kitada *et al.*, 2016).

Conversely, growing evidence has shown that miR-34a is a senescence promoter, as it inhibits SIRT1 through a miR-34a-binding site within the 3' UTR of SIRT1 (Zhao *et al.*, 2010). Furthermore, miR-21, a tumor inducer, is also involved in EPC senescence (Zhu S. *et al.*, 2013). The antioxidant enzymes and pro-senescence miRNAs underlie the molecular basis for endothelial senescence and aging-associated diseases. Therefore, exploration of effective molecules or compounds that stimulate longevity gene expression and inhibit the effects of negative regulators may lead to a prospective enhancement of vascular integrity and lifespan.

Kallistatin treatment increases circulating EPC number and reduces aortic oxidative stress in hypertensive rats, whereas kallistatin deficiency decreases EPC levels and exacerbates oxidative vascular injury (Liu Y. *et al.*, 2012, Gao *et al.*, 2014). In addition, kallistatin promotes vascular repair by enhancing the viability, migration, and function of EPCs (Gao *et al.,* 2014). Kallistatin, via NO stimulation, reduces TNF-α induced superoxide production and NADPH oxidase activity in endothelial cells (Shen *et al*., 2010). Moreover, in Chapter II we showed that kallistatin prevented endothelial–mesenchymal transition (EndMT) by inhibiting TGF-β-induced miR-21 and increasing SIRT1 synthesis (Guo *et al.*, 2015). However, whether kallistatin through regulating miR-34a-SIRT1 pathway affects endothelial senescence has not been explored, in this study we investigated the potential role of kallistatin in vascular senescence and aging, using both *in vitro* and *in vivo* models.

Materials and Methods

Isolation and Culture of EPCs

EPCs were isolated from human umbilical cord blood as described (Gao *et al.*, 2014). The study was approved by the Medical University of South Carolina Human Research (Pro00017277). EPCs were isolated by density gradient centrifugation using Ficoll-Paque PLUS (GE Healthcare,) and cultured in endothelial basal medium with 10% fetal bovine serum and supplements (Lonza).

Senescence-associated β-Galactosidase Staining

EPCs at 80% confluency in 12-well plates were pre-incubated with kallistatin (1 μM) for 30 min and then treated with TNF-α (10 ng/mL) for 6 days. The senescence phenotype was detected using the β-galactosidase staining kit (Cell Signaling). The number of positive senescence-associated β-galactosidase (SA-β-gal) cells was observed by light microscopy (Olympus CK40) in 10 randomly chosen low-power fields (× 200) and expressed as a percentage of counted cells.

Telomerase Activity Assay

EPCs were pre-incubated with or without kallistatin (1 μM) for 30 min prior to the addition of TNF-α (10 ng/mL) for 24 h. Cells were lysed with non-denaturing lysis buffer. Telomerase activity was measured using TRAPEZE RT telomerase detection kit (EMD Millipore).

NADPH Oxidase Activity Assay

The enzymatic activity of NADPH oxidase was assessed as described in Chapter II. Fluorescence intensity was continuously monitored for 15 min with a TD20/20 luminometer.

Detection of Superoxide Formation

Cellular ROS generation was detected using the peroxide-sensitive fluorescent probe 2', 7'-dichlorodihydrofluorescein diacetate (DCFH-DA; 10 μM, Sigma). To determine the role of PI3K-Akt-eNOS pathway, EPCs were pretreated with PI3K inhibitor LY294002 (5 μM) or iNOS inhibitor L-NAME (100 μM) for 30 min in prior to kallistatin treatment. To quantify ROS levels, EPCs were seeded onto a 96-well fluorescence plate and treated as above. Relative fluorescence was measured using the fluorescence plate reader at 485-nm excitation and 535-nm emission. Superoxide levels in aortas were determined by red fluorescent probe dihydroethidium (DHE; 3 μM Sigma) incubation at 37°C for 30 min at dark. For ROS staining in *C. elegans*, worms were washed, incubated with 3 μM DHE for 30 min and anesthetized with 5 mM levamisole (Sigma). *C. elegans* were then transferred to glass slides, sealed with 70% glycerol, and imaged with a fluorescence microscope (Olympus CK40). Fluorescence intensity was analyzed using IMAGE J software (National Institutes of Health).

RNA Extraction and qRT-PCR

Total RNA was extracted and reversely transcribed as in Chapter II. RT primers for miRNAs were used as follows: U6 for EPCs and mice, has-miR-34a and has-miR-21 for EPCs, mmu-miR-34a-3p and mmu-miR-21 for mice, and U18 and cel-miR-34 for *C. elegans*. Human 18S was internal control gene for quantifying mRNA expression. Mouse or *C. elegans* GAPDH was used as internal control gene for quantifying mRNA expression. The following primers were used: 18S (Hs99999901_s1), U6 snRNA (001973), $p16^{INK4a}$ (Hs00923894_m1), has-miR-34a (002316), eNOS (Hs01574659_m1), SIRT1 (Hs01009006_m1), catalase (Hs00156308_m1), PAI-1 (Hs01126606_m1), GAPDH (Mm99999915_g1), eNOS (Mm00435217_m1), SIRT1 (Mm00490758_m1), catalase (Mm00437992_m1), U18 (001764), miR-34 (Ce241995_mat), GAPDH

(Ce02425762_m1), sir-2.1 (Ce02459018_g1), and sod-3 (Ce02404515_g1). Data were analyzed with $2^{-\Delta Ct}$ value calculation using control genes for normalization.

Western Blot

Proteins from cell lysates or tissue lysates were separated by SDS-PAGE and immunoblotted as previously described in Chapter II. Primary antibodies were anti-SIRT1, anti-eNOS, anti-β-actin, and anti-GAPDH. Chemiluminescence was detected by the ECL-plus kit (GE Healthcare).

miRNA Transfection

For miR-34a overexpression, EPCs were transfected with 5 pM of miR- 34a mimic or control miRNA (Fisher Scientific) with Lipofectamine RNAiMAX reagent (Fisher Scientific) for 12 h according to the manufacturer's protocol.

Diabetic Mouse Experiments

All procedures complied with the standards for care and use of animal subjects as stated in the Guide for the Care and Use of Laboratory Animals. The protocol for all animal studies was approved by the Institutional Animal Care and Use Committee at the Medical University of South Carolina. Male wild-type C57/BL6 mice (7–8 weeks of age) were purchased from Harlan. Mice (male, 12-week-old) were fasted for 16 h and subjected to 6-day continuous intraperitoneal injections of streptozotocin (STZ, 60 mg/kg; Sigma) to induce type 1 diabetes. Sodium citrate buffer alone (0.1 M, pH 4.5) was injected in control animals. Mice with blood glucose > 250 mg/dL were considered diabetic and used in this study. A total of 18 mice were randomly assigned to three groups: control group (n = 6), diabetes group (n = 6), and diabetes + kallistatin group (20 mg/kg body weight, n = 6). Mice were injected with kallistatin intraperitoneally every 2

days after verification of diabetes. One week after kallistatin injection, the thoracic aorta was collected for histological analysis or gene expression analysis.

C.elegans Treatments

Wild-type (N2) *C. elegans*, sir-2.1 mutant strain VC199 (ok434), miR-34 mutant strain (gk437), and SOD-3::GFP strain CF1553 (muIs84) were obtained from the Caenorhabditis Genetics Center. *C. elegans* were cultured and maintained at 25°C on nematode growth medium (NGM) seeded with *E. coli* OP50. N2 worms were treated with different concentrations of kallistatin (1 or 5 μM) from L4 stage (adult) for 3 days. Total RNA was extracted for QPCR.

Stress Resistance Assay

For heat-shock assay, age-synchronized N2 L4 worms (n = 30) were pre-incubated with kallistatin (1 or 5 μM), and were cultured with daily exchanged fresh medium plates. Two days later, adult worms were exposed at 35°C for 6 h. The survival of worms was recorded after thermal stress by touching or tapping as monitored under microscope (AmScope). For oxidative stress resistance assay, age-synchronized N2 L4 worms (n = 50) were pre-incubated with or without kallistatin (1 or 5 μM). Next, the three groups were separately transferred to NGM plates containing 2 mM paraquat (Sigma). Survival of the worms was scored daily until the death of last worm.

Statistical Analysis

Data are expressed as means ± SE of three independent experiments. Student t-test and analysis of variants were used to assess differences. Survival curves between treatment groups were compared using the nonparametric log-rank test. A value of $P < 0.05$ was considered statistically significant.

Results

Kallistatin Inhibits TNF-α-Induced Cellular Senescence in EPCs

To identify the effect of kallistatin on cellular senescence in cultured EPCs, we evaluated three senescent markers, including SA-β-gal activity, plasminogen activator inhibitor-1 (PAI-1) synthesis, and telomerase activity. Six days' treatment of TNF-α caused marked increased SA-β-gal positive cell numbers compared with the control group, whereas pre-incubation with purified human kallistatin significantly reduced TNF-α-induced SA-β-gal-positive cells. Kallistatin alone had no effect on EPC senescence (Figure 3-1 A). Quantitative analysis of SA-β-gal staining confirmed these results (Figure 3-1 B). TNF-α increased PAI-1 synthesis, whereas kallistatin significantly suppressed PAI-1 expression with or without TNF-α treatment (Figure 3-1 C). Moreover, kallistatin prevented TNF-α-mediated suppression of telomerase activity in EPCs (Figure 3-1 D). These results indicate that kallistatin is capable of blocking TNF-α-induced EPC senescence.

Kallistatin Inhibits TNF-α-Induced Oxidative Stress, and miR-21 and $p16^{INK4a}$ Synthesis

To further determine kallistatin's effect on senescence-associated oxidative stress in EPCs, fluorescence probe DCFH-DA was used to detect cellular ROS formation. Representative images show that kallistatin inhibited TNF-α-induced accumulation of cellular ROS in EPCs, and kallistatin's effect was abolished by pretreatment with the PI3K inhibitor LY294002 or the NOS inhibitor L-NAME (Figure 3-2 A). Quantitative analysis verified kallistatin's inhibitory effect on ROS formation (Figure 3-2 B). Likewise, kallistatin suppressed TNF-α-induced NADPH oxidase activity, which was again abolished by LY294002 or L-NAME (Figure 3-2 C). Kallistatin alone had no effect on oxidative stress (Figure 3-2 A–C). These results indicate that kallistatin inhibits

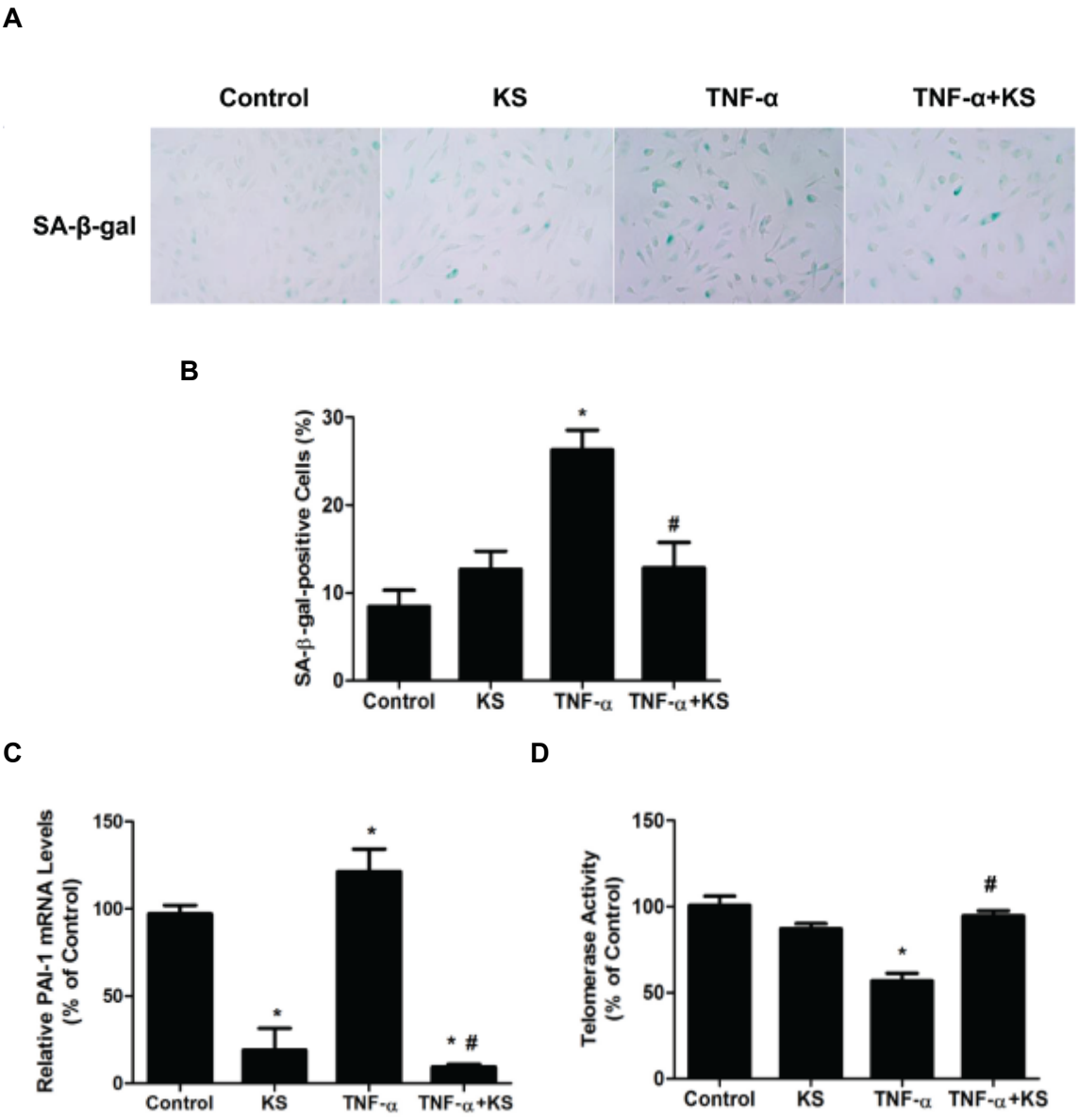

Figure 3-1. Kallistatin (KS) inhibits TNF-α-induced EPC senescence. (A) Representative images of senescence-associated β-gal staining in EPCs. (B) Quantification of positive gal staining cells. (C) QPCR analysis of PAI-1. (D) QPCR detection of telomerase activity. n = 3. $^{*}P < 0.05$ vs. control, $^{\#}P < 0.05$ vs. TNF-α group.

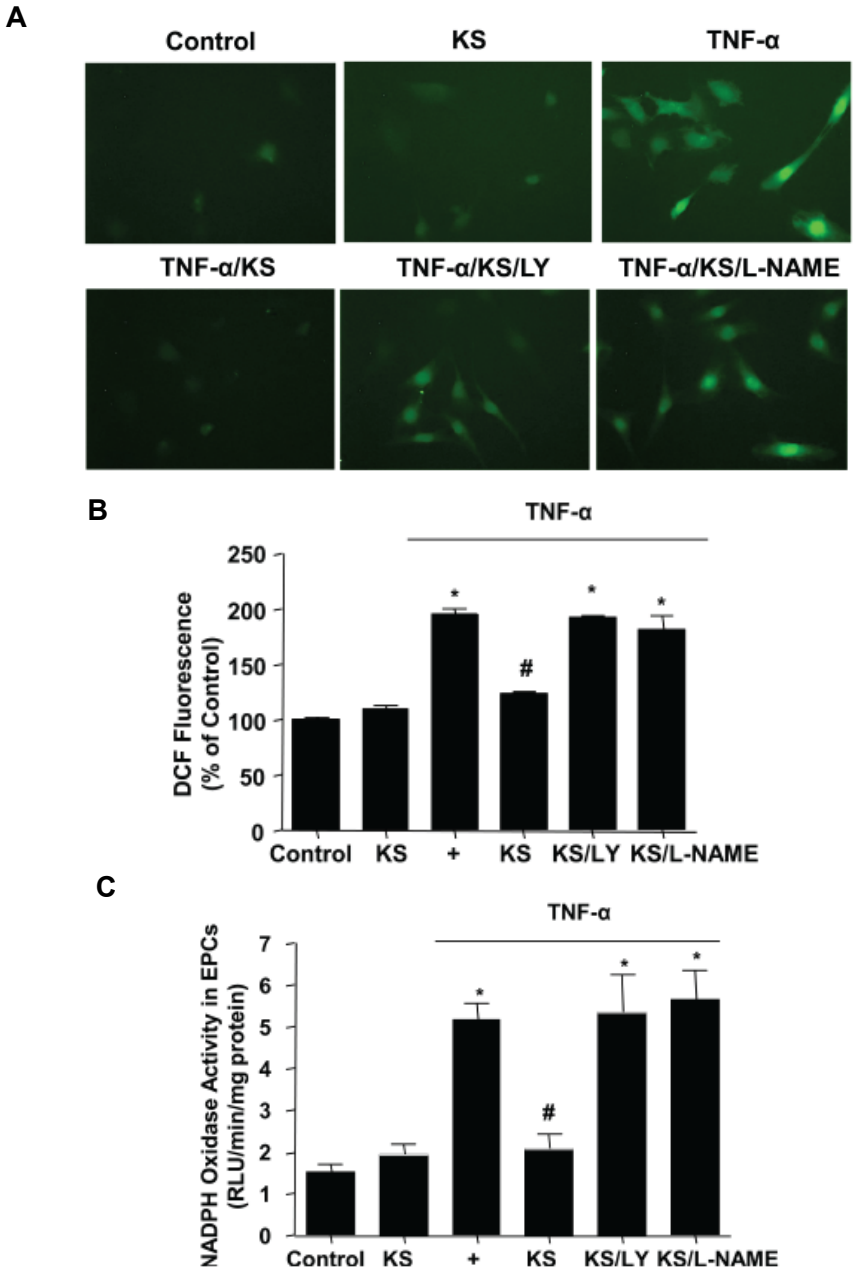

Figure 3-2 A-C. Kallistatin (KS) inhibits TNF-α-induced oxidative stress in EPCs. (A) Representative images of ROS formation using fluorescent probe DCFH-DA. (B) Quantification analysis of ROS production. (C) NADPH oxidase activity determined by lucigenin chemiluminescence assay. n = 3. $^{*}P < 0.05$ vs. control, $^{\#}P < 0.05$ vs. TNF-α group.

TNF-α-induced oxidative stress via activation of the PI3K-Akt-eNOS signaling pathway. Kallistatin also antagonized TNF-α-induced miR-21 synthesis (Figure 3-2 D). Moreover, kallistatin markedly reduced the expression of $p16^{INK4a}$, a cyclin-dependent kinase inhibitor known to be a senescence-associated inducer of cell cycle arrest (Figure 3-2 E). Collectively, these results indicate that kallistatin inhibits TNF-α-induced oxidative stress, and miR-21 and $p16^{INK4a}$ synthesis.

Kallistatin Prevents TNF-α-Mediated Inhibition of SIRT1, eNOS, and Catalase and Stimulates Antioxidant Gene Expression

We next determined the effect of kallistatin on the antioxidant genes of SIRT1, eNOS, and catalase. Kallistatin treatment increased SIRT1 protein levels, as determined by western blot (Figure 3-3 A, top panel). Moreover, kallistatin reversed TNF-α-mediated inhibition of SIRT1, eNOS, and catalase expression (Figure 3-3 A–C). Additionally, kallistatin alone stimulated the synthesis of these antioxidant enzymes (Figure 3-3 A–C). Therefore, kallistatin not only prevented TNF-α-mediated inhibition of eNOS, SIRT1, and catalase, but also increased the expression levels of antioxidant enzymes.

Kallistatin Stimulates Antioxidant Gene Expression through miR-34a Inhibition

As miR-34a is a key senescence mediator, we examined kallistatin's effect on miR-34a. Our results showed that kallistatin markedly inhibited miR-34a synthesis in EPCs (Figure 3-4 A). To further determine the role of miR-34a in kallistatin-mediated stimulation of antioxidant genes, miR-34a was overexpressed by transfection of miR-34a mimic to EPCs. miR-34a overexpression suppressed SIRT1, eNOS, and catalase expression compared to the mimic control group, and also abolished kallistatin's stimulatory effect on these antioxidant genes (Figure 3-4 B–D). Moreover, miR-34a overexpression abolished kallistatin's anti-senescence effect, evidenced by SA-β-gal

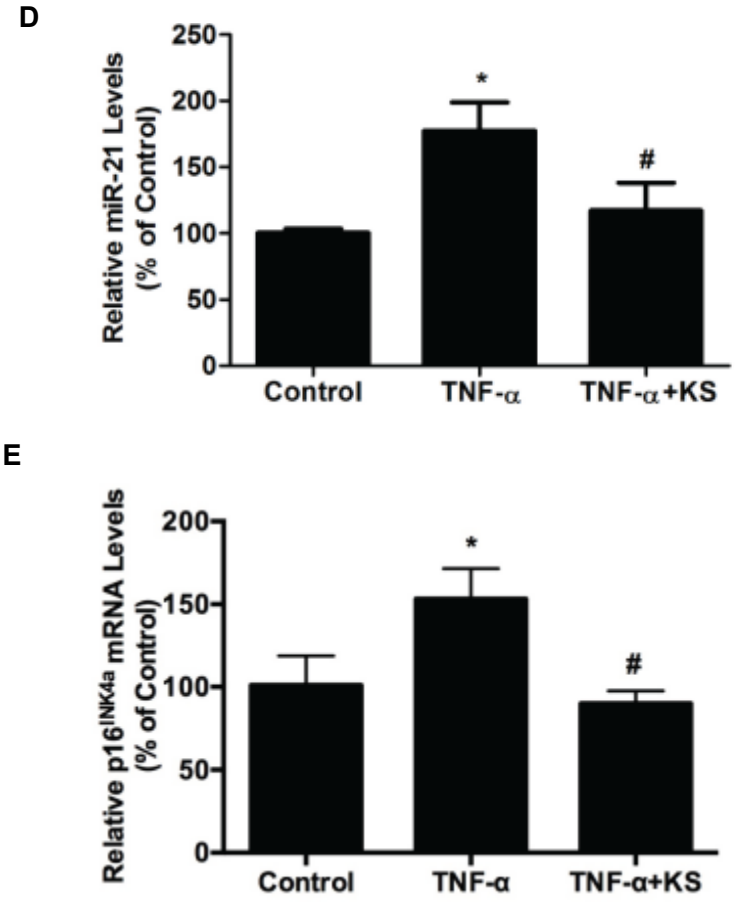

Figure 3-2 D&E. Kallistatin (KS) inhibits TNF-α-induced miR-21 and $p16^{INK4a}$ synthesis in EPCs. QPCR analysis of (D) miR-21 and (E) $p16^{INK4a}$ gene expression. n = 3. $^{*}P < 0.05$ vs. control, $^{\#}P < 0.05$ vs. TNF-α group.

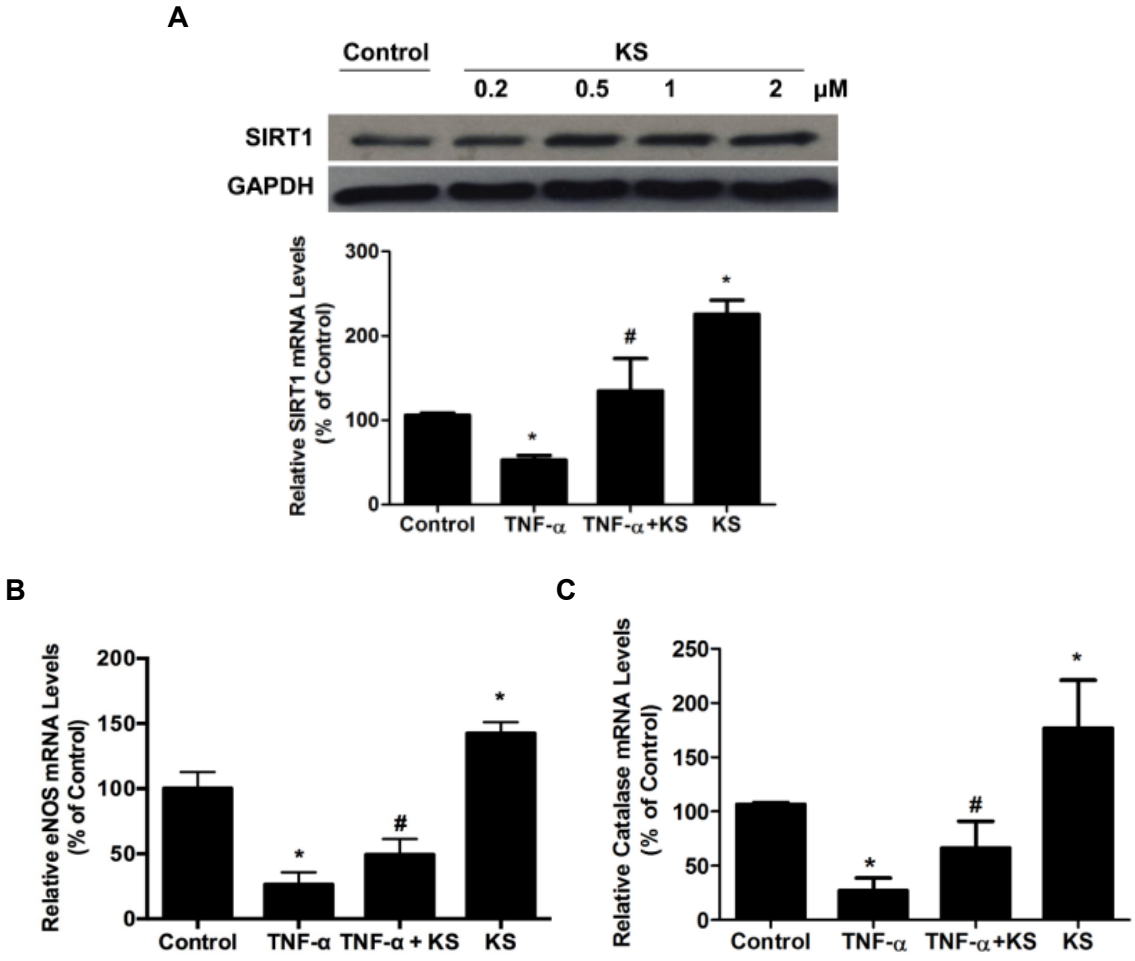

Figure 3-3. Kallistatin (KS) stimulates SIRT1, eNOS, and catalase expression and prevents TNF-α-mediated inhibition of these genes in EPCs. (A) Representative western blot of SIRT1 and QPCR analysis of SIRT1 mRNA levels. (B) QPCR of eNOS mRNA levels. (C) QPCR analysis of catalase mRNA levels. n = 3. *$P < 0.05$ vs. control, $^{\#}P < 0.05$ vs. TNF-α group.

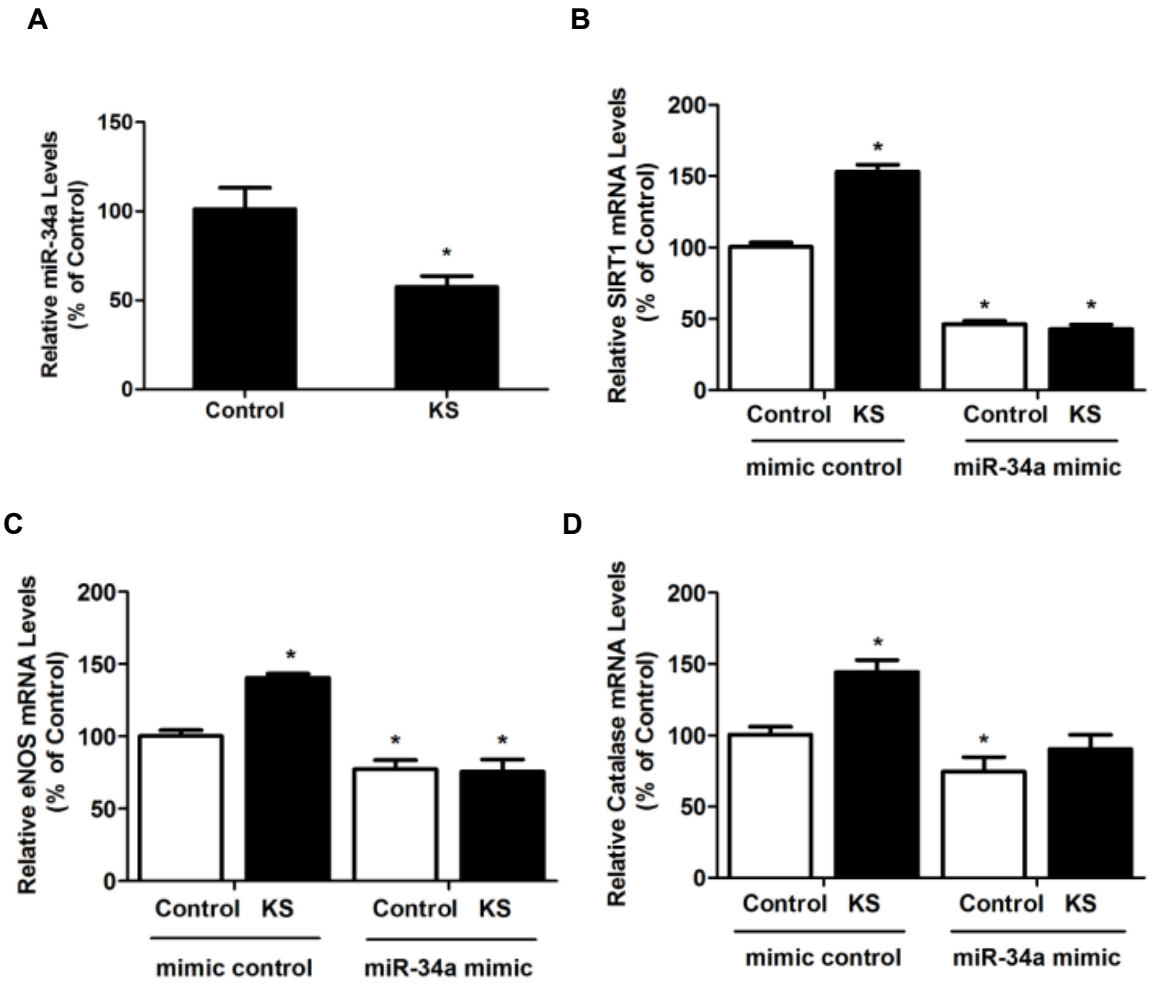

Figure 3-4 A-D. Kallistatin (KS) though inhibiting miR-34a upregulates antioxidant genes SIRT1, eNOS and catalase in EPCs. QPCR analysis of (A) miR-34a in kallistatin treated EPCs. QPCR analysis of (B) SIRT1, (C) eNOS and (D) catalase mRNA levels in mimic control group or miR-34a mimic group. n = 6. *$P < 0.05$ vs. control or mimic control.

staining (Figure 3-4 E). These results indicate that kallistatin, by inhibiting miR-34a synthesis, prevents miR-34a-mediated inhibition of SIRT1 and eNOS expression to alleviate EPC senescence.

Kallistatin's Active site Is Essential for Stimulating Antioxidant Gene Expression: Role of Tyrosine Kinase

To determine which functional domain of kallistatin is essential for the regulation of miR-34a-SIRT1 pathway, three types of kallistatin, including wild-type kallistatin, heparin-binding site mutant kallistatin, and active site mutant kallistatin, were used. We found that both wild-type kallistatin and heparin-binding site mutant kallistatin effectively inhibited miR-34a synthesis and elevated SIRT1 and eNOS mRNA levels in EPCs, but active site mutant kallistatin had no such effects (Figure 3-5 A–C). The results indicate that kallistatin's active site is essential for modulating the expression of miR-34a, SIRT1, and eNOS in EPCs. Moreover, genistein, a tyrosine kinase inhibitor, blocked wild-type kallistatin's effect in modulating miR-34a, SIRT1, and eNOS synthesis (Figure 3-5 A–C), implicating the involvement of a tyrosine kinase. Thus, kallistatin's active site is critical for downregulation of miR-34a and upregulation of SIRT1 and eNOS.

Kallistatin Attenuates Aortic Senescence, Superoxide Formation Associated with Decreased miR-34a and miR-21 Synthesis and Increased SIRT1, eNOS, and Catalase Levels in Diabetic Mice

We further determined kallistatin's *in vivo* effect on vascular senescence and oxidative stress in aortas of STZ-induced diabetic mice. Aortic senescence, identified by SA-β-gal staining, was increased in diabetic mice compared to control mice, while kallistatin treatment prevented STZ-induced effect (Figure 3-6 A). Moreover, higher levels of superoxide formation and NADPH oxidase activity were observed in the aortas

E

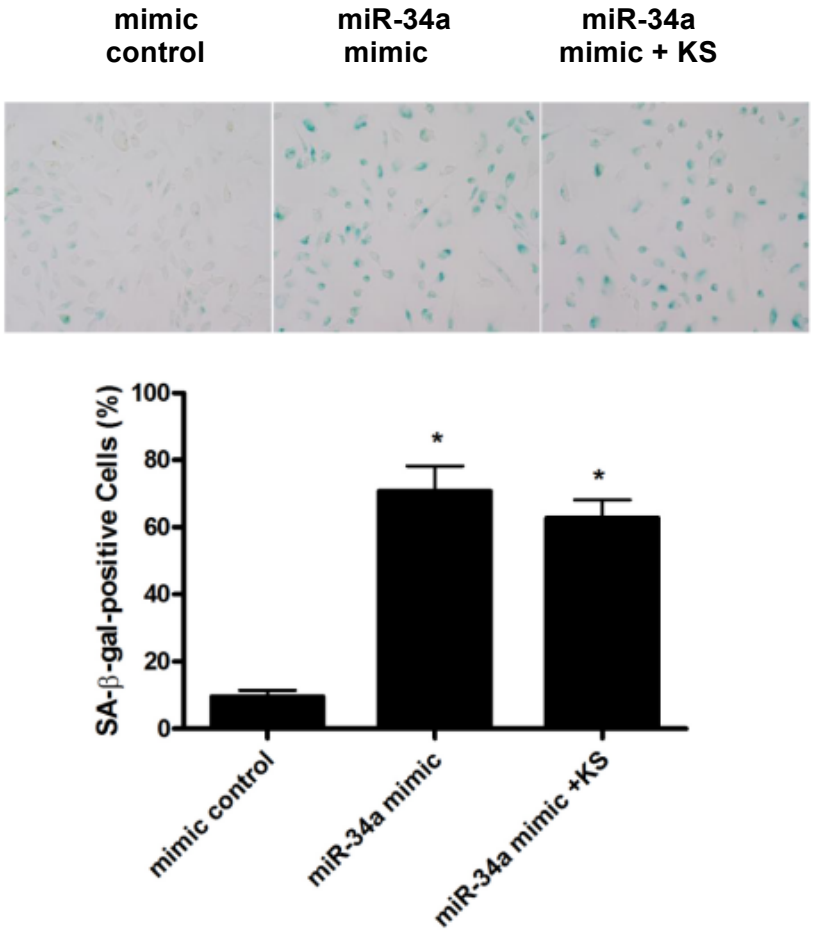

Figure 3-4 E. miR-34a mimic abolishes the anti-senescent effect of kallistatin (KS) in EPCs. (E) Representative images of positive SA-β-gal staining in mimic control and miR-34a-overexpressing EPCs, and quantification analysis is shown. n = 6. **P* < 0.05 vs. mimic control.

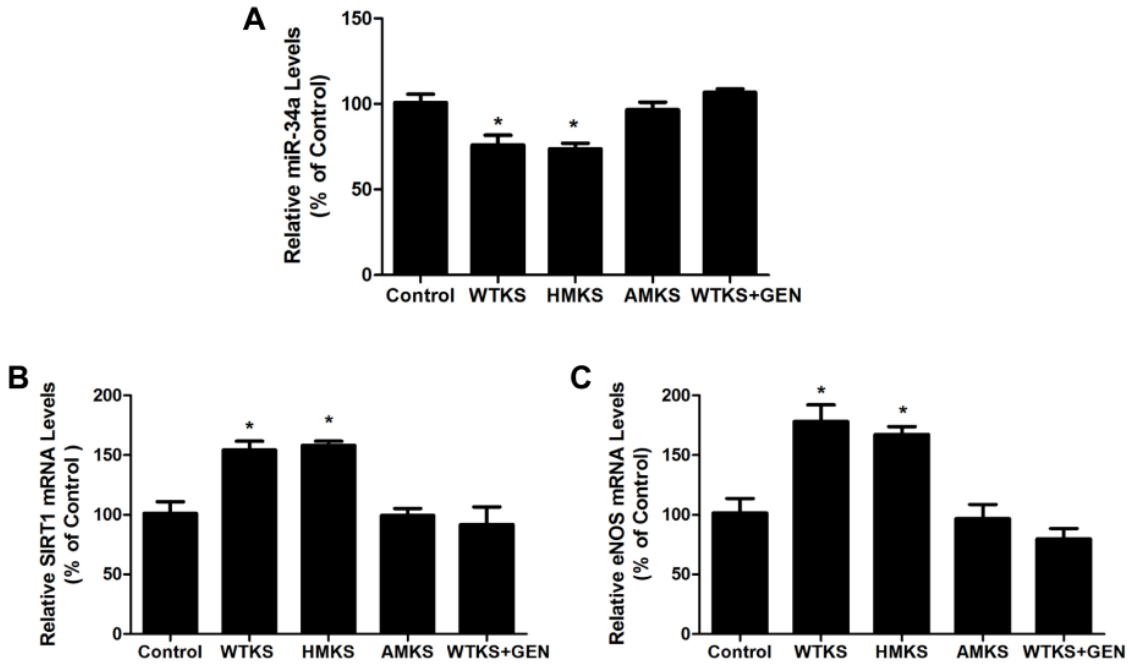

Figure 3-5. The active site of kallistatin is essential for modulating miR-34a, eNOS, and SIRT1 synthesis through interacting with a tyrosine kinase in EPCs. QPCR analysis of (A) miR-34a, (B) SIRT1 and (C) eNOS. GEN: genistein, a tyrosine kinase inhibitor. WTKS: wild-type kallistatin; HMKS: heparin-binding site mutant kallistatin; AMKS: active site mutant kallistatin. n = 3. *P < 0.05 vs. control.

of STZ-induced diabetic mice, but this observation was reversed by kallistatin administration (Figure 3-6 B&C). Furthermore, STZ induced a significant increase of miR-34a and miR-21 synthesis, as well as reduced SIRT1, eNOS, and catalase mRNA levels in aortas of diabetic mice compared to control mice, while kallistatin administration reversed STZ-mediated effect (Figure 3-6 D–H). Consistently, aortic SIRT1 and eNOS protein levels were markedly reduced in diabetic mice compared to control mice, but were restored by kallistatin administration, as determined by western blot (Figure 3-6 I&J). Consistent with the results derived from cultured EPCs, kallistatin treatment protects against vascular aging and oxidative stress in diabetic mice by decreasing miR-34a and miR-21 synthesis and increasing SIRT1, eNOS, and catalase levels.

Kallistatin Enhances Wild-type *C. elegans* Lifespan under Oxidative or Heat Stress Independent of the Presence of miR-34 and sir-2.1

As stress conditions impair *C. elegans* longevity and induce premature senescence, we investigated the effect of kallistatin on *C. elegans* survival under oxidative or thermal stress. Paraquat was used to induce oxidative damage in three strains of *C. elegans*, including wild-type (N2), miR-34 mutant, and sir-2.1 (SIRT1 analogue) mutant worms. Representative images showed that kallistatin (1 or 5 μM) markedly reduced paraquatinduced superoxide formation in *C. elegans*, as identified by red fluorescence probe DHE, and the result was confirmed by quantitative analysis (Figure 3-7 A). Moreover, the mean lifespan of wild-type *C. elegans* was 13.3 ± 0.9 days under normal condition at 25°C, but was shortened to 7.7 ± 0.3 days under paraquat-induced oxidative stress. Pretreatment with 1 or 5 μM kallistatin reduced the sensitivity to paraquat and increased mean lifespan of *C. elegans* by 5.8% or 20.5% (8.2 ± 0.3 or 9.3 ± 0.4 days), respectively (Figure 3-7 B). However, kallistatin treatment had no effect on the lifespan of miR-34 or sir-2.1 mutant worms under oxidative stress (Figure 3-7 C&D).

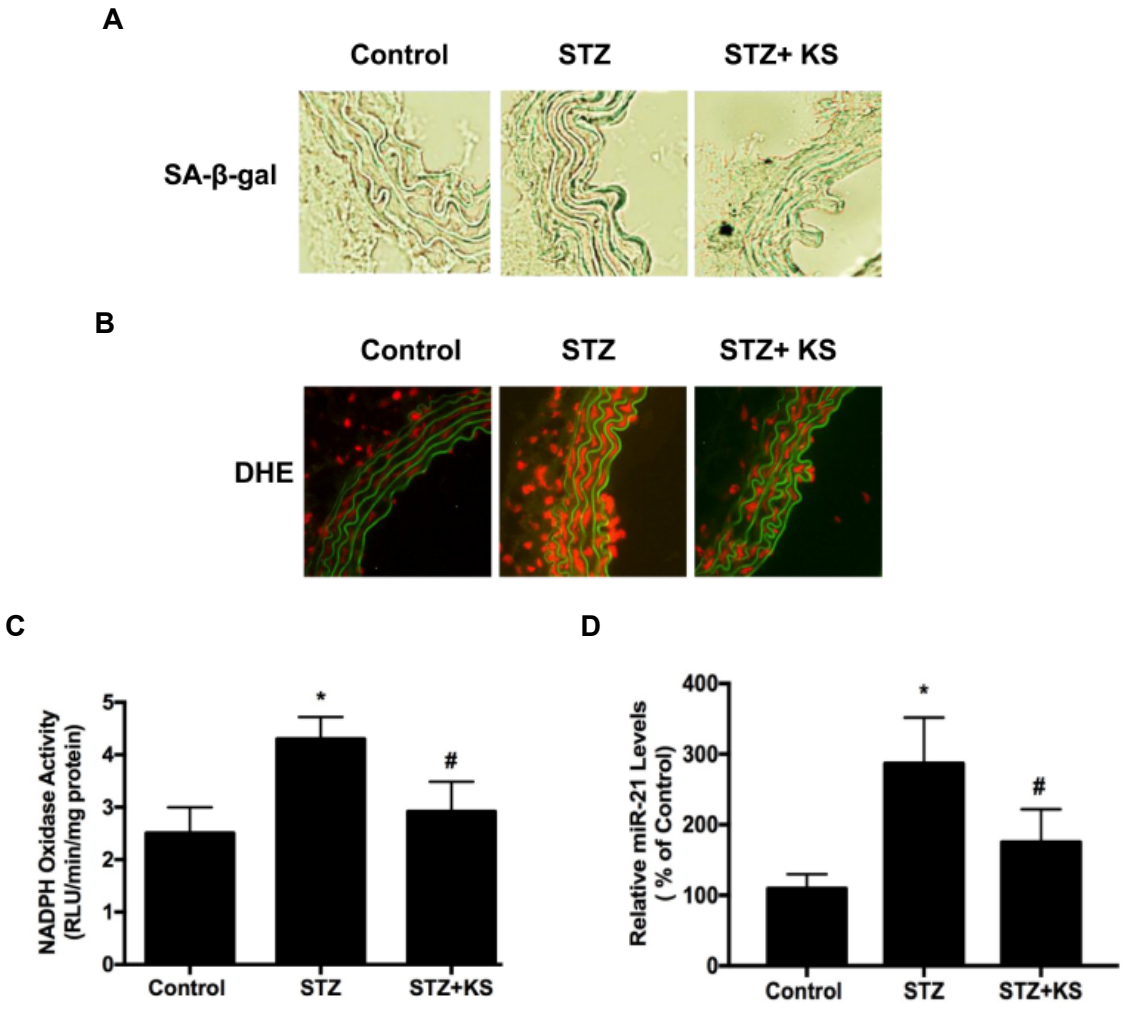

Figure 3-6 A-D. Kallistatin (KS) attenuates vascular aging, superoxide production, and miR-21 synthesis in aortas of diabetic mice. (A) Representative images of SA-β-gal staining in thoracic aortas from control mice, STZ-induced diabetic mice, and KS-treated diabetic mice. (B) Representative images of superoxide formation labeled by red fluorescence dye hydroethidine (DHE). (C) NADPH oxidase activity measured by lucigenin chemiluminescence assay in mouse aortas. (D) QPCR analysis of miR-21 in mouse aorta. STZ: streptozotocin. n=6. $^{*}P < 0.05$ vs. control group; $^{\#}P < 0.05$ vs. STZ group.

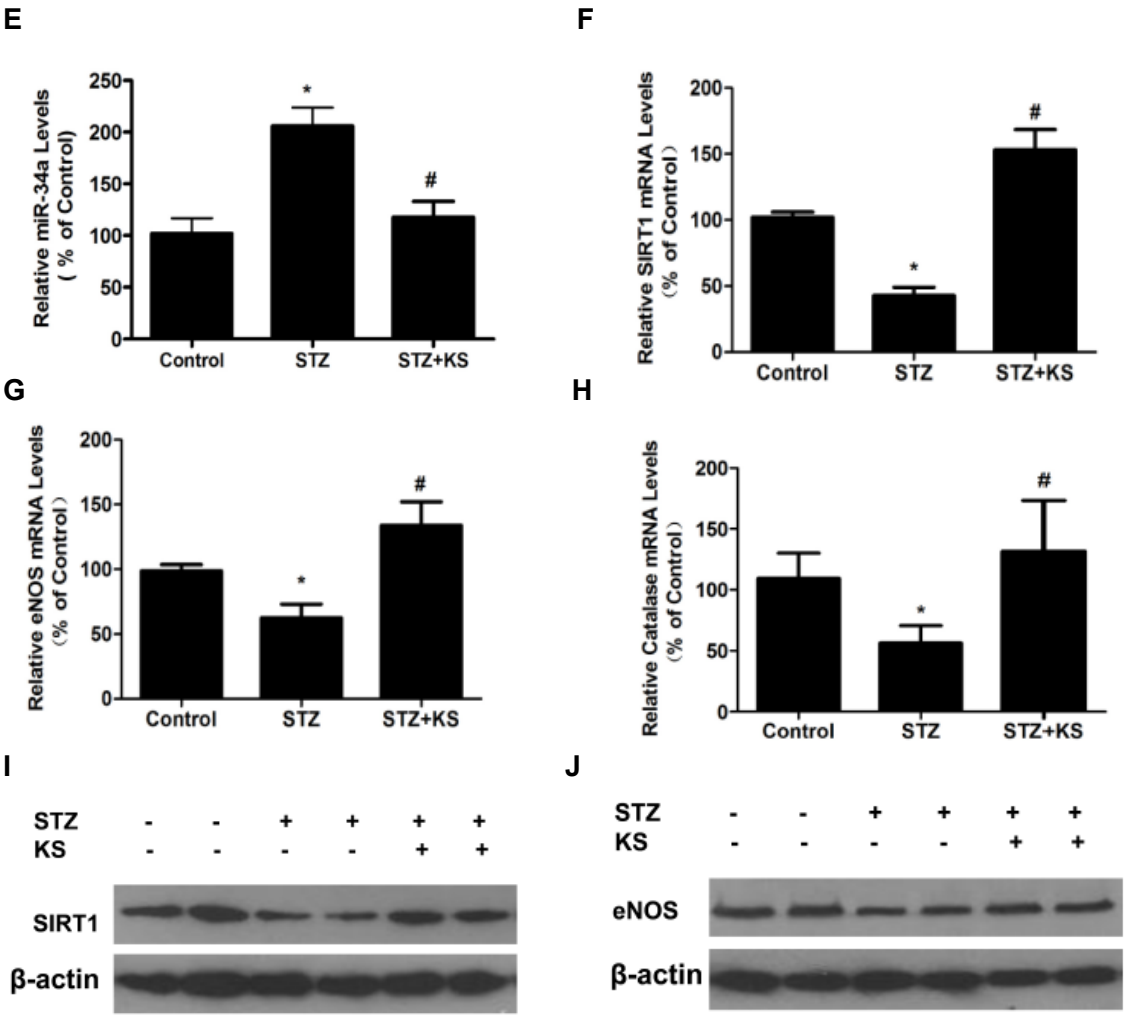

Figure 3-6 E-J. Kallistatin (KS) inhibits miR-34a synthesis and stimulates antioxidant gene expression in the aorta of diabetic mice. QPCR analysis of (E) miR-34a, (F) SIRT1, (G) eNOS and (H) catalase in mouse aorta. Representative western blots of (I) SIRT1 and (J) eNOS in mouse aorta. STZ: streptozotocin. n=6. *P < 0.05 vs. control group; $^{\#}P$ < 0.05 vs. STZ group.

A

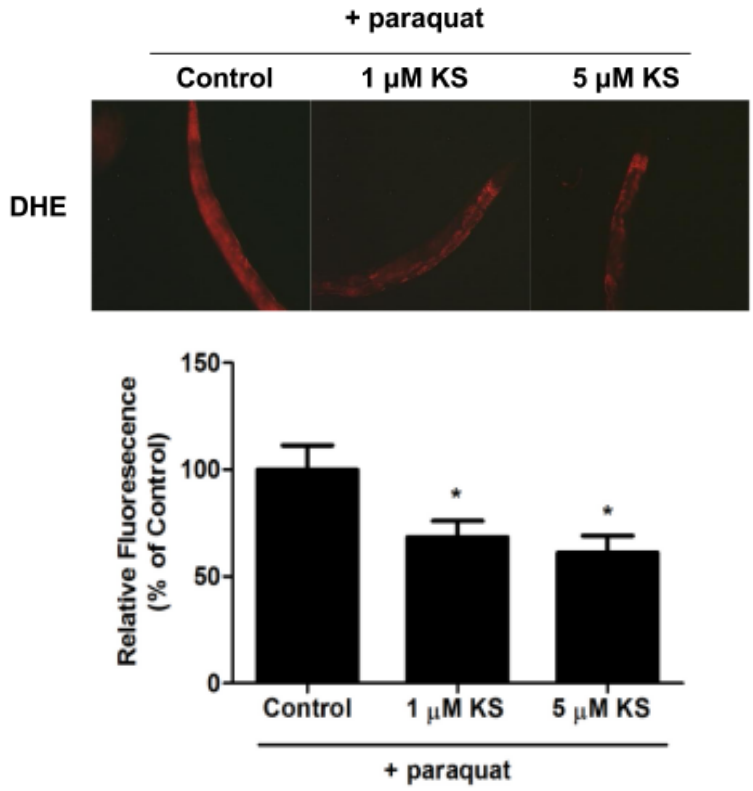

Figure 3-7 A. Kallistatin (KS) inhibits paraquat-induced superoxide formation in *C. elegans*. (A) Representative images of superoxide formation in wild-type *C. elegans*. n=10 worms per group. **P* < 0.05 vs. control.

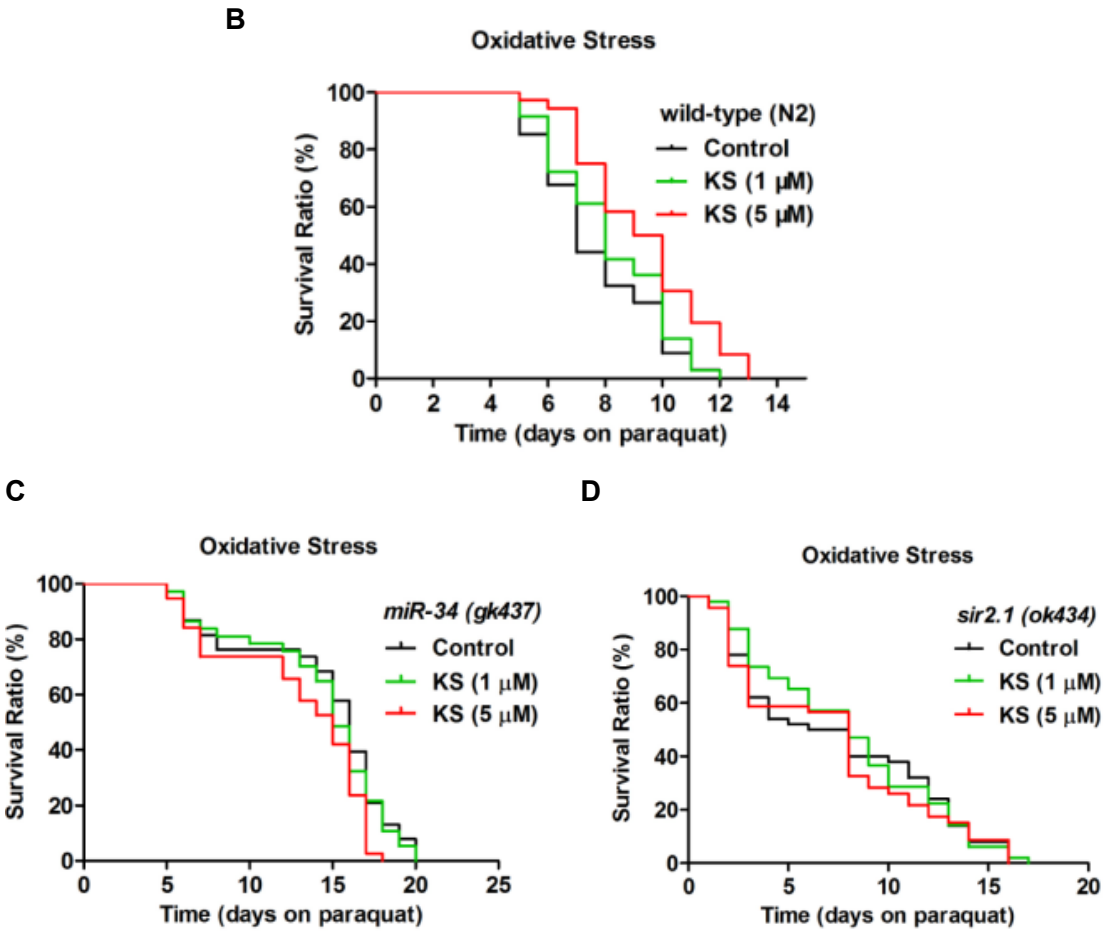

Figure 3-7 B-D. Kallistatin (KS) enhances *C. elegans* longevity under oxidative stress. Survival curves of (B) wild-type (N2) strain, (C) miR-34 mutant (gk437) and (D) sir-2.1 mutant (ok434). n=50 worms per group.

The results indicate that miR-34 and sir-2.1 are essential for kallistatin-mediated *C. elegans* longevity under oxidative stress. Kallistatin significantly increased *C. elegans* thermo-tolerance at 35 °C. Wild-type worm survival rate was 38.9 ± 3.9% under thermal condition, but kallistatin treatment at 1 and 5 lM markedly enhanced worm survival to 63.3 ± 4.4% and 72.1 ± 10.5%, respectively (Figure 3-7 E). However, kallistatin (1 or 5 μM) had no effect on the survival of miR-34 mutant or sir-2.1 mutant worms at 35 °C (Figure 3-7 F&G). Similar to oxidative stress, these results confirm that kallistatin promotes *C. elegans* survival under heat stress via regulating miR-34 and sir-2.1. Moreover, kallistatin treatment inhibited miR-34, but increased sir-2.1 and sod-3 (MnSOD analogue) synthesis (Figure 3-7 H–J). Likewise, SOD-3 protein levels were elevated by kallistatin treatment, as evidenced using SOD-3::GFP co-expression *C. elegans* as a sod-3 indicator (Figure 3-7 K). Collectively, kallistatin inhibits miR-34 synthesis and stimulates sir-2.1 and sod-3 levels in *C. elegans*, and the regulatory mechanisms parallel those observed in cultured EPCs and in aortas of diabetic mice.

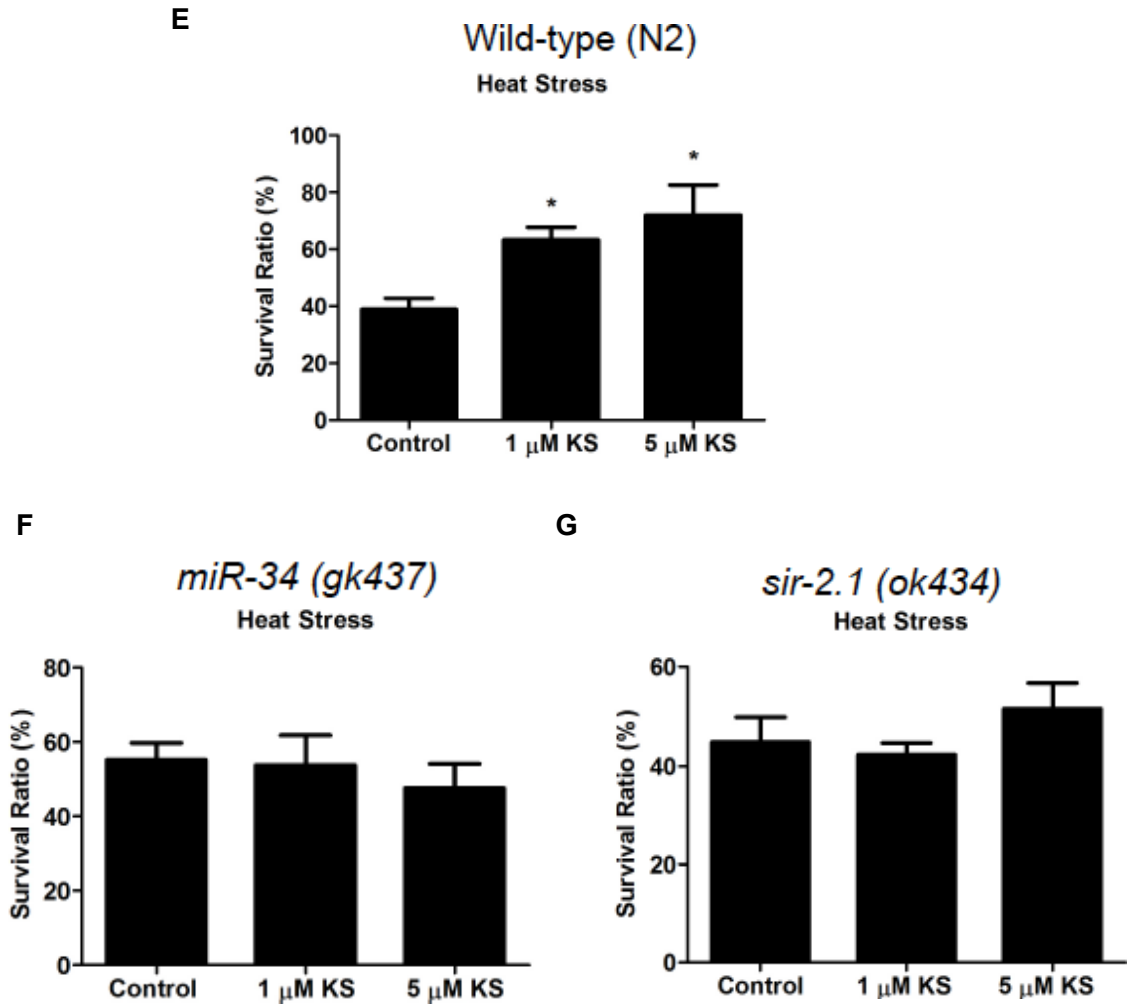

Figure 3-7 E-G. Kallistatin (KS) enhances *C. elegans* survival under heat stress. Average survival ratios of (E) wild-type (N2), (F) miR-34a mutant (gk437) and (G) sir-2.1 mutant (ok434). n=30 worms per group. *$P < 0.05$ vs. control.

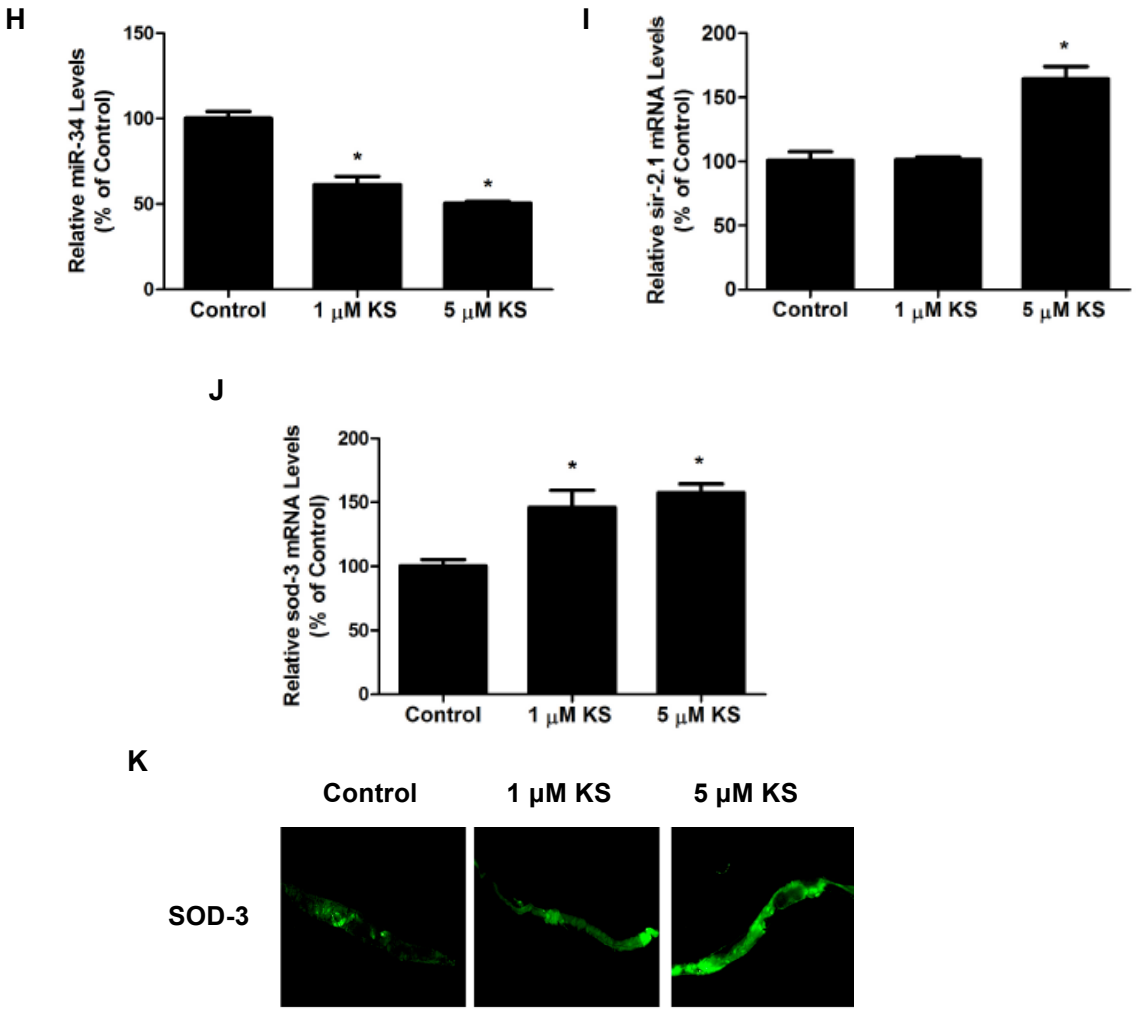

Figure 3-7 H-K. Kallistatin inhibits miR-34 but stimulates sir-2.1 and sod-3 expression in *C. elegans*. QPCR analysis of (H) miR-34, (I) sir-2.1, (J) sod-3 mRNA levels. (K) Representative images of SOD3 expression in SOD-3::GFP *C. elegans.* n=100 worms per group. **P* < 0.05 vs. control.

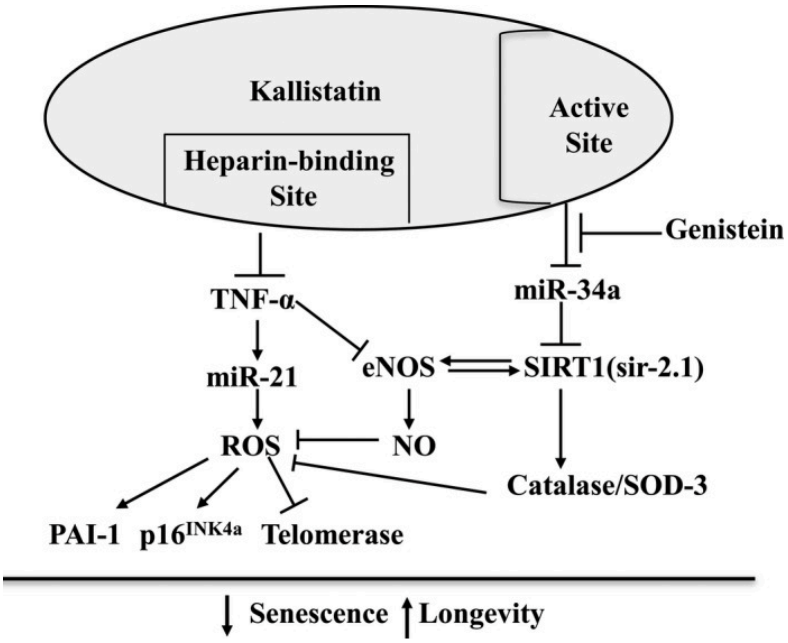

Figure 3-8. Signaling mechanism by which kallistatin inhibits vascular senescence and aging. Kallistatin via its heparin-binding site antagonizes TNF-α mediated miR-21 synthesis, ROS formation, PAI-1 and $p16^{INK4a}$ expression, and telomerase activity in EPCs. Kallistatin via its active site prevents miR-34a-mediated inhibition of antioxidant genes SIRT1, eNOS, and catalase and SOD-3. The tyrosine kinase inhibitor, genistein, blocks kallistatin's ability to modulate miR-34a and antioxidant gene expression.

Discussion

This study demonstrates a novel role of kallistatin in vascular senescence and aging using cultured EPCs, STZ-induced diabetic mice, and *C. elegans*. Recombinant human kallistatin treatment significantly reduced EPC senescence by blocking TNF-α-induced oxidative stress, and decreased the senescence markers, PAI-1, miR-21, and $p16^{INK4a}$, but increased telomerase activity. Kallistatin via its active site inhibited miR-34a and stimulated SIRT1, eNOS, and catalase synthesis, whereas overexpression of miR-34a abolished kallistatin's effects on these antioxidant enzymes and anti-senescence action. Moreover, kallistatin suppressed miR-34a and stimulated SIRT1 and eNOS expression, through interaction with cell surface tyrosine kinase in EPCs. Likewise, kallistatin administration in STZ-induced diabetic mice alleviated aortic senescence and oxidative stress associated with reduced miR-34a and miR-21 synthesis and increased SIRT1, eNOS, and catalase levels. Moreover, kallistatin prolonged wild-type *C. elegans* lifespan under heat or oxidative stress conditions by inhibiting miR-34, and stimulating sir-2.1 (SIRT1). These *in vitro* and *in vivo* studies support the view that kallistatin protects against vascular senescence and aging by preventing miR-34a-mediated inhibition of SIRT1 and eNOS, thus inhibiting oxidative stress. The signaling mechanisms of kallistatin's anti-senescence actions are depicted in Figure 3-8.

Oxidative stress is the leading cause of endothelial dysfunction and senescence. The inflammatory factor TNF-α has the ability to potentiate ROS generation by activating NADPH oxidase on the endothelial cell surface (Yoshida & Tsunawaki, 2008). Conversely, eNOS reduces intracellular superoxide levels through NO formation, which inhibits NADPH oxidase activity (Fujii *et al*., 1997). In this study, we demonstrated that kallistatin inhibited TNF-α-induced oxidative stress via activation of the PI3K-Akt-eNOS

signaling pathway, as kallistatin's effect was blocked by LY294002 and L-NAME. Likewise, our previous report showed that kallistatin antagonized TNF-α-mediated apoptosis through increased Akt-eNOS phosphorylation in endothelial cells (Shen *et al*., 2010). Kallistatin also promoted the proliferation and migration of EPCs via activation of Akt-eNOS signaling pathway (Gao *et al*., 2014). Thus, it is likely that kallistatin antagonizes TNF-α-induced senescence by activation of Akt and eNOS phosphorylation in EPCs. In addition, miR-21 modulates ROS production in several cell types (Zhang *et al.*, 2012, Jiang *et al.*, 2014), and kallistatin inhibited TGF-β induced miR-21 synthesis and oxidative stress in endothelial cells (Guo *et al.*, 2015). Our current data showed that kallistatin also blocked TNF-α-mediated miR-21 expression and ROS production in EPCs. Kallistatin's vasoprotective effect has been shown in animal models of salt-induced hypertension, renal injury, and chronic myocardial infarction through inhibiting oxidative stress (Gao *et al.*, 2008; Shen *et al.*, 2008, 2010). Consistently, our current study showed that kallistatin attenuated vascular aging and oxidative stress in conjunction with increased antioxidant protein levels in the aortas of STZ-induced diabetic mice. Collectively, these studies indicate that kallistatin, via inhibiting oxidative stress, protects against vascular senescence.

The longevity factor SIRT1 is a NAD+-dependent histone deacetylase, and high levels of SIRT1 were shown to inhibit oxidative stress and DNA damage (Alcendor *et al.*, 2007). SIRT1 activates antioxidant enzymes, including catalase and MnSOD, by stimulating the FOXO transcription factors (Brunet *et al.*, 2004). Through a positive feedback loop, SIRT1 activates eNOS, which in turn activates SIRT1 (Ota *et al.*, 2010). Importantly, SIRT1 is highly expressed during angiogenesis in endothelial cells, and disrupting SIRT1 abrogates vascular endothelial homeostasis and remodeling (Potente *et al.*, 2007). Our results indicate that kallistatin treatment stimulated the expression of

SIRT1 and its downstream antioxidant enzymes eNOS and catalase, as well as antagonized TNF-α-mediated inhibition of SIRT1, eNOS, and catalase synthesis in cultured EPCs. Similarly, kallistatin elevated the levels of these antioxidant enzymes in the aortas of STZ-induced diabetic mice. In *C. elegans*, SIRT1 homolog sir-2.1 and MnSOD homolog sod-3 were also increased upon kallistatin treatment, whereas sir-2.1 mutant abolished kallistatin mediated stress resistance. Collectively, these combined results reveal a critical role of SIRT1 in mediating kallistatin's effect on oxidative stress and vascular aging.

The role of miR-34a in regulating cell senescence, differentiation, and vitality has been extensively highlighted in a wide variety of cells (Tazawa *et al.*, 2007, Zhao *et al.*, 2010). miR-34a triggers senescence partly through genetic inhibition of SIRT1 in EPCs (Zhao *et al*., 2010). This observation inspired us to explore the potential role of kallistatin in modulating miR-34a-dependent SIRT1 expression in EPCs. Our results showed that kallistatin significantly suppressed miR-34a synthesis, but stimulated eNOS, SIRT1, and catalase expression in EPCs and aortas of diabetic mice. Intriguingly, overexpression of miR-34a by transfection of miR-34a mimic abolished kallistatin-induced antioxidant gene expression. Moreover, miR-34a mimic markedly induced EPC senescence; however, kallistatin had no effect on miR-34a-induced EPC senescence. These findings indicate that kallistatin's anti-senescent effect is mediated by suppressing miR-34a synthesis in EPCs. Furthermore, genistein, a tyrosine kinase inhibitor, blocked kallistatin's effects on the expression of miR-34a, eNOS, and SIRT1, which is partially in consistent with our previous findings in human endothelial cells (Guo *et al*., 2015). The results reveal that kallistatin, through interacting with tyrosine kinase, downregulates miR-34a leading to vascular senescence attenuation.

Kallistatin via its two structural elements regulates differential signaling pathways (Chao *et al*., 2016). Kallistatin via its heparin-binding site antagonized TNF-α-induced NF-κB activation and thus inflammatory gene expression (Yin *et al*., 2010). Our current finding indicates that kallistatin also antagonized TNF-α-induced senescence and oxidative stress in EPCs. Kallistatin blocks TNF-α-induced endothelial senescence mediators, miR-21 and $p16^{INK4a}$. Likewise, kallistatin markedly downregulated TNF-α-induced expression of PAI-1, a pro-atherogenic factor and an endothelial aging marker. Furthermore, kallistatin reversed TNF-α-mediated inhibition of telomerase, which is responsible for maintaining telomere length and cellular integrity. Consistently, our recent report showed that circulatory kallistatin levels are positively associated with leukocyte telomere length in humans (Zhu *et al*., 2016), indicating a potential role of kallistatin in maintaining telomere length. Therefore, kallistatin via its heparin-binding site blocks TNF-α-mediated effects in EPCs. Meanwhile, kallistatin's active site is essential for stimulating eNOS and SIRT1 in endothelial cells (Guo *et al*., 2015). In this study, we showed that kallistatin through its active site inhibited miR-34a synthesis and stimulated eNOS and SITR1 expression in EPCs. Therefore, kallistatin, through its two functional domains, displays anti-senescence actions by blocking TNF-α-induced effects, and preventing miR-34amediated inhibition of SIRT1 and eNOS.

The STZ-induced diabetic mouse is a popular model for studying vascular injury and aging. Kallistatin levels are markedly reduced in vitreous fluids of patients with diabetic retinopathy and in the retinas in STZ-induced diabetic rats (Ma *et al.*, 1996, Hatcher *et al.*, 1997). Decreased kallistatin levels are also observed in the kidney of STZ-induced diabetic mice and in TNF-α-induced senescent human EPCs. Moreover, endogenous kallistatin plays a protective role in multi-organ function, as depletion of kallistatin by neutralizing antibody injection augmented cardiovascular and renal

damage, and increased oxidative stress, inflammation, and endothelial cell loss in hypertensive rats (Liu *et al*., 2012). Furthermore, kallistatin treatment exerts renoprotective effects in diabetic nephropathy by suppressing ROS and inflammatory gene expression in mice (Yiu *et al*., 2016). Accumulating evidence indicates that kallistatin acts as a potent antioxidant and anti-inflammatory agent in cultured cells and animal models (Gao *et al*., 2008; Shen *et al*., 2010; Yin *et al*., 2010; Li *et a*l., 2014; Guo *et al*., 2015). As oxidative endothelial injury and aging are observed in diabetes, kallistatin may have a role in protection against vascular damage in diabetic disease. Indeed, our current study showed that kallistatin treatment in STZ-induced diabetic mice attenuated aortic senescence and superoxide formation, in association with reduced miR-34a and miR-21, and increased SIRT1, eNOS, and catalase synthesis. The findings in diabetic mice support the concept that kallistatin plays a protective role in vascular injury and aging by regulating miR-34a, SIRT1, and eNOS synthesis.

C. elegans is a prominent model for aging study, as pathways mediating longevity and metabolism are conserved from *C. elegans* to mammals. Heat or oxidative stress induces elevated levels of ROS and cellular damage in *C. elegans*, leading to accelerated aging (Rodriguez *et al.*, 2013). In this study, we demonstrated that kallistatin treatment improved *C. elegans* lifespan or survival under oxidative stress or heat conditions. Previous studies showed that miR-34 loss-offunction mutation or sir-2.1 (SIRT1 homolog) overexpression in *C. elegans* markedly delayed the age-related physiological decline and prolonged lifespan in response to stress conditions (Tissenbaum & Guarente, 2001, Yang *et al.*, 2013). Herein, we showed that kallistatin treatment inhibited miR-34 and stimulated sir-2.1 and sod-3 synthesis in wild-type *C. elegans*. Kallistatin's protective effect in the longevity of wild-type *C. elegans* was abolished in miR-34 or sir-2.1 mutant *C. elegans* under stress conditions. Consistent

with the findings in EPCs and diabetic mice, these results further verify that kallistatin's anti-aging effect is dependent on miR-34 inhibition and sir-2.1 (SIRT1) activation. Collectively, these findings provide significant insights regarding the mechanism of kallistatin in regulating the aging process via miR-34a-SIRT1 pathway.

In conclusion, this is the first study to demonstrate the protective role of kallistatin in vascular senescence and aging. Kallistatin's anti-aging effect is mainly attributed to suppression of oxidative stress by preventing miR-34a-mediated inhibition of antioxidant gene expression. This study established an essential role of kallistatin's active site in the regulation of miR-34a, SIRT1, and eNOS synthesis by interaction with a tyrosine kinase. As kallistatin is an endogenous protein, minimal side effects are expected with kallistatin treatment. Therefore, this study opens a new prospective in kallistatin-based therapeutic intervention in age-associated cardiovascular diseases.

CHAPTER IV

TO DETERMINE THE ROLE OF ENDOGENOUS KALLISTATIN IN ENDOTHELIAL SENESCENCE, VASCULAR AND ORGAN INJURY

Summary

This study is aimed to further investigate the role and mechanism of endogenous kallistatin in endothelial senescence, vascular and organ injury. Kallistatin treatment inhibited H_2O_2-induced senescence in human endothelial cells, as indicated by reduced senescence-associated-β-galactosidase activity, $p16^{INK4a}$ and plasminogen activator inhibitor-1 expression, and elevated telomerase activity. Kallistatin blocked H_2O_2-induced superoxide formation, NADPH oxidase levels, and VCAM-1, ICAM-1, IL-6, and miR-34a synthesis. Kallistatin reversed H_2O_2-mediated inhibition of eNOS, SIRT1, catalase and superoxide dismutase (SOD)-2 expression, and directly stimulated these genes. Moreover, kallistatin's anti-senescence and antioxidant effects were attributed to SIRT1-mediated eNOS pathway. Kallistatin, via interaction with tyrosine kinase, upregulated Let-7g, whereas Let-7g inhibitor abolished kallistatin's effects on miR-34a and SIRT1/eNOS synthesis, leading to inhibition of senescence, oxidative stress and inflammation. Furthermore, lung endothelial cells isolated from endothelium-specific kallistatin knockout mice displayed marked reduction of mouse kallistatin expression. Kallistatin deficiency in mouse endothelial cells exacerbated senescence, oxidative stress and inflammation compared to wild-type mouse endothelial cells, and H_2O_2 treatment further magnified these effects. Kallistatin deficiency caused marked reduction of Let-7g, SIRT1, eNOS, catalase and SOD-1 mRNA levels, and elevated miR-34a synthesis in mouse endothelial cells. Moreover, systemic depletion of kallistatin resulted in worsened aortic oxidative stress and renal injury and fibrosis in general kallistatin knockout mice with diabetes. These findings indicate that endogenous kallistatin protects against endothelial senescence, vascular and organ injury and kallistatin treatment reduces endothelial senescence by modulating Let-7g-mediated miR-34a-SIRT1-eNOS pathway.

Introduction

Endothelial senescence contributes to the onset and development of vascular injury and age-associated vascular diseases, such as atherosclerosis, diabetes, and coronary artery diseases (Minamino *et al.*, 2004, Minamino & Komuro, 2007). Vascular senescence gives rise to the alteration of morphological features and functional physiology in blood vessels (Cavallaro *et al.*, 2000). The key features of senescent cells are: permanent growth arrest state, flattened morphology, elevation of SA-β-gal activity, cell cycle inhibitor $p16^{INK4a}$ expression, and endothelial dysfunction marker plasminogen activator inhibitor-1 (PAI-1) expression. Moreover, cellular senescence is characterized by shortened telomere length or reduced telomerase activity (Hornsby, 2007). Oxidative stress and inflammation have been implicated in the aging process and adversely affect endothelial availability and function (Freund *et al.*, 2010, Bhayadia *et al.*, 2016). Oxidative stress compromises telomere integrity and nitric oxide (NO) bioavailability to accelerate cellular senescence in endothelial cells (Kurz *et al.*, 2004). Vascular senescence is also associated with enhanced expression of the inflammatory molecules, vascular cell adhesion molecule-1 (VCAM-1) and intercellular adhesion molecule-1 (ICAM-1), which leads to augmented adhesion of monocytes into vascular wall, facilitating the ignition and progression of aging-associated vascular diseases (Gorgoulis *et al.*, 2005, Powter *et al.*, 2015). Therefore, inhibition of oxidative stress and inflammation is of great significance for controlling endothelial senescence.

miRNAs are essential regulators for a plethora of cellular processes. A highly evolutionarily conserved miRNA Let-7g has been reported to inhibit oxLDL-induced apoptosis of endothelial cells and alleviate atherosclerosis in mice (Zhang *et al.*, 2013, Liu *et al.*, 2017). Let-7g also has the ability to improve multiple endothelial functions by stimulating SIRT1 signaling (Liao *et al.*, 2014). Furthermore, miR-34a, a well-recognized

tumor suppressor and a senescent inducer, triggers endothelial senescence by directly suppressing the target gene SIRT1 (Ito *et al.*, 2010). SIRT1, an NAD+-dependent deacetylase and anti-aging molecule, is decreased in vascular tissue undergoing senescence. Evidence has indicated a positive feedback regulation between SIRT1 and eNOS. SIRT1 promotes the expression of eNOS and activates eNOS by its deacetylase activity, while eNOS through NO production stimulates SIRT1 expression (Mattagajasingh *et al.*, 2007, Potente & Dimmeler, 2008, Xia *et al.*, 2013). NO produced from eNOS has a wide range of biological properties to maintain vascular homeostasis, including vascular dilation, and inhibition of oxidative stress and inflammation. Therefore, Let-7g, miR-34a, and antioxidant genes SIRT1 and eNOS are key signaling molecules for regulating endothelial senescence.

Recently plasma kallistatin levels have been shown to be positively associated with leukocyte telomere length in young African Americans, implicating the involvement of kallistatin in anti-aging process (Zhu *et al*., 2016). Moreover, kallistatin depletion by neutralizing antibody injection worsens cardiovascular and renal injury, oxidative stress and inflammation in hypertensive rats (Liu *et al*., 2011), indicating endogenous kallistatin may have a role in vascular and organ injury. H_2O_2 is widely used to achieve oxidative stress-induced premature senescence in endothelial cells and fibroblasts (Chen J. H. *et al.*, 2007, Liu D. H. *et al.*, 2012). According to previous findings, the dose of H_2O_2 (100 μM) represents subcytotoxic conditions to induce senescence (Frippiat *et al.*, 2001, Li R. L. *et al*., 2016). In this study, we further investigated the role and mechanism of kallistatin in oxidative stress-induced endothelial senescence by 1) exogenous kallistatin treatment in human endothelial cells, and 2) endogenous kallistatin deficiency in mouse lung endothelial cells isolated from endothelium-specific kallistatin-deficient ($KS^{endo-/-}$) mice. General kallistatin knockout ($KS^{-/-}$) mice were also generated and subjected to

streptozotocin (STZ) challenge, which is a chemical agent to induce diabetes by damaging islet β-cells. We further determined the role of endogenous kallistatin in diabetes-induced vascular and organ injury.

Material and Methods

Human Endothelial Cell Culture and Treatments

Human umbilical vein endothelial cells (HUVECs) were cultured as previously described in Chapter II. HUVECs at 80% confluency were pre-treated with kallistatin (1 μM) followed by hydrogen peroxide (H_2O_2, 100 μM; Fisher Scientific) challenge for 3 days in serum-free EBM-2 medium; senescent markers and oxidative stress indicators were evaluated. To measure gene expression, HUVECs were pre-incubated with kallistatin (1 μM) followed by H_2O_2 (100 μM) treated for 24 h. To determine the causal relationship of SIRT1 and eNOS, HUVECs were pre-treated with SIRT1 inhibitor nicotinamide (NAM, 5 mM; Sigma) or NOS inhibitor Nω-nitro-L-arginine methyl ester hydrochloride (L-NAME, 100 μM; Sigma) for 30 min, followed by kallistatin (1 μM) and H_2O_2 (100 μM) treatment for 24 h. Similarly, cultured primary mouse lung endothelial cells at 80% confluency were treated with or without H_2O_2 (100 μM) for 3 days to evaluate senescent markers and oxidative stress indicators, and for 24 h to measure gene expression

SA-β-gal Staining

Cellular senescence of HUVECs or mouse lung endothelial cells in 12-well plates was determined with SA-β-gal staining kit (Cell Signaling).

Telomerase Activity Assay

Telomerase activity was measured using TRAPEZE RT telomerase detection kit (EMD Millipore).

NADPH Oxidase Activity Assay

The enzymatic activity of NADPH oxidase was assessed by a luminescence assay in the presence of lucigenin (250 μM; Sigma) and NADPH (100 μM; Sigma).

Detection of Superoxide Formation

HUVECs superoxide generation was detected using the fluorescent probe 2', 7'-dichlorodihydrofluorescein diacetate (DCFH-DA; 10 μM, Sigma). Superoxide levels in mouse lung endothelial cells and mouse thoracic aortas were determined by fluorescent probe dihydroethidium (DHE; 3 μM, Sigma).

miRNA Transfection

HUVECs were grown in antibiotic-free EBM-2 on plates for 24 h, and then transfected with Let-7g inhibitor (10 pM, antisense RNA Let-7g), miR-34a mimic or control miRNA (10 pM; Life Technologies) with Lipofectamine RNAiMAX reagent (Life Technologies) according to the manufacturer's protocol.

Quantitation of mRNA by qRT-PCR

RNA extraction, reverse transcription and Real-time PCR were performed as previously described in Chapter II method section. The following primers were used: human 18S, $p16^{INK4a}$, eNOS, SIRT1, catalase, PAI-1, NADPH oxidase 4 and miR-34a; mouse GAPDH, eNOS, SIRT1, catalase and miR-34a as described in Chaper III. Superoxide dismutase (SOD)-2 (Hs00167309_ml), ICAM-1 (Hs00277001_ml), interleukin (IL)-6 (Hs00174131_ml), VCAM-1 (Hs00365486_ml), Let-7g (002282), mouse SOD-1 (Mm01344233_gl), mouse VCAM1 (Mm01320970_ml), mouse IL-6 (Mm00446190_ml), mouse ICAM-1 (Mm00516024_gl), mouse kallistatin (Mm00434669_ml), mouse PAI-1 (Mm00435858_ml), mouse $p16^{INK4a}$

(Mm00494449_ml). Data were analyzed with $2^{-\Delta\Delta Ct}$ value calculation using control genes for normalization.

Western Blot

Lysed cell sample were lysed, separated and immunobloted as previously described in Chapter II. Primary antibodies were anti-SIRT1, anti-eNOS, anti-mouse kallistatin, anti-β-actin, anti-Tie2, anti-fibronectin, anti-α-SMA and anti-α-tubulin (Cell Signaling).

Generation of Endothelium-Specific Kallistatin Knockout Mice

Heterozygous kallistatin floxing mice in C57/BL6 strain (male and female, $KS^{fl/+}$) were obtained from Biocytogen, LLC (Worcester), and male wild-type C57/BL6 mice (7-8 weeks of age) were purchased from Harlan (Indianapolis). These mice were housed in a germ-free environment. All procedures complied with the standard for care and use of animal subjects as stated in the Guide for the Care and Use of Laboratory Animals (Institute of Laboratory Resources, National Academy of Sciences). $KS^{fl/+}$ mice were inbred to produce homozygous floxed kallistatin mice ($KS^{fl/fl}$). To generate endothelium-specific heterozygous kallistatin knockout mice ($Tie2Cre^{+}KS^{fl/+}$), female $KS^{fl/fl}$ mice were crossed with male Tie2-Cre mice (The Jackson Laboratories). $Tie2Cre+KS^{fl/+}$ mice were then crossed with $KS^{fl/fl}$ mice to generate endothelium-specific kallistatin knockout ($KS^{endo-/-}$) mice. The expression of mouse kallistatin null allele in endothelium of $KS^{endo-/-}$ mice was determined by PCR with a pair of custom primers: 5'-TCA AGT CCC TCA TGT GCG TTG GTA G-3', and 5'-ATG TCA ATC ACA ATG CCC TCT GCC T-3'. The amplification conditions are 95°C for 5 min and 35 cycles of 95°C for 30 s, 63°C for 30 s, and 72°C for 1 min, followed by a 10-min incubation at 72°C at the end of the run.

Amplification products were resolved on a 3% agarose gel. Mouse kallistatin deficiency in isolated mouse lung endothelial cells was verified by qRT-PCR and western blot.

Isolation and Identification of Mouse Lung Endothelial Cells

Mouse lung endothelial cells were isolated from 8-week-old $KS^{endo-/-}$ and WT mice as described (Alphonse *et al.*, 2015). Mice were euthanized by CO_2 inhalation followed by cervical dislocation. The lungs were digested with 0.1% collagenase in PBS for 45 min. The cell suspension was isolated by magnetic immunoselection with CD31-conjugated magnetic beads (Miltenyi Biotec) using the magnetic-activated cell sorting system (MACS, Miltenyi Biotec). Purified mouse lung endothelial cells were cultured on gelatin-coated tissue culture dishes with EBM-2 medium with 10% FBS and 1% antibiotics until they became confluent. Newly grown colonies were digested, incubated with CD31 magnetic beads and selected through MACS again. After the second selection, mouse lung endothelial cells were seeded in a T75 flask provided with complete EBM-2 medium to grow robustly. Mouse endothelial cells were characterized with endothelial marker CD31 by PCR and immunostaining. For immunostaining, mouse endothelial cells were fixed with 4% paraformaldehyde, incubated with blocking buffer, and followed with rat anti-mouse CD31 antibody (Santa Cruz Biotechnology) overnight at 4°C. After washing with PBS, cells were incubated with anti-rat FITC secondary antibody (Sigma) for 1 h at room temperature, washed with PBS, and counterstained with Hoechst 33342 (1 μg/ml; Sigma).

Generation and Identification of General Kallistatin Knockout Mice

To generate heterozygous kallistatin knockout mice ($CAGCre^{+}KS^{fl/+}$), female $KS^{fl/fl}$ mice were crossed with male CAG-Cre mice (The Jackson Laboratories). $CAGCre^{+}KS^{fl/+}$ mice were then crossed with $KS^{fl/fl}$ mice to produce $CAGCre^{+}KS^{fl/fl}$ mice.

Mice at the age of 4-5 week-old were subcutaneously injected with tamoxifen (75mg/kg, dissolved in corn oil) for 5 days to induce Cre recombinase activity. Genotyping were performed after one week of tamoxifen induction using 0.5 cm tail biopsy. Serpina3c-A1Loxp-F 5'-CTG CTC ATG ATG TAG GAG ATC TTA GC-3', Serpina3c-A1Loxp-R 5'-TCC AGT CAT GGT TTG GAT AGT GG-3'; Cre-F: 5'-GCG GTC TGG CAG TAA AAA CTA TC-3', Cre-R: 5'-GTG AAA CAG CAT TGC TGT CAC TT-3'. The amplification conditions are described as above. Mouse kallistatin ablation was also verified by western blot.

Diabetes Model

Male $KS^{-/-}$ mice and WT littermates (12 weeks of age) were subjected to 6-day continuous intraperitoneal injections of STZ (60 mg/kg; Sigma). Sodium citrate buffer (0.1 M, pH 4.5) was injected in control animals. Mice with blood glucose > 250 mg/dL were considered diabetic. A total of 24 mice were randomly assigned to three groups: WT group (n = 6), $KS^{-/-}$ group, WT+STZ group (n = 6), and $KS^{-/-}$ +STZ group (n = 6). Two months after blood glucose stabilization, thoracic aortas and kidney samples were collected for histological analysis or western blot analysis.

Morphological Investigations

5 μm-thick renal sections and 8 μm-thick aortic sections were obtained from each sample. Renal sections were stained with Sirius red to determine the extent of fibrosis. Artery sections were stained with dihydroethidium (DHE; Signma) at 37°C for superoxide determination. Primary antibodies for VE-cadherin, CD31 and α-SMA were used to detect in HUVECs with fluorescence microscopy. Briefly, cells were fixed with 4% paraformaldehyde and permeabilized with 0.2% Triton X-100, and blocked with 3% BSA in PBS for 1 h at room temperature, followed by incubation with primary antibody

overnight at 4°C. After incubation, cells were rinsed three times with PBS and incubated with fluorochrome-conjugated secondary antibody for 2 h at room temperature in the dark. Cells were then washed with PBS and counter stained with Hoechst 33342 (5 μg/ml; Cell Signaling Technology) for 5 min. Plates were then observed under a fluorescence microscope.

Assays for Plasma Creatinine and Blood Urea Nitrogen (BUN) Levels

Plasma was collected from each sample. Protein levels in plasma were measured by Pierce BCA protein assay kit (Thermo Fisher Scientific). Plasma creatinine or BUN levels were determined using Quantichrom creatinine assay kit (DITC500) or Quantichrom urea assay kit (DIUR-500) (BioAssay Systems).

Statistical Analysis

Data are presented as mean ± S.E.M. Statistical analyses were performed with GraphPad Prism 7 (GraphPad Software). ANOVA and Student's t-test analysis were used to assess differences between data means as appropriate. A value of $P < 0.05$ was considered statistically significant.

Results

Kallistatin Attenuates H_2O_2-Induced Cellular Senescence in Human Endothelial Cells

Representative images showed that H_2O_2 treatment induced pronounced cellular senescence in HUVECs, characterized by increased senescent marker SA-β-gal activity compared with the control group, while purified recombinant human kallistatin pretreatment reversed the effect (Figure 4-1 A). Quantitative analysis of positive SA-β-gal staining cells confirmed the results (Figure 4-1 B). Senescent markers $p16^{INK4A}$, PAI-1 and telomerase were also evaluated. Kallistatin blocked H_2O_2-induced $p16^{INK4A}$ and PAI-1 expression, and prevented H_2O_2-mediated inhibition of telomerase activity (Figure 4-1 C-E). Therefore, kallistatin is capable of blocking oxidative stress-induced endothelial senescence.

Kallistatin Inhibits H_2O_2-Induced Oxidative Stress and Inflammation

Representative images showed that kallistatin attenuated H_2O_2-induced superoxide formation in human endothelial cells, which was verified by quantitative analysis (Figure 4-2 A&B). Similarly, kallistatin antagonized H_2O_2-induced NADPH oxidase activity and NADPH oxidase 4 mRNA levels (Figure 4-2 C&D). Moreover, kallistatin inhibited H_2O_2-mediated expression of the pro-inflammatory genes VCAM-1, ICAM-1 and IL-6 (Figure 4-2 E-G). Kallistatin alone inhibited miR-34a, and prevented H_2O_2-induced miR-34a synthesis (Figure 4-2 H). These results indicate that kallistatin inhibits H_2O_2-induced oxidative stress and inflammation in endothelial cells.

Kallistatin Inhibits Endothelial Senescence and Oxidative Stress through SIRT1-Mediated eNOS Pathway

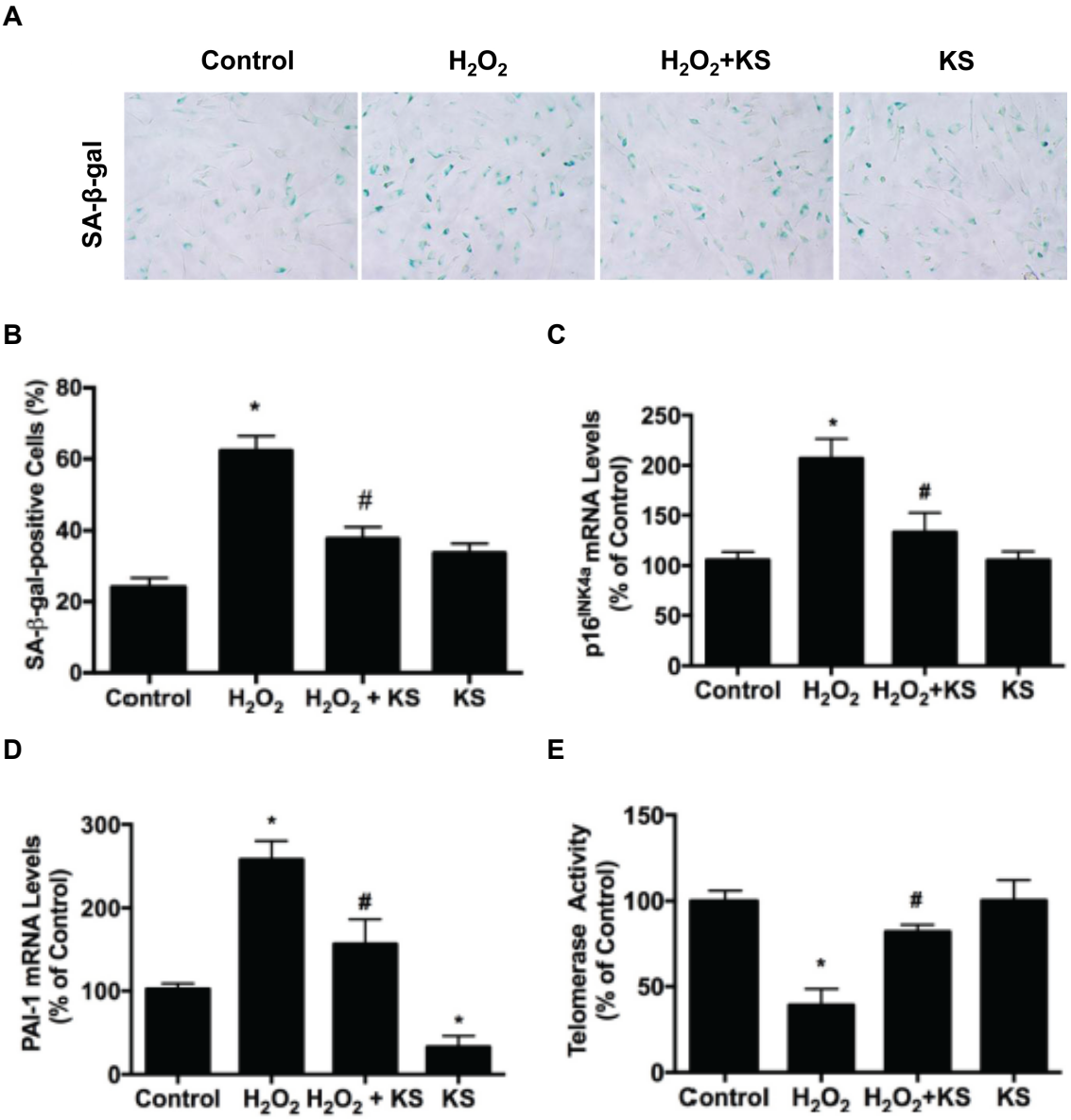

Figure 4-1. Kallistatin (KS) alleviates H_2O_2-induced endothelial senescence in human endothelial cells. (A) Representative images of SA-β-gal staining. (B) Quantification analysis of positive SA-β-gal staining cells. (C) QPC analysis of $p16^{INK4a}$. (D) QPCR analysis of PAI-1 mRNA levels. (E) Telomerase activity determined by QPCR (C-D). n=3. $^{*}P < 0.05$ vs. control, $^{\#}P < 0.05$ vs. H_2O_2 group.

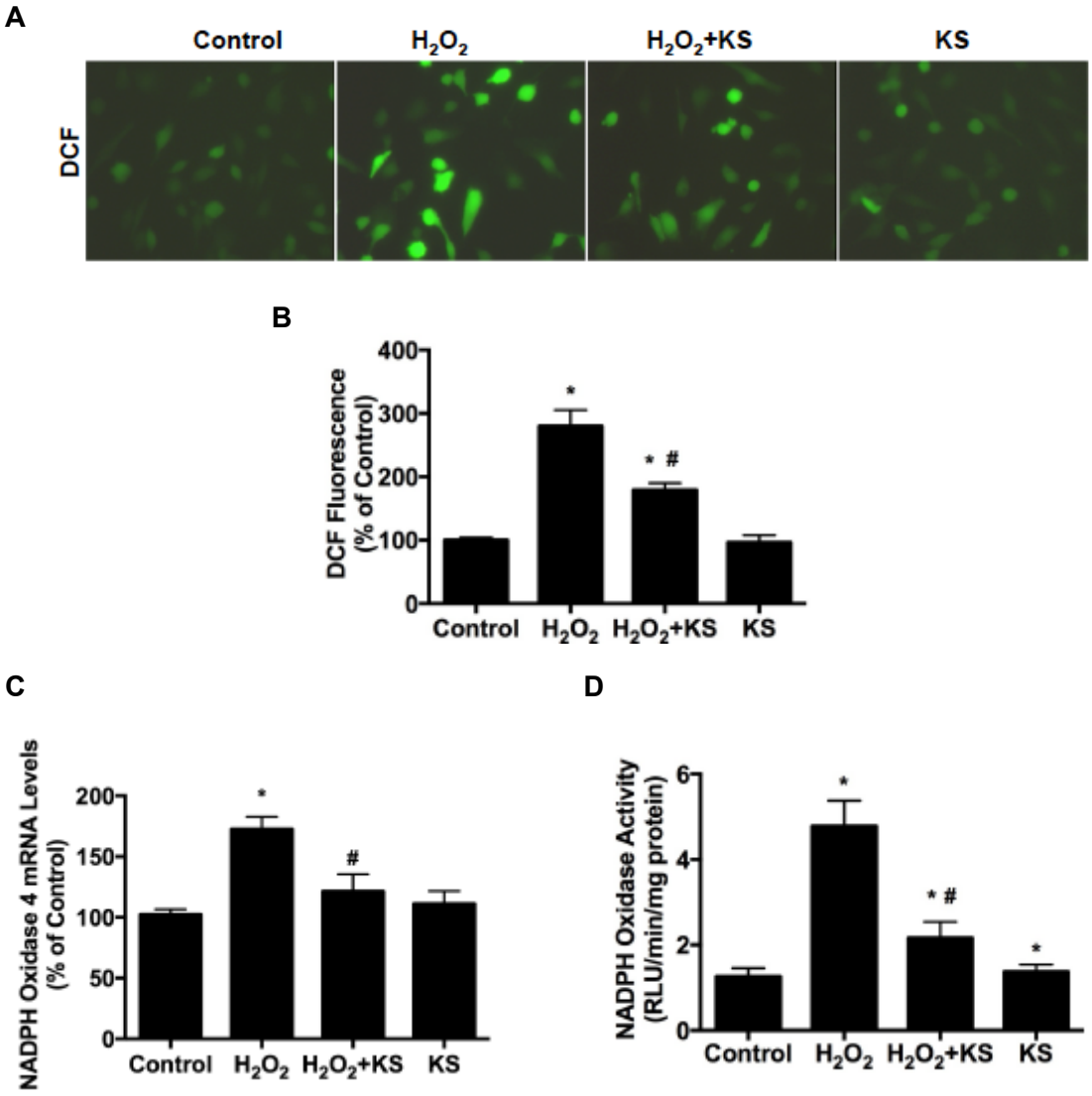

Figure 4-2 A-D. Kallistatin (KS) suppresses H_2O_2-induced oxidative stress in human endothelial cells. (A) Representative images of superoxide formation determined by fluorescence dye oxidized DCF. (B) Quantitative analysis of fluorescent counts. (C) QPCR analysis of NADPH oxidase 4 mRNA levels. (D) NADPH oxidase activity determined by lucigenin chemiluminescence assay. n=3. $^{*}P < 0.05$ vs. control, $^{\#}P < 0.05$ vs. H_2O_2 group.

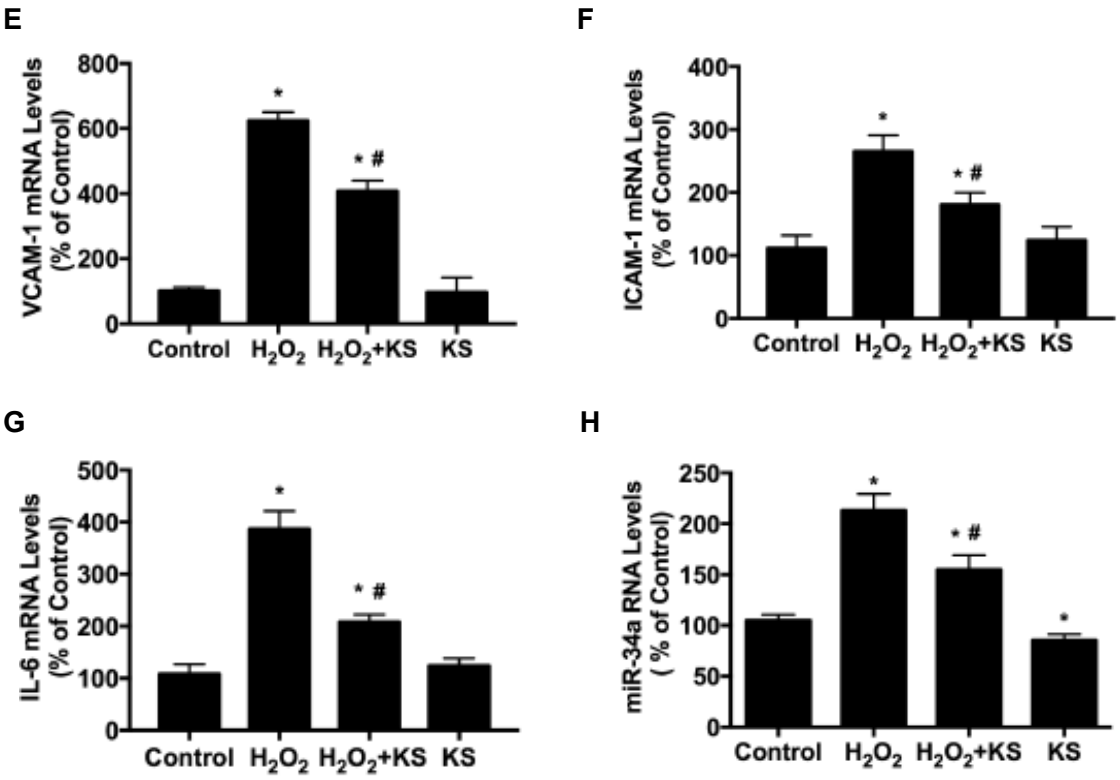

Figure 4-2 E-H. Kallistatin (KS) suppresses H_2O_2-induced inflammation and miR-34a synthesis in human endothelial cells. QPCR analysis of (A) VCAM-1, (B) ICAM-1, (C) IL-6 and (D) miR-34a RNA levels. n=3. *P<0.05 *vs.* control, $^{\#}P$<0.05 *vs.* H_2O_2 group.

In order to determine whether the kallistatin-mediated protection against endothelial senescence is associated with antioxidant gene regulation, the effects of kallistatin on the regulation of SIRT1, eNOS, catalase and SOD-2 were determined. Kallistatin treatment not only markedly enhanced SIRT1, eNOS, catalase and SOD-2 expression, but also prevented H_2O_2-mediated inhibition of these antioxidant genes (Figure 4-3 A-D). Moreover, NAM, a potent inhibitor of SIRT1 activity, blocked kallistatin-stimulated eNOS expression, whereas L-NAME, an NOS inhibitor, had no effect on kallistatin-stimulated SIRT1 expression (Figure 4-3 E&F), indicating that kallistatin via SIRT1 elevation stimulates eNOS. Furthermore, NAM abolished kallistatin's antioxidant activity and anti-senescent action, as evidenced by reversing kallistatin's inhibition of SA-β-gal activity and NADPH oxidase activity in HUVECs (Figure 4-3 G&H). These results indicate that the SIRT1-mediated eNOS pathway plays a crucial role in kallistatin's inhibition of endothelial senescence and oxidative stress.

Kallistatin by Let-7g Upregulation Blocks miR-34a-Mediated Inhibition of SIRT1-eNOS Pathway, and Reduces Endothelial Senescence, Oxidative Stress and Inflammation

To illustrate whether kallistatin-mediated inhibition of endothelial senescence was associated with upregulation of Let-7g, the effect of kallistatin on Let-7g expression was determined. Kallistatin treatment significantly increased Let-7g synthesis, whereas genistein, a tyrosine kinase inhibitor, blocked kallistatin's effect (Figure 4-4 A), implicating that kallistatin interacts with a cell surface tyrosine kinase to stimulate Let-7g synthesis. Let-7g inhibitor (Let-7g anti-sense RNA) blocked kallistatin's inhibition of miR-34a synthesis (Figure 4-4 B), indicating that kallistatin regulates Let-7g-mediated miR-34a pathway. Conversely, miR-34a mimic had no effect on kallistatin-induced Let-7g

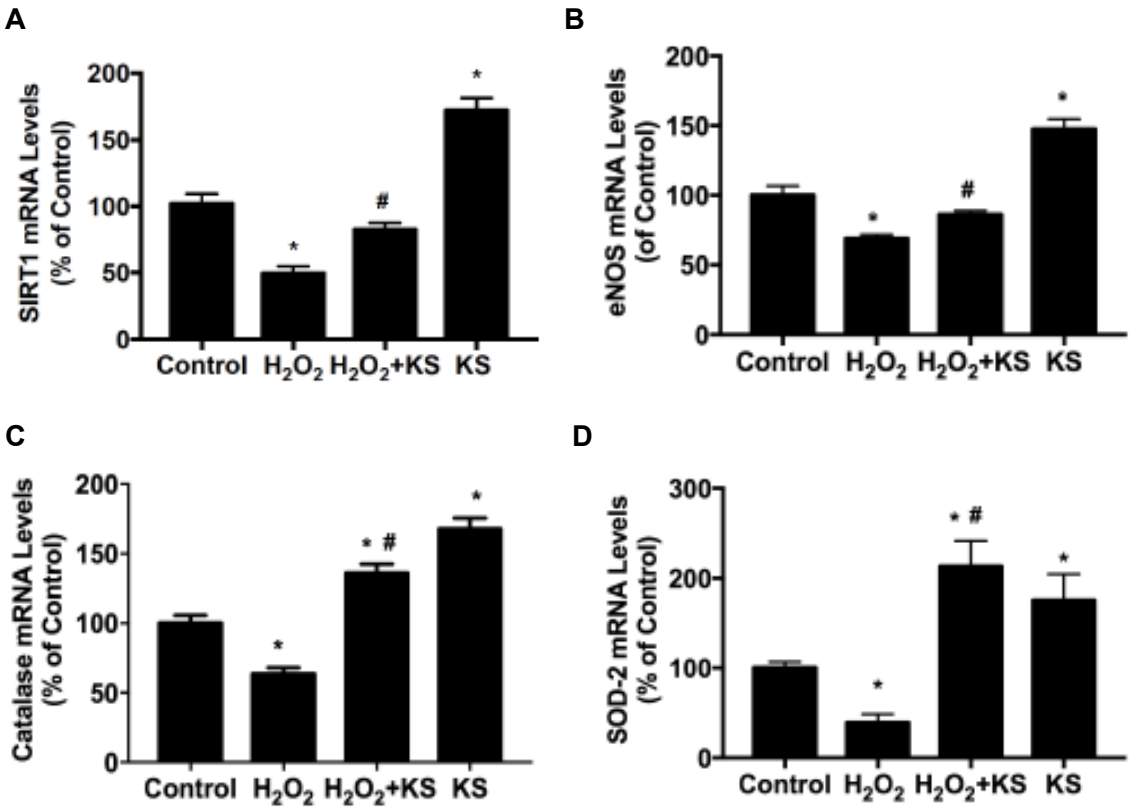

Figure 4-3 A-D. Kallistatin (KS) stimulates antioxidant gene expression and prevents H_2O_2-mediated inhibition of these genes in human endothelial cells. QPCR analysis of (A) SIRT1, (B) eNOS, (C) catalase and (D) SOD-2 mRNA levels. n=3. $^{*}P < 0.05$ *vs.* control, $^{\#}P < 0.05$ *vs.* H_2O_2 group.

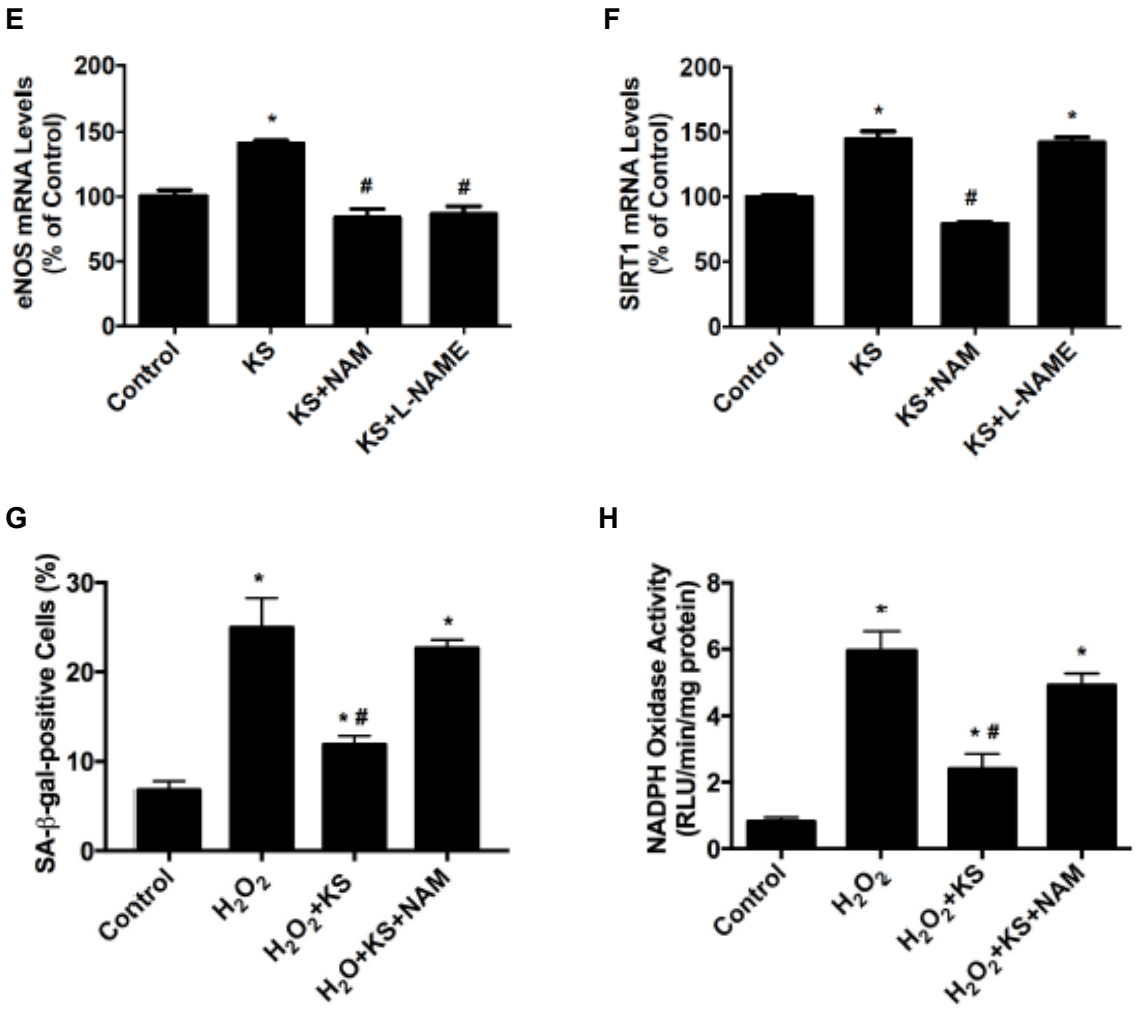

Figure 4-3 E-H. Kallistatin (KS) inhibits H_2O_2-induced senescence and oxidative stress through SIRT1-eNOS pathway in human endothelial cells. QPCR analysis of (E) eNOS and (F) SIRT1 mRNA levels. (G) Quantification analysis of SA-β-gal positive staining cells. (H) NADPH oxidase activity determined by lucigenin chemiluminescence. n=3. $^{*}P < 0.05$ *vs.* control, $^{\#}P < 0.05$ *vs.* KS group or H_2O_2 group.

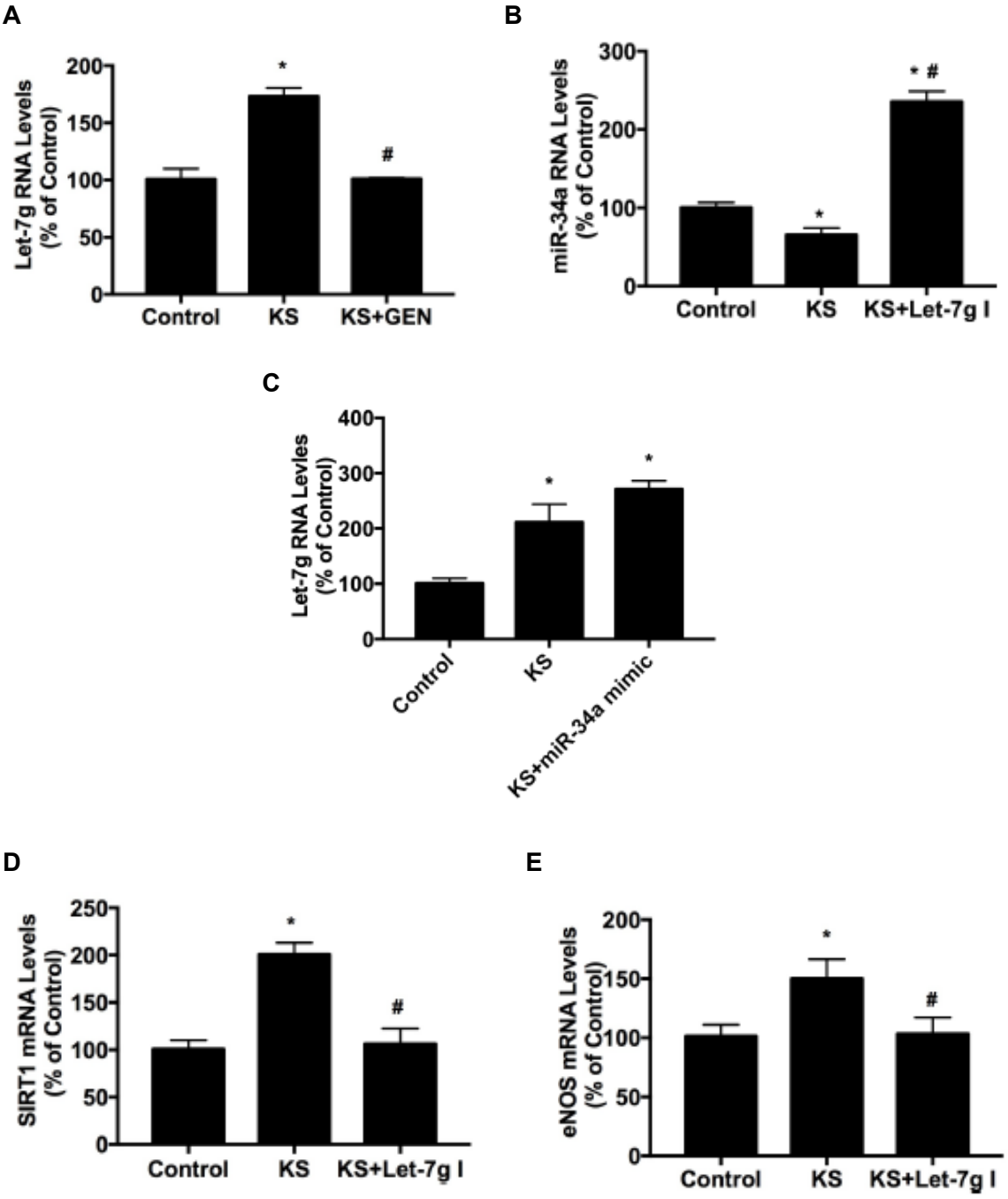

Figure 4-4 A-E. Kallistatin (KS) through Let-7g to inhibit miR-34a and elevate SIRT1 and eNOS synthesis in human endothelial cells. QPCR analysis of (A) Let-7g, (B) miR-34a, (C) Let-7g, (D) SIRT1 and (E) eNOS mRNA levels. GEN: genistein, a tyrosine kinase inhibitor; Let-7g I: Let-7g inhibitor. n=3. **P* < 0.05 *vs.* control, $^{\#}P$ < 0.05 *vs.* KS group or H_2O_2 group.

expression (Figure 4-4 C), thus kallistatin's effect on Let-7g upregulation is independent of miR-34a. Moreover, Let-7g inhibitor abolished kallistatin-induced SIRT1 and eNOS mRNA levels, and blocked kallistatin-mediated elevation of SIRT1 and eNOS levels by western blot (Figure 4-4 D-F), indicating an essential role of Let-7g in kallistatin's induction of antioxidant genes. Furthermore, Let-7g inhibitor abolished kallistatin's inhibitory effect on H_2O_2-induced senescence, characterized by elevated $p16^{INK4a}$ and PAI-1 mRNA levels in endothelial cells (Figure 4-4 G&H). Likewise, Let-7g inhibitor blocked kallistatin's effect on H_2O_2-induced NADPH oxidase activity and VCAM-1 expression (Figure 4-4 I&J). These combined findings indicate that kallistatin, by interacting with a tyrosine kinase, upregulates Let-7g, thus inhibiting miR-34a-SIRT1-eNOS pathway. Therefore, Let-7g plays a crucial role in mediating kallistatin's inhibitory effects on endothelial senescence.

Identification of Kallistatin Deficiency in Mouse Lung Endothelial Cells

We generated endothelium-specific kallistatin knockout ($KS^{endo-/-}$) mice by crossing $KS^{fl/fl}$ mice with Tie2Cre+$KS^{fl/+}$ mice. Lung endothelial cells were isolated from WT mice and $KS^{endo-/-}$ mice. Cultured primary mouse lung endothelial cells were identified by CD31 expression and immunostaining (Figure 4-5 A&B). In lysed mouse endothelial cell DNA samples, kallistatin null allele (del) was detected only in $KS^{endo-/-}$ mice, but not in WT mice (Figure 4-5 C), indicating that endogenous kallistatin is ablated in mouse endothelial cells. Moreover, the protein and mRNA levels of mouse kallistatin were markedly diminished in endothelial cells from $KS^{endo-/-}$ mice, compared with endothelial cells from WT mice (Figure 4-5 D&E). These results confirm that mouse endogenous kallistatin is deficient in $KS^{endo-/-}$ mouse endothelial cells.

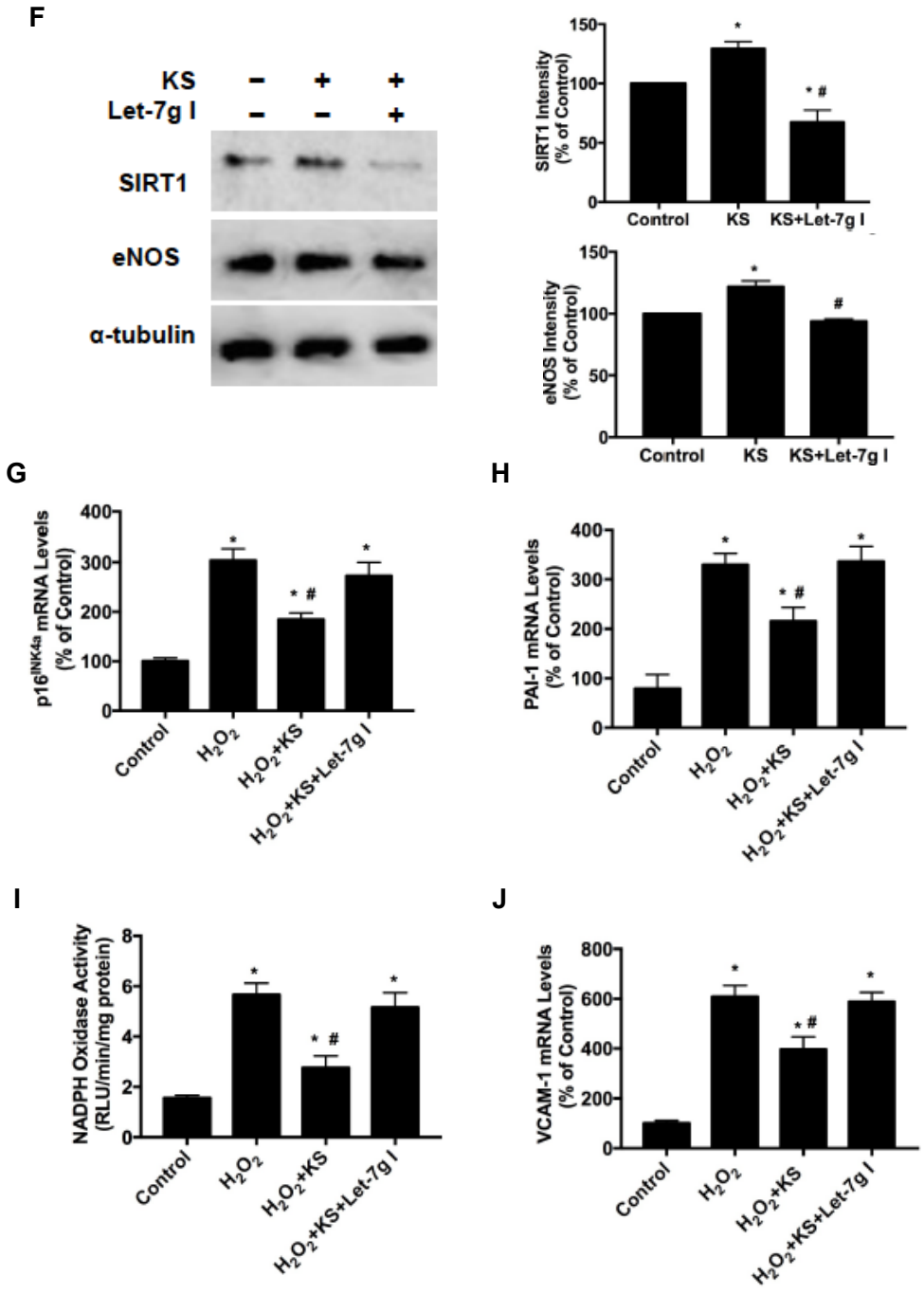

Figure 4-4 F-J. Kallistatin through Let-7g induction stimulates SIRT1 and eNOS, and inhibits endothelial senescence, oxidative stress and inflammation. (F) Representative western blot of SIRT1 and eNOS and quantification. QPCR of (G) $p16^{INK4a}$ and (H) PAI-1. (I) Chemiluminescence analysis of NADPH oxidase activity. (J) QPCR analysis of VCAM-1. Let-7g I: Let-7g inhibitor. n=3. $^{*}P < 0.05$ *vs.* control, $^{\#}P < 0.05$ *vs.* KS group or H_2O_2 group.

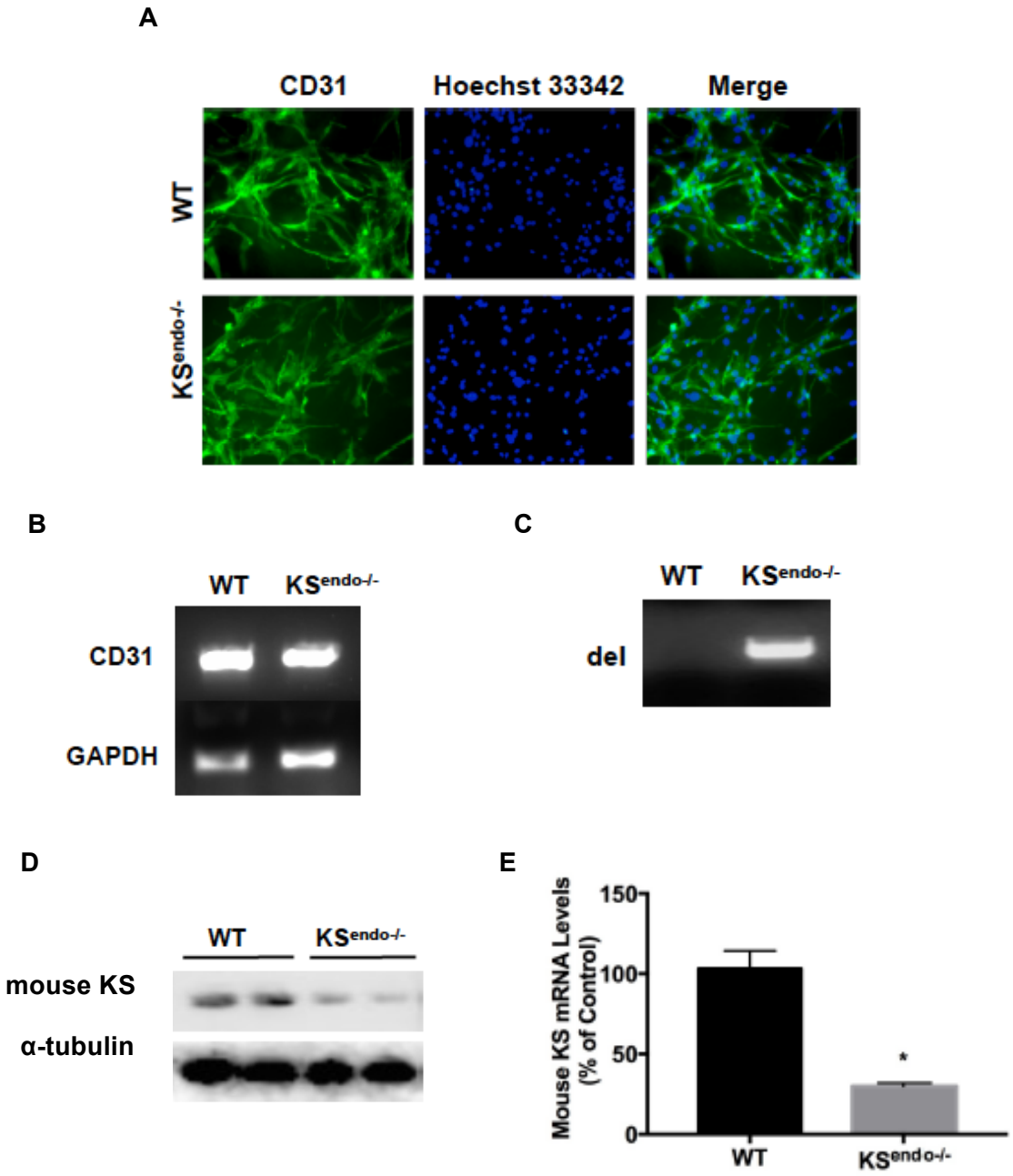

Figure 4-5. Identification of kallistatin (KS) deficiency in isolated mouse lung endothelial cells. (A) Representative images of immunostaining of endothelial marker CD31 expression in mouse lung endothelial cells. (B) CD31 expression determined by PCR. (C) Identification of mouse kallistatin depletion (del) by target null gene DNA electrophoresis. (D) Representative immunoblots of mouse KS protein. (E) QPCR analysis of mouse kallistatin mRNA levels. n=3. *$P < 0.05$ *vs.* control.

Kallistatin Deficiency Aggravates Oxidative Stress-Induced Senescence, Oxidative Stress and Inflammation in Mouse Endothelial Cells

Cultured primary mouse lung endothelial cells with or without H_2O_2 treatment were used to determine the effect of kallistatin deficiency on endothelial senescence, oxidative stress and inflammation. In the non-H_2O_2-treated groups, kallistatin-deficient endothelial cells displayed increased SA-β-gal activity, $p16^{INK4a}$ and PAI-1 expression, compared to WT mouse endothelial cells (Figure 4-6 A-C). Mouse kallistatin deficiency in H_2O_2–treated endothelial cells further enhanced the levels of senescence makers, compared to H_2O_2–treated WT mouse endothelial cells (Figure 4-6 A-C). Moreover, cellular superoxide formation and NADPH oxidase activity were increased upon H_2O_2 treatment, and kallistatin deficiency further enhanced superoxide formation and NADPH oxidase activity (Figure 4-6 D&E). Likewise, kallistatin deficiency increased H_2O_2-induced VCAM-1, ICAM-1 and IL-6 mRNA levels in kallistatin-deficient endothelial cells (Figure 4-6 F-H). Therefore, kallistatin deficiency in mouse endothelial cells exacerbates endothelial senescence, oxidative stress and inflammation. These findings implicate a protective role of endogenous kallistatin in stress-induced endothelial senescence.

Kallistatin Deficiency Reduces Let-7g and Antioxidant Gene Expression and Increases miR-34a Synthesis in Mouse Endothelial Cells

Kallistatin deficiency in $KS^{endo-/-}$ mouse endothelial cells caused a significant reduction of Let-7g, SIRT1, eNOS, catalase and SOD-1 expression compared with WT mouse cells (Figure 4-7 A-E). Moreover, H_2O_2 treatment reduced the expression of Let-7g and antioxidant genes in endothelial cells from WT mice, and kallistatin deficiency further reduced the expression of these genes (Figure 4-7 A-E). Conversely, kallistatin deficiency increased miR-34a synthesis in mouse lung endothelial cells, compared with WT endothelial cells, with or without H_2O_2 treatment (Figure 4-7 F). These results

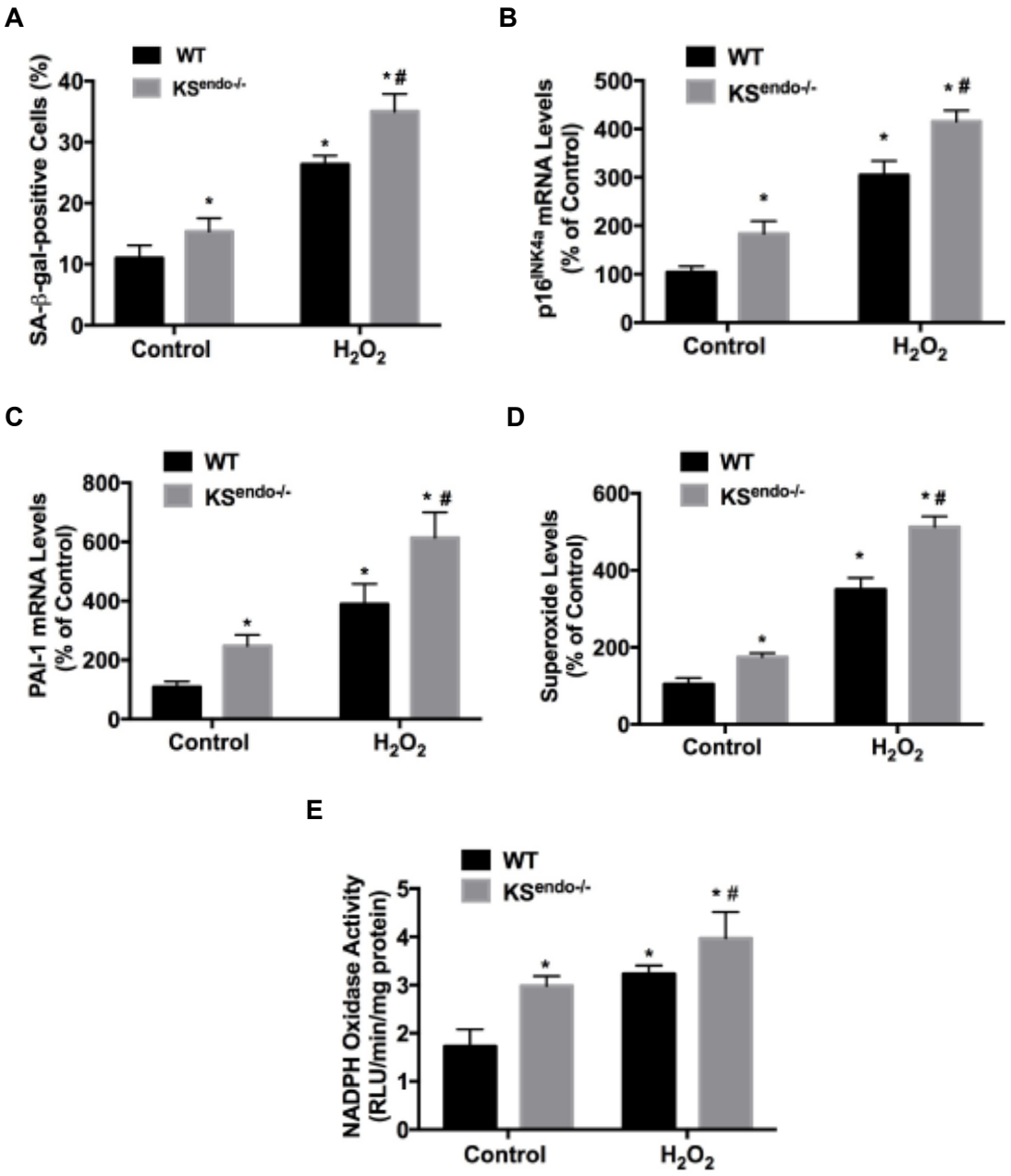

Figure 4-6 A-E. Kallistatin (KS) deficiency in mouse lung endothelial cells increases senescence and oxidative stress. (A) Quantitative analysis of SA-β-gal activity. QPCR analysis of (B) $p16^{INK4a}$ and (C) PAI-1 mRNA levels. (D) Superoxide formation determined by oxidized DCF fluorescent probe. (E) NADPH oxidative activity determined by lucigenin chemiluminescence. $^{*}P < 0.05$ *vs.* WT control group, $^{\#}P < 0.05$ *vs.* WT H_2O_2 group.

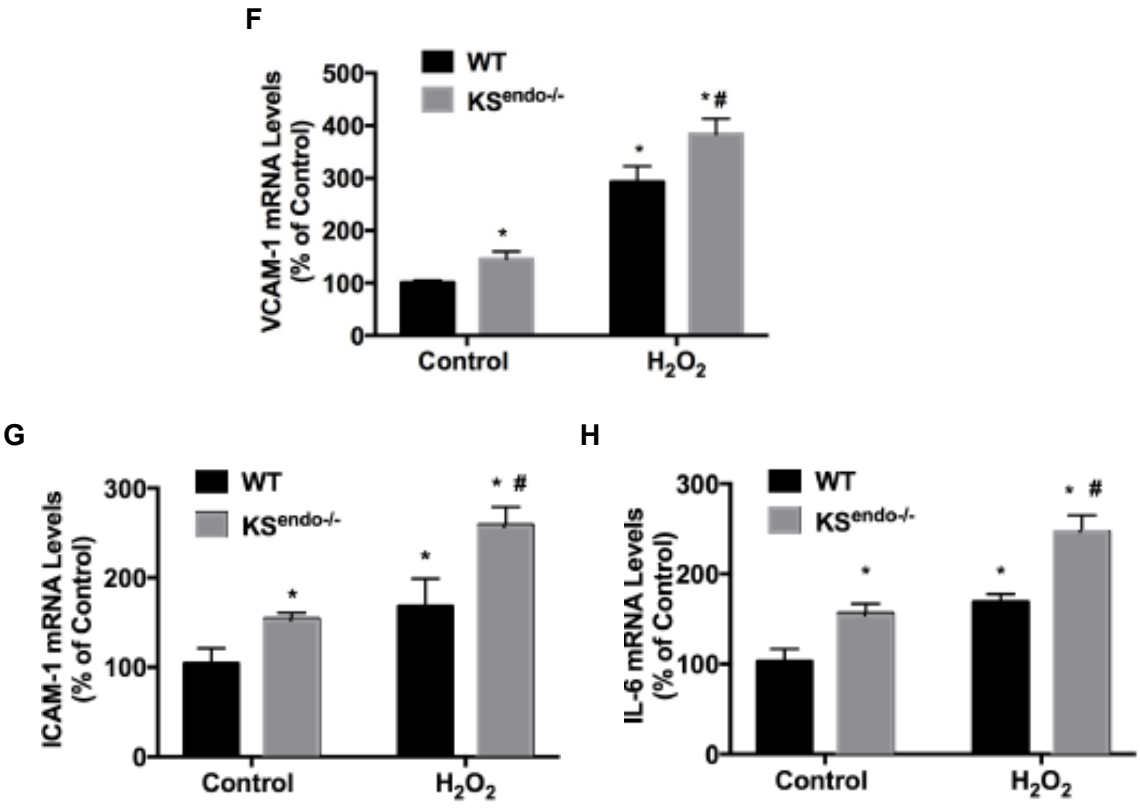

Figure 4-6 F-H. Kallistatin (KS) deficiency in mouse lung endothelial cells exacerbates inflammatory gene expression. QPCR analysis of (F) VCAM-1, (G) ICAM-1 and (H) IL-6 mRNA levels. n=3. $^{*}P < 0.05$ *vs.* WT control group, $^{\#}P < 0.05$ *vs.* WT H_2O_2 group.

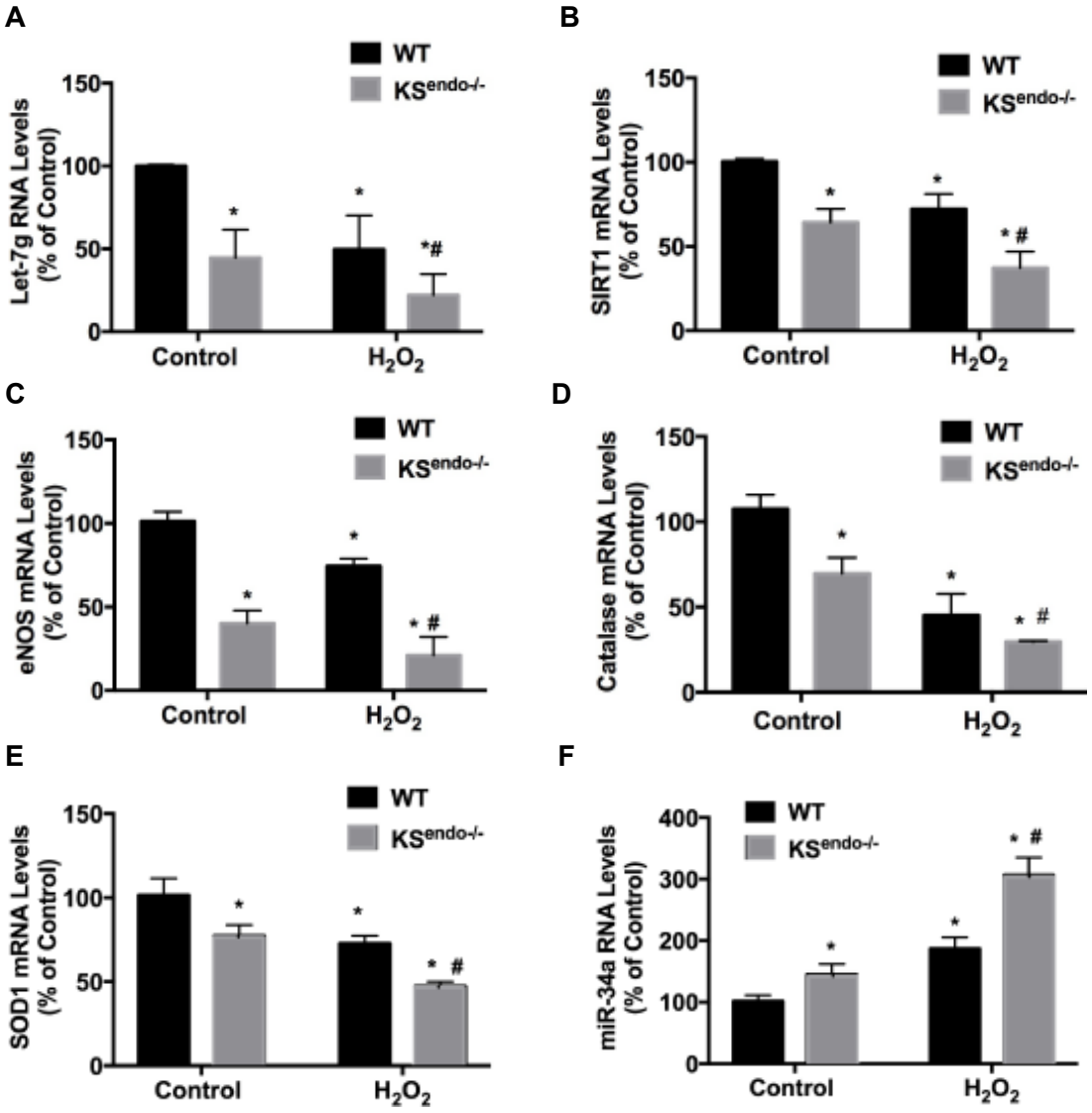

Figure 4-7. Kallistatin (KS) deficiency inhibits the synthesis of Let-7g and antioxidant genes and elevates miR-34a in mouse lung endothelial cells. QPCR analysis of (A) Let-7g, (B) SIRT1, (C) eNOS, (D) catalase, (E) SOD1 and (F) miR-34a. n=3. $^{*}P < 0.05$ *vs.* WT control group, $^{\#}P < 0.05$ *vs.* WT H_2O_2 group.

indicate that endothelial senescence in kallistatin-deficient mouse endothelial cells is attributed to downregulation of Let-7g and antioxidant genes, and elevation of miR-34a.

Systemic Depletion of Kallistatin Aggravates Aortic Oxidative Stress and Renal Fibrosis in Diabetic Mice

We generated general kallistatin knockout ($KS^{-/-}$) mice. Kallistatin null allele (del) was only detected in $KS^{-/-}$ mice (Figure 4-8 A). Kallistatin depletion was also identified by the dramatic reduction of protein levels of mouse kallistatin in the kidney of $KS^{-/-}$ mice (Figure 4-8 B). Kallistatin ablation exacerbated STZ-induced superoxide formation and NADPH oxidase activity in aortas of diabetic mice, compared with aortas of diabetic WT mice (Figure 4-8 C&D). Compared with STZ WT mice, kallistatin ablation also caused the rupture of neointima and thickening of the smooth muscle layer of mouse aorta (Figure 4-8 C), indicating that kallistatin deficiency exacerbates vascular injury. Moreover, kallistatin depletion decreased SIRT1 and eNOS expression in aorta, STZ treatment further downregulated these protein levels (Figure 4-8 E). Regarding diabetes-associated renal injury, we found that kallistatin knockout aggravated renal dysfunction as increased plasma creatinine and BUN levels (Figure 4-8 F&G). Sirius red staining result showed that kallistatin depletion markedly increased STZ-induced renal interstitial fibrosis compared with the kidney of WT diabetic mice (Figure 4-8 H&I). To determine whether EndMT occurs in diabetes-induced renal fibrosis, we evaluated the expression of endothelial marker Tie2, and mesenchymal markers such as α-SMA and fibronectin (Figure 4-8 J). STZ treatment decreased Tie2, but elevated α-SMA and fibronectin protein levels; and kallistatin deficiency further augmented STZ-mediated effects on these markers, implicating that more fibrosis emerges in the kidney of diabetic $KS^{-/-}$ mice. Collectively, endogenous kallistatin is essential for protection against vascular injury and renal fibrosis in diabetic mice.

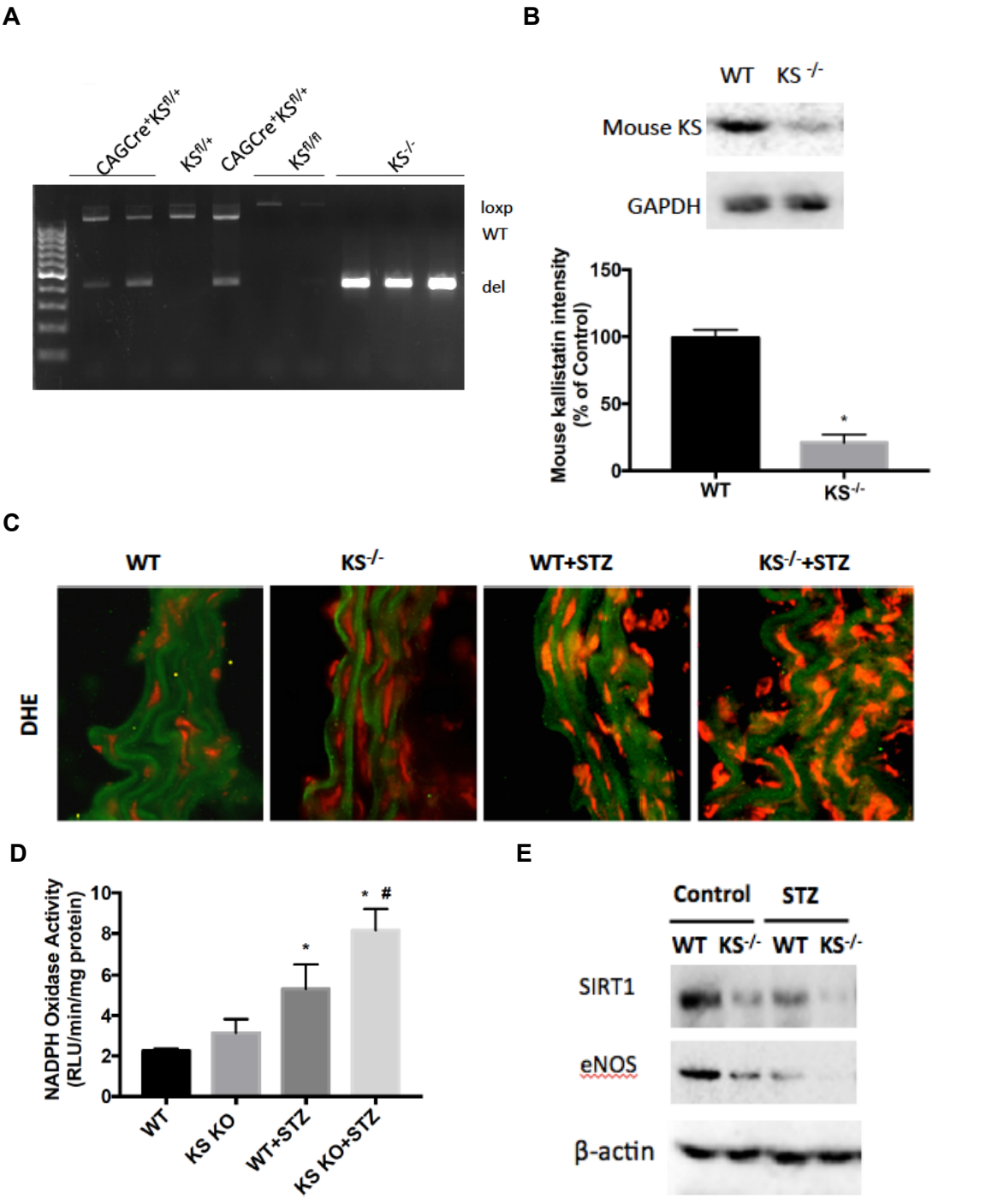

Figure 4-8 A-E. Kallistatin (KS) depletion exacerbates aortic oxidative stress in STZ-induced diabetic mice. (A) Genotyping PCR. (B) Representative western blot of mouse kallistatin in kidney samples and quantification analysis. (C) Representative images of aortic superoxide formation labeled by red fluorescence dye DHE. (D) Aortic NADPH oxidase activity chemiluminescence. (E) Representative western blots of aortic SIRT1 and eNOS. del: kallistatin null gene. n=4. $^{*}P < 0.05$ vs. WT group; $^{\#}P < 0.05$ vs. WT+STZ group.

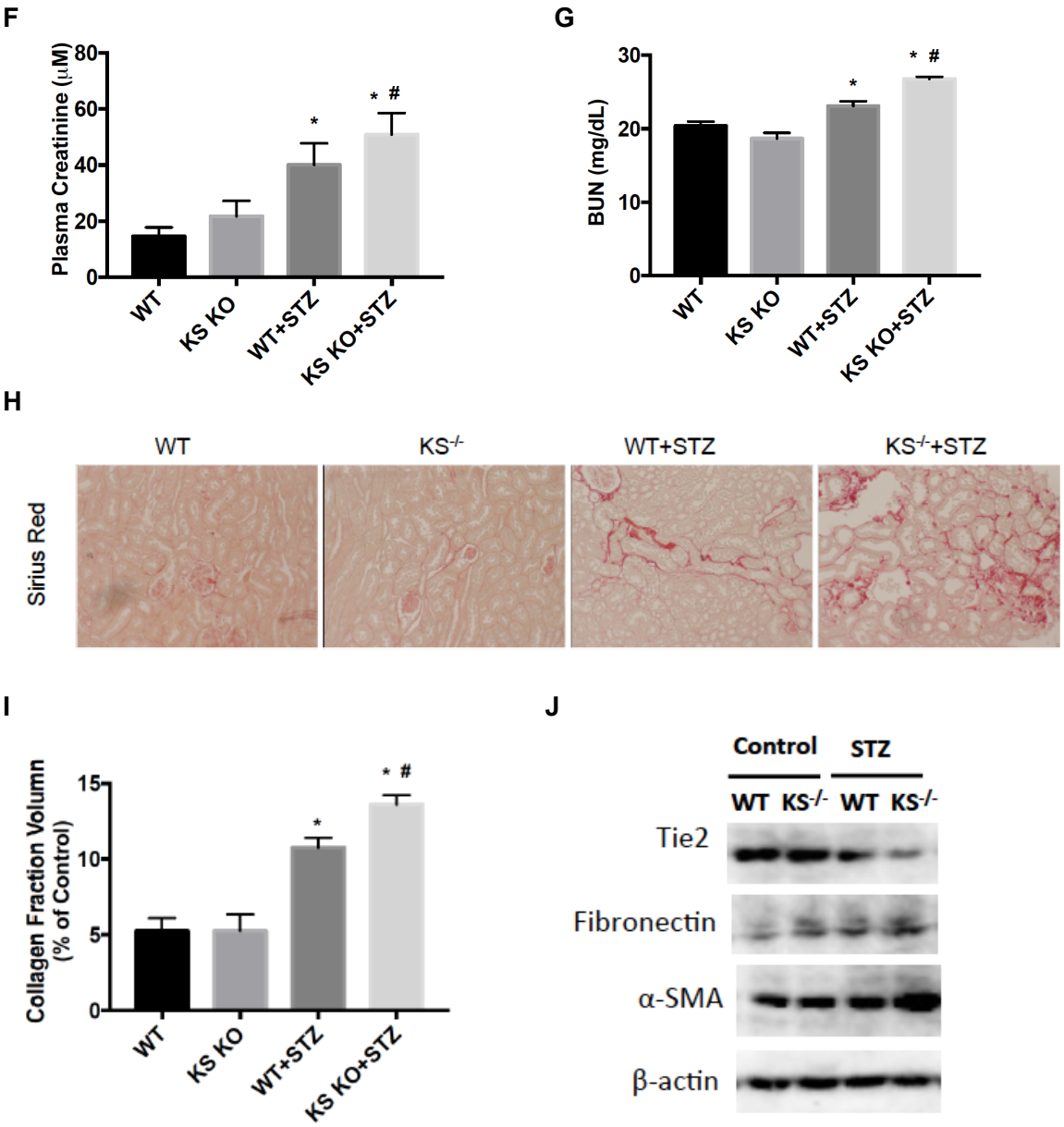

Figure 4-8 F-J. Kallistatin (KS) depletion exacerbates renal injury and fibrosis in STZ-induced diabetic mice. (F) Plasma creatinine levels. (G) Plasma BUN levels. (H) Representative images of sirius red staining in kidney sections. (I) Quantification of collagen fraction. (J) Representative western blots of endothelial marker Tie2, and mesenchymal markers fibronection and α-SMA. n=4. *P < 0.05 vs. WT group; #P < 0.05 vs. WT+STZ group.

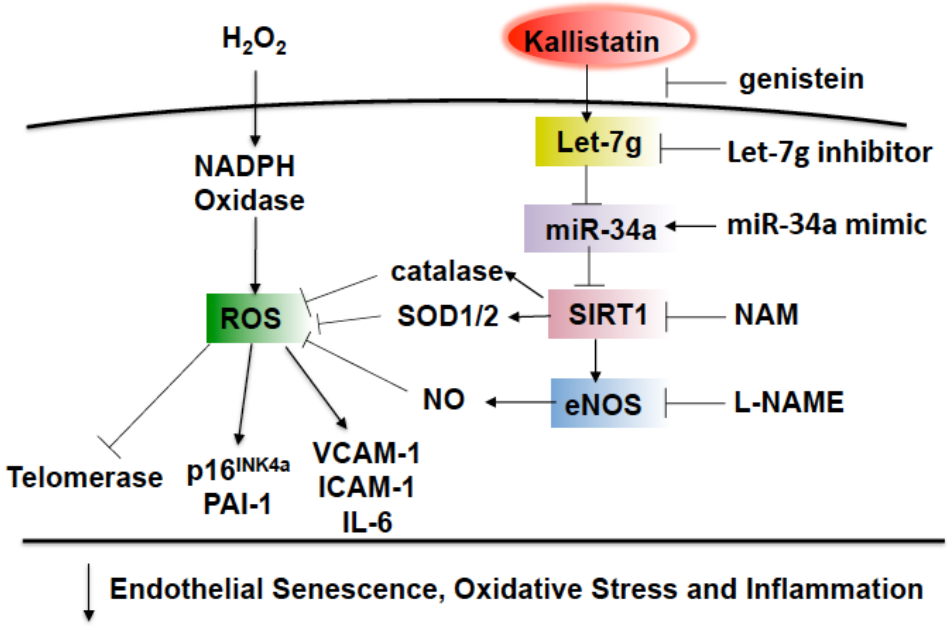

Figure 4-9. Signaling pathway by which kallistatin inhibits endothelial senescence, oxidative stress and inflammation. Kallistatin through tyrosine kinase stimulates Let-7g synthesis, inhibits miR-34 and upregulates SIRT1-mediated-eNOS pathway, thereby elevating catalase, SOD-1/2 and NO levels, leading to blockade of H_2O_2-modulated ROS formation, $p16^{INK4a}$, PAI-1, VCAM-1, ICAM-1, and IL-6 expression, and telomerase activity in endothelial cells. Genistein, tyrosine kinase inhibitor; NAM, SIRT1 inhibitor; L-NAME, NOS inhibitor.

Discussion

This study demonstrates that endogenous kallistatin plays a protective role in endothelial senescence, aorta oxidative stress and organ injury, and kallistatin through a novel mechanism inhibits cellular senescence, oxidative stress and inflammation. Kallistatin antagonized oxidative stress-induced senescence, as indicated by inhibiting $p16^{INK4a}$ and PAI-1 levels and increasing telomerase activity in human endothelial cells. Moreover, kallistatin, via tyrosine kinase, upregulated Let-7g, thus preventing miR-34a-mediated inhibition of the SIRT1-eNOS pathway. Activation of SIRT1-eNOS signaling resulted in increased catalase, SOD-1/2 and NO levels, and decreased ROS formation, VCAM-1, ICAM-1 and IL-6 expression. The signaling mechanism by which kallistatin inhibits endothelial senescence, oxidative stress and inflammation is shown in Figure 4-9. To confirm the pivotal role of endogenous kallistatin in protection against endothelial senescence, we generated endothelial cell-specific kallistatin knockout ($KS^{endo-/-}$) mice and general kallistatin knockout mice ($KS^{-/-}$ mice). The protective actions of endogenous kallistatin in vascular senescence were validated by exacerbated senescence, oxidative stress and inflammation in mouse lung endothelial cells isolated from $KS^{endo-/-}$ mice. Importantly, kallistatin is essential for protection of vascular and organ injury as systemic depletion of kallistatin aggravated vascular oxidative stress and renal interstitial fibrosis in diabetic mice. The current study indicates an important role of kallistatin in vascular injury and age-related vascular diseases.

Oxidative stress and inflammation are hallmarks of endothelial senescence (Erusalimsky, 2009, Salminen *et al.*, 2012). Kallistatin administration has been shown to attenuate vascular injury and organ damage and aging, in conjunction with reduced oxidative stress and inflammation in animal models with hypertension, arthritis, diabetes and sepsis (Shen *et al.*, 2008, Shen *et al.*, 2010, Yin *et al.*, 2010, Li *et al.*, 2014, Lin *et*

al., 2015, Yiu *et al.*, 2016). In this study, we showed that kallistatin inhibited H_2O_2-induced oxidative stress and pro-inflammatory gene expression, including VCAM-1, ICAM-1 and IL-6, in human endothelial cells. Moreover, kallistatin stimulated antioxidant gene expression, including SIRT1, eNOS, catalase and SOD-2. NO production by eNOS inhibits superoxide formation and inflammation. Catalase, one of SIRT1's downstream antioxidant enzymes, is decreased in H_2O_2-induced premature senescence. Human SOD-2 and mouse SOD-1 are antioxidant enzymes and play an important role in the prevention of endothelial senescence and inflammation (Velarde *et al.*, 2012, Zhang *et al.*, 2017). Previous reports indicated a reciprocal positive feedback regulation between SIRT1 and eNOS. SIRT1 has been shown to induce eNOS expression and activity, and eNOS through NO formation upregulates SIRT1 and maintains vascular homeostasis. Kallistatin was shown to increase SIRT1 and eNOS synthesis in human endothelial cells and EPCs (Guo *et al*., 2015, 2017). Moreover, kallistatin treatment increased eNOS activity and NO formation in human endothelial cells (Shen *et al.,* 2010). The present study shows that kallistatin stimulates SIRT1-mediated eNOS pathway, as kallistatin-induced eNOS expression was blocked by SIRT1 inhibitor NAM, but kallistatin-mediated SIRT1 expression was not affected by NOS inhibitor L-NAME. Collectively, kallistatin through stimulating SIRT1-mediated eNOS pathway protects against senescence, oxidative stress and inflammation.

Let-7g was recently recognized as an anti-aging miRNA to improve endothelial functions (Liao *et al.,* 2014). Let-7g negatively regulated apoptosis, senescence and inflammation in endothelial cells (Zhang *et al*., 2013; Liao *et al*., 2014; Liu *et al*. 2017). Upregulation of SIRT1 levels was involved in Let-7g-mediated inhibition of endothelial senescence. In this study, we showed that kallistatin increased Let-7g synthesis, and kallistatin, via Let-7g induction, stimulated SIRT1 and eNOS, leading to inhibition of

endothelial senescence, oxidative stress and inflammation in endothelial cells. Importantly, kallistatin harbors two structural elements, an active site and a heparin-binding domain. Kallistatin's active site is essential for eNOS and SIRT1 expression through interacting with a tyrosine kinase in EPCs and endothelial cells (Guo *et al*. 2015, 2017). It is likely that kallistatin via the active site interacts with tyrosine kinase to stimulate Let-7g synthesis. Moreover, miR-34a-SIRT1 axis has been regarded to be one of critical pathways to regulate endothelial senescence (Ito *et al*. 2010). Our previous study showed that kallistatin reduced EPC senescence and aorta aging by inhibiting the synthesis of miR-34a, a pro-senescent miRNA. Consistently, the current study indicates that kallistatin treatment prevented H_2O_2-induced miR-34a synthesis in endothelial cells. Importantly, we found that Let-7g is the upstream regulator of miR-34a in response to kallistatin treatment. These results indicate that kallistatin protects against endothelial senescence by upregulating Let-7g to inhibit miR-34a-SIRT1-eNOS pathway.

To further investigate the role of endogenous kallistatin in vascular senescence, $KS^{endo-/-}$ mice were produced by loxp/Cre technology, and lung endothelial cells from $KS^{endo-/-}$ mice and WT littermates were isolated and cultured. Kallistatin deficiency in mouse endothelial cells accelerated replicative senescence and superoxide formation. Upon H_2O_2 treatment, kallistatin deficiency further aggravated stress-induced senescence, oxidative stress and inflammation, indicating a protective role of endogenous kallistatin in maintaining endothelial viability and function. Furthermore, exacerbated senescence in $KS^{endo-/-}$ endothelial cells was associated with elevation of miR-34a, and reduction of Let-7g, SIRT1, eNOS, catalase and SOD-1. Thus, Let-7g-mediated inhibition of miR-34a-SIRT1-eNOS pathway is suppressed when kallistatin is deficient. These combined findings support the notion that endogenous kallistatin acts as

a protective molecule in vascular injury and senescence by stimulating Let-7g, SIRT1 and eNOS, and suppressing miR-34a synthesis.

We generated general kallistatin knockout mice for the first time. There were no physiological changes except lighter body weight in male $KS^{-/-}$ mice. Kallistatin gene delivery has been shown to decrease aortic superoxide levels and glomerular endothelial loss, and reduce renal fibrosis in hypertensive rats (Shen *et al*., 2008; Shen *et al.,* 2010). Conversely, kallistatin depletion by neutralizing kallistatin antibody injection exacerbated renal and cardiovascular oxidative stress, inflammation and organ injury in hypertensive rats (Liu *et al*., 2012). Here we used STZ-induced diabetic $KS^{-/-}$ mice to further confirm the role of kallistatin in vascular oxidative injury and renal fibrosis. In keeping with previous findings regarding kallistatin's inhibition in EndMT, organ fibrosis and vascular injury (*Shen et al.*, 2008; Shen *et al.,* 2010; Guo *et al.,* 2015), kallistatin depletion aggravated vascular oxidative stress and renal dysfunction and fibrosis. SIRT1 and eNOS expression was significantly suppressed in aorta of $KS^{-/-}$ mice. EndMT markers were regulated towards pro-EndMT occurrence. Further studies need to perform to validate whether the interstitial fibrosis is originated from EndMT. These findings suggest that endogenous kallistatin plays a protective role in diabetes-induced vascular injury and renal fibrosis.

Overall, this study indicates that kallistatin inhibits cellular senescence, oxidative stress and inflammation by promoting Let-7g-mediated inhibition of miR-34a-SIRT1-eNOS pathway in human endothelial cells. Moreover, endogenous kallistatin plays a protective role in endothelial senescence, vascular and organ injury. Therefore, kallistatin could potentially be used as a promising new therapeutic strategy for vascular aging and dysfunction in humans.

CHAPTER VI

GENERAL DISCUSSION

Discussion:

The goal of this research project is to gain insights into the role and mechanism of kallistatin in vascular injury, senescence and aging, using cultured endothelial cells, EPCs, STZ-induced diabetic mice, kallistatin deficient mice ($KS^{endo-/-}$ and $KS^{-/-}$) and *C. elegans*. Vascular-related diseases progress with advancing age, which is primarily attributed to pathophysiological changes in blood vessels (Strait & Lakatta, 2012). The structural remodeling is featured with neointima thickening, rarefaction of endothelial cells, increased oxidative stress and inflammation (Asahara *et al.*, 1997, Lakatta, 2002, Foreman & Tang, 2003). Endothelial cells upon injury insults can undergo EndMT, senescence or inflammation (Erusalimsky, 2009, Agarwal *et al.*, 2016). We first demonstrated the efficacy of kallistatin in preventing EndMT, a process mediating vascular injury, organ fibrosis and tumor progression. Moreover, kallistatin treatment reduced senescence and aging in cultured EPCs and endothelial cells, mouse aorta, and *C. elegans*. We found that the central mechanism for kallistatin in suppression of EndMT and vascular senescence is mediated by stimulating antioxidant gene expression. Conversely, endogenous kallistatin deficiency exacerbated endothelial senescence, oxidative stress and inflammation in mouse endothelial cells. In contrast to kallistatin's efficacy in aortic injury and EndMT, systemic kallistatin depletion in $KS^{-/-}$ mice aggravated diabetes-induced vascular oxidative stress and renal fibrosis. These findings imply a crucial role of endogenous kallistatin in protection against vascular injury, senescence and aging.

Our previous studies showed that kallistatin gene delivery inhibited renal fibrosis in hypertensive rats, cardiac fibrosis in rats with myocardial infarction, and tumor growth in mice with tumor xenografts (Miao *et al.*, 2002, Gao *et al.*, 2008, Shen *et al.*, 2008). EndMT is a process mediating neo-intimal thickening by promoting endothelial cell

differentiation to matrix-producing fibroblasts (Arciniegas *et al*., 1992). Accumulating evidence indicates the involvement of EndMT in renal interstitial fibrosis, pulmonary fibrosis and cardiac fibrosis (Jimenez, 2013, Kong *et al*., 2014). Aberrant TGF-β-Akt signaling is primarily activated to drive fibrosis (Meadows *et al*., 2009). TGF-β promotes superoxide generation and matrix protein deposition and makes endothelial cells lose cell-cell junction and be invasive. miR-21, an oncogenic miRNA potentiates TGF-β responses by inhibiting phosphatase and tensin homolog (PTEN), an inhibitor of Akt phosphorylation (Kumarswamy *et al*., 2012). Our current study showed that kallistatin antagonized TGF-β-induced EndMT by blocking miR-21-Akt pathway and inhibiting oxidative stress. This study provided new insights that kallistatin via its active site stimulated eNOS and SIRT1 synthesis and via its heparin-binding domain blocked TGF-β-induced miR-21-Akt pathway. These findings not only revealed the mechanism by which kallistatin inhibits EndMT but also provided supportive evidence that kallistatin through inhibiting EndMT protects against vascular injury, organ fibrosis and tumor progression.

The supply of *de novo* endothelial cells by EPC pool renders EPCs essential for vascular repair (Rumpold *et al*., 2004). However, EPC senescence directly affects its normal rejuvenation capacity, leading to vascular injury (Heiss *et al*., 2005). Kallistatin has been found to increase circulating EPC number in hypertensive rats, and enhance EPC proliferation, migration, adhesion and tube formation *in vitro* by activation of PI3K-Akt-eNOS pathway (Gao *et al*., 2014). Consistently, this study showed that kallistatin inhibited senescence-associated oxidative stress in EPCs by stimulating antioxidant genes, eNOS and SIRT1 synthesis. SIRT1 is a longevity gene, which is inversely regulated by miR-34a, a pro-senescent miRNA (Ito *et al*., 2010). Likewise, miR-21 is

involved in accelerating cellular senescence in EPCs (Zhu *et al*., 2013). This is the first study to demonstrate that kallistatin inhibits EPC senescence associated with reduction of miR-34a, miR-21 and elevation of eNOS and SIRT1 levels. Inhibition of miR-21 and stimulation of antioxidant genes may extend kallistatin's efficacy in EndMT to senescence. Notably, overexpression of miR-34a abolished kallistatin's protective effect on senescence and SIRT1/eNOS stimulation, highlighting the important role of miR-34a in kallistatin-mediated anti-senescence in EPCs. Type 1 diabetes has been documented to be associated with aortic senescence (Ota *et al*., 2010). We used STZ to establish type 1 diabetes in mice. Our study supports the notion that kallistatin inhibits diabetes-induced aortic senescence and oxidative stress by preventing miR-34a-SIRT1/eNOS pathway.

Recent study reported that plasma kallistatin levels were positively associated with leukocyte telomere length in young African Americans (Zhu *et al*., 2016). Telomere length is a decisive factor for cellular lifespan, thus kallistatin may have a potential anti-aging effect. Indeed, our study showed that kallistatin could suppress *in situ* superoxide formation and delay the aging process under heat or oxidative stress conditions in *C. elegans*. *C. elegans* possesses a short lifespan and conservative longevity gene expression. Two of the pronounced regulatory genes are miR-34 and sir-2.1 (SIRT1 homolog). Kallistatin enhanced *C. elegans* survival under stress conditions in wild-type *C. elegans* but not in miR-34 mutant or sir-2.1 mutant worms, indicating a crucial role of miR-34 and SIRT1 in kallistatin–regulated longevity. This study demonstrated a role of kallistatin in delaying the aging process at the organismal level.

It is well known that oxidative stress, inflammation and senescence are intricately related (Erusalimsky, 2009, Guzik & Touyz, 2017). Oxidative stress and inflammation

are implicated in various age-associated cardiovascular diseases (Guzik & Touyz, 2017). Our study showed that kallistatin inhibited H_2O_2-induced endothelial senescence, associated with elevated antioxidant gene synthesis, and reduced pro-inflammatory gene expression in human endothelial cells. Using pharmacological inhibitors of eNOS and SIRT1, this study further revealed that kallistatin through SIRT1 stimulated eNOS synthesis. Let-7g has been shown to inhibit endothelial senescence, apoptosis and inflammation (Zhang *et al*., 2013, Liao *et al*., 2014). We found that kallistatin through Let-7g upregulation prevented miR-34a-SIRT1-eNOS pathway to achieve its anti-senescent, antioxidant and anti-inflammatory actions. Moreover, kallistatin deficiency in mouse lung endothelia cells exacerbated senescence, superoxide formation and inflammation in conjunction with reduced Let-7g and antioxidant gene expression, and elevated miR-34a synthesis. These studies confirmed that endogenous kallistatin is crucial for reducing endothelial senescence, oxidative stress and inflammation. These combined findings provided new insight into the mechanism of kallistatin in protection against endothelial senescence by regulating Let-7g-mediated miR-34a-SIRT1-eNOS pathway.

In this study, we generated two strains of kallistatin knockout mice, endothelial cell-specific kallistatin deficient ($KS^{endo-/-}$) mice and general kallistatin knockout ($KS^{-/-}$) mice, using Loxp-Cre recombination technique. To avoid potential embryonic fatality of $KS^{-/-}$ mice, Cre recombinase activity in $KS^{-/-}$ mice were induced by tamoxifen at four to five weeks of age. Our previous report showed that kallistatin depletion by neutralized antibody injection exacerbates renal and cardiovascular injury in hypertensive rats (Liu Y. *et al.*, 2012). Likewise, we observed that systemic depletion of kallistatin in general knockout mice worsened aortic oxidative stress and renal fibrosis in STZ-induced diabetes. Kallistatin deficiency reduced eNOS and SIRT1 levels and elevated oxidative stress in the aorta of diabetic mice. In parallel with the EndMT study, interstitial fibrosis,

as indicated by collagen deposition, was further aggravated in kidney of systemic kallistatin knockout mice with STZ-induced diabetes. Renal fibrosis was associated with reduced capillary density and increased fibroblasts in diabetic $KS^{-/-}$ mice, as evidenced by decreased endothelial marker Tie2 and increased mesenchymal marker expression, fibronectin and α-SMA. These findings confirmed the protective role of endogenous kallistatin in vascular and organ injury.

Besides kallistatin's beneficial effects on vascular oxidative stress and organ fibrosis, our future study will further determine the role of endogenous kallistatin in vascular senescence and inflammation using general kallistatin knockout mice with STZ-induced diabetes. Senescent phenotype and biomarkers in aortas of diabetic $KS^{-/-}$ mice will be evaluated. Inflammatory gene expression and histologic investigation for inflammatory cell infiltration in vascular or renal section will be examined. We expect that the future study could substantiate kallistatin's crucial role in vascular injury and senescence by its antioxidant and anti-inflammatory actions.

Appendix 1

Tissue Homogenization and Plasma Collection

Tissue Homogenization

1. Mince mouse tissues on ice into small pieces and homogenize 10 mg of tissue in 500 µL ice-cold lysis buffer (50 mM Tris-HCl, 150 mM NaCl, 1 mM disodium EDTA, 0.1 mM EGTA, 1% Nonidet P-40, 0.1% sodium dodecyl sulfate, 0.5% sodium dexoycholate) with 1% protease inhibitor.

2. Homogenize thoroughly and keep tissues on ice for 30 min.

3. Centrifuge the homogenate at high speed (12000 × g) for 30 min at 4°C.

4. Transfer the supernatant into a new tube and store at -80°C.

Plasma Collection

1. Collect whole blood into commercially available anticoagulant EDTA-treated capillary tubes.

2. Stand the sample on ice at least 30 min.

3. Centrifuge at 3000 rpm for 30 min at 4°C.

4. Collect supernatant (plasma) and store at -80°C.

Appendix 2

RNA Extraction

1. Add 0.3-0.4 mL of TRIzol Reagent per 1×10^5-10^7 cells to lyse the cells. Add 1 mL of TRIzol reagent per 100 mg of tissue to homogenize samples.

2. Incubate for 20 min at room temperature to permit the complete dissociation of nucleoprotein complexes.

3. Add 0.2 mL of chloroform per 1 mL of TRIzol Reagent for phase separation.

4. Incubate for 2-3 min at room temperature.

5. Centrifuge the sample for 15 min at 12000 × g at 4°C.

6. Transfer the aqueous phase to a new tube. Add 0.5 ml of isopropanol to the aqueous phase, per 1 mL of TRIzol Reagent used for lysis.

7. Shake vigorously by hand for 15 s and incubate for 10 min at room temperature.

8. Centrifuge for 10 min at 12000 × g at 4°C.

9. Remove the supernatant, wash the RNA pellet once in 1 mL of 75% ethanol per 1 ml of TRIzol Reagent used for lysis.

10. Vortex the sample briefly and centrifuge for 5 min at 7500 × g at 4°C.

11. Air-dry RNA pellet for 5-10 min.

12. Dissolve RNA in 20-30 µL DEPC water and incubate in a heat block set at 55-60 °C for 10-15 min.

13. Determine RNA concentration using Nano-drop instrument.

Appendix 3

Reverse Transcription-Polymerase Chain Reaction (RT-PCR)

For mRNA RT-PCR:

1. Dilute RNA to 0.2 μg/μL in DEPC H_2O.

2. Prepare the 2 × RT master mix on ice (per 20 μL reaction, Life Technologies)

Component	Volume/ Reaction (μL)
10×RT buffer	2.0
25× dNTP Mix (100 mM)	0.8
10× RT Random Primers	2.0
MultiScribe Reverse transcriptase	1.0
RNase Inhibitor	1.0
Nuclease-free H_2O	3.2
Total volume:	10.0

3. Mix 2 × RT master mix briefly.

4. Add10 μl of RNA sample to 10 μL of 2 × RT master mix.

5. Mix well and centrifuge, then load the thermal cycler.

6. Run PCR cycles (25°C for 10 min, 37°C for 120 min, 85°C for 5 min and 4°C forever).

For miRNA RT-PCR:

1. Dilute RNA to 0.2 μg/μL in DEPC H_2O.

2. Prepare the RT master mix on ice (per 15 μL reaction, Life Technologies)

Component	Volume/ Reaction (μL)
10 × RT buffer	1.50
25 × dNTP Mix (100 mM)	0.15

MultiScribe Reverse transcriptase	1.00
RNase Inhibitor	0.19
Nuclease-free H_2O	4.16
Total volume:	7.00

---

3. Add 3 µL of 5 × RT primers and 5 µL of RNA sample to each 7 µL master mix.

4. Mix gently and centrifuge, then load the thermal cycler.

5. Run PCR cycles (16°C for 30 min, 42°C for 30 min, 85°C for 5 min and 4°C forever).

Appendix 4

Quantitative Real-time Polymerase Chain Reaction (qRT-PCR)

For cDNA qPCR amplication

1. Dilute cDNA to 5-10 ng/µL.

2. TaqMan® Gene Expression Assay (20 X, primers and probe) is thawed on ice, resuspended completely by gently vortexing, then centrifuged briefly.

3. Mix the master mix reagent by gently swirling the bottle.

4. Prepare a PCR reaction mix (per 20 µL reaction):

Component	Volume per 20 µL Sample	Final Concentration
TaqMan master mix (2 X)	10.0	1 X
Taqman Primer	1.0	50 nM
Water	7.0	_
Total Volume	18.0	_

5. Mix and transfer 18 µL reaction mix to each well of a 96-well PCR plate.

6. Add 2.0 µL DNA sample to reaction mix per replicate.

7. Seal the plate and centrifuge the plate briefly.

8. Load the plate into the BioRad PCR instrument.

9. Set thermal cycling conditions: UDG incubation at 50°C for 2 min, AmpliTaq Gold enzyme activation at 95°C for 10 min; PCR cycle (X 40): denature at 95°C for 15 s and anneal/extend at 60°C for 1 min.

For Small RNA qPCR amplification

1. Obtain a sterile 1.5 mL microcentrifuge tube for each sample.

2. Prepare PCR reaction mix (per 20 µL reaction)

Component	Volume per 20 µL Reaction (µL)

Taqman Small	
RNA Assay (20X)	1.00
Product form RT reaction	1.33
Taqman Master Mix (2X)	10.00
Nuclease-free water	7.67
Total volume	20.00

3. Cap the tube and invert several times to mix.

4. Centrifuge the tube briefly.

5. Transfer 20 µL of the complete PCR reaction mix into each well on a 96-well plate.

6. Seal the plate and centrifuge the plate briefly.

7. Load the plate into PCR instrument.

8. Run the PCR cycle as above.

Appendix 5

Recombinant Human Kallistatin Purification

1. Culture 293T HEK His-tag kallistatin cells to 90% confluency at 37°C in 5% CO_2 incubator.

2. Collect the media and centrifuge at 12000 rpm at 4°C for 30 min.

3. Suspend supernatant in 80% of ammoniums sulfate. Stir for 2-3 hrs at 4°C.

4. Centrifuge at 12000 rpm at 4°C for 30 min.

5. Suspend the pellet in 30 mL of cold ddH_2O and then stir at 4°C for 30 min.

6. Dialyze with 1 mM EDTA 4 × of one litter at 4°C using10000 MW dialysis cassette. Centrifuge at 12000 rpm at 4°C for 30 min.

7. Dialyze with 0.02 M Na_2HPO_4/0.5 M NaCl, 2 × of one litter.

8. His-Tag resin (4-5 mL). Mix the protein with His-Tag resin, rotate over night at 4°C.

9. Next day stop rotating, let it sit for 1 h. Pack the column and wash with 300 mL of washing buffer (0.02 M Na_2HPO_4, 0.5 M NaCl, and 10 mM Imidazole).

10. Elute with 1 mL of 4 × elution buffer and 5 mL of H_2O.

11. Dialyze with 1 × PBS and measure protein concentration at OD280.

Appendix 6

Gelatin Zymography

Prepare the samples:

1. Homogenize samples in ice-cold lysis buffer (pH 5.0, cacodylic acid 10 mM; NaCl 0.15 M; ZnCl 20 mM; NaN_3 1.5 mM; Triton X-100 0.01% and proteinase inhibitor). 1:3 (wt/vol).
2. Centrifuge the homogenates for 10 min at 14000 rpm at 4°C.
3. Measure the protein concentration with pierce BCA assay kit (Thermo scientific).

SDS-PAGE

1. Prepare the gel: 4% stacking gel and 10% SDS-PAGE polymerized with gelatin type I in a final concentration of 1 mg/mL (heat 30 s in microwave).
2. Load samples: loading buffer (non-reducing: 10% SDS; 4% sucrose; 0.25M Tris HCl and 0.1% bromophenol blue pH 6.8). 50 µg sample is diluted at 3:1 with loading buffer, without boiling.
3. Run the gel at 15 mA in stacking gel and 20 mA in separating gel at 4°C.

Gel Washing and Staining:

1. Incubate gel in renaturing buffer (2.5% Triton-X-100) for 30 min to remove SDS. First time 100 mL for 10 min, then change to 100 ml for 20 min.
2. Wash in 150 mL ddH_2O for 10-30 min.
3. Incubate gel in developing buffer (50 mM Tris pH 8.0; 5 mM $CaCl_2$; 0.2 M NaCl; 0.02% Brij-35) for 30 min and change to fresh developing buffer for 16 h at 37°C.
4. Stain gel with Coomassie blue G-250 solution (dissolve 1.25 g Coomassie Blue G-250 in 250 mL methanol, then add 250 mL ddH_2O and 50 ml acetic acid) for 30 min.
5. Destain gel with 7% acetic acid, 20% methanol and 73% H_2O solution until bands can be clearly seen.

Appendix 7

SDS-PAGE and Western Blot Analysis

SDS-PAGE Solutions

Separating gel buffer (pH 8.8): 7.38 g Tris-HCl, 30.7 g Tris-Base, 0.8 g SDS in 200 mL ddH_2O.

Stacking gel buffer (pH 6.8): 7.9 g Tris-HCl, 0.4 g SDS in 100 mL ddH_2O.

10% ammonium persulfate (AP): 1.0 g AP in 10 mL ddH_2O.

30% acrylamide: 75 g acrylamide, 2 g methylenebisacrylamide in 250 mL ddH_2O.

10 × running buffer (pH 8.3): Tris-Base 30.35 g, glycine 144.0 g, SDS 10.0 g. Bring to 1 L with ddH_2O.

5 ×SDS loading buffer (pH 6.8): 1 M Tris-HCl (pH 6.8) 3.75 mL, SDS 1.5 g, DTT 1.16 g, bromophenol blue 1.5 mg, glycerol 7.5 mL, ddH_2O 7.5 mL.

Prepare SDS-PAGE gel:

1. Clean the small and large glass plates with ddH_2O and 70% ethanol. Set up the glass casting apparatus.

2. Prepare polyacrylamide separating gel solution (for 2 gels, 10 wells):

Mixture	10%
ddH_2O	4.2 mL
30% acrylamide	3.3mL
Separating buffer	2.5mL
10% AP	55 µL
TEMED	3 µL

3. Dispense the solution into the casting chamber. Add water slowly until full. Wait 40 min or until polymerized.

4. Prepare polyacrylamide stacking solution (for 2 gels, 10 wells):

ddH_2O	1.5 mL
30% acrylamide	375 µL
Stacking buffer	625 µL
10% AP	7.5 µL
TEMED	4 µL

5. Remove the water overlay and dispense the stacking gel solution. Insert the comb. Allow 30 min for polymerization. Remove the comb.

6.Transfer the polymerized gel to the running apparatus. Pour the 1 × running buffer until it covers the plates.

7. Load sample (15-50 µg) after boiling at 100°C for 5 min into the wells.

8. Run at 180 V for 40-60 min.

Western Blot Solutions

1 x Transfer buffer (pH 8.3): 3.03 g Tris-Base, 14.4 g glycine, 200 mL methanol, bring to 1 L with ddH_2O.

10 X Tris-buffered saline (TBS), pH 7.6: 24.2 g Tris-Base, 80 g NaCl dissolved in 1L ddH_2O. Adjust pH to 7.6 with HCl.

Tris-buffered saline, 0.1% Tween 20 (TBST): Add 1 mL Tween-20 to 1 L 1 X TBS buffer.

Gel transfer

1. Pre-soak sponges, blotting paper and membrane. Add transfer buffer to a plastic tub. Place the stack to the black side of the plastic holder in the following order: sponge, blotting paper, membrane, gel, blotting pager and sponge.

2. Remove all air bubbles and close the plastic holder. Place the transfer sandwich into the running chamber. Add ice holder and fill with transfer buffer.

3. Run at 100 V at 4°C for 1 h.

Detection using chemiluminescence (ECL+Plus)

1. Rinse the membrane briefly with TBST for 5 min X 2. Block the membrane with 7% milk in TBST for 1 hr at room temperature on an orbital shaker.

2. Wash twice with TBST, 5 min each.

3. Incubate with primary antibody in 5% milk TBST overnight at 4°C with shaking.

4. Wash the membrane for 3 X 5 min with TBST.

4. Incubate with appropriate secondary antibody (1:5000 to 1: 10000 in 5% milk TBST) for 1 hr at room temperature. Wash 3 X 10 min with TBST.

5. Apply chemiluminescence chemicals solution A and solution B at a ratio of 1: 1 (500 µL each) at dark, for each membrane add enhancer solution A and B (80 µL each).

6. Drain off excess detection solution and wrap the membrane in Saran Wrap.

7. Capture the chemiluminescent signals using a bio-rad camera-based imager.

8. Use image analysis software to read the band intensity of the target proteins.

Appendix 8

NAD(P)H Oxidase Activity Assay

Solutions:

Reaction Buffer: 50 mM Na phosphate, pH 7.2, 0.01 mM EDTA, pH 8.0.

5 mM lucigenin (Sigma M-8010, store at RT) in reaction buffer.

2 mM NADH (Sigma N8129, stored at 4°C) in reaction buffer.

2 mM NADPH (Sigma N1630, store at -20°C) in reaction buffer.

Activity Procedure:

1. Let the TD-20/20 luminometer warm up for 5 min and set up as follows:

   a. Inj 1: OFF, Inj 2: OFF

   b. Set up: Delay = 5 sec, Integrate = 900 sec, Replicate = 1

   c. Set up: 888, set sensitivity to 60.1 %

2. Once set up is complete, prepare NADPH blanks in cuvettes and record light intensity.

reaction buffer	1.37 mL
5 mM lucigenin	75 µL (250 µM)
2 mM NADH or NADPH	55 µL (100 µM)
	1.5 mL

3. Prepare sample reaction mixtures in cuvettes and record light intensity.

reaction buffer	1.35 mL
5 mM lucigenin	75 µL (250 µM)
2 mM NADH or NADPH	55 µL (100 µM)
sample	20 µL
	1.5 mL

4. Calculate activity as follows:

$$\frac{\text{(sample intensity - blank intensity)}}{\text{protein conc. (mg/mL) x 0.02 mL x time (min)}} = \text{rlu/mg protein/min}$$

Appendix 9

Transfection of MicroRNA-34a Mimic or Let-7g Inhibitor

1. One day before transfection, culture cells (in 12-well plate) in 500 µL of growth medium without antibiotics such that they will be 30-50% confluent at the time of transfection.

2. For each well to be transfected, prepare RNAi duplex-Lipofectamine® RNAiMAX complexes as follows:

A. Dilute 6 pmol miRN-34a mimic or control siRNA in 50 µL Opti-MEM® I Reduced Serum Medium without serum. Mix gently.

B. Mix Lipofectamine™ RNAiMAX gently before use, then dilute 1 µL in 50 µL Opti-MEM® I Reduced Serum Medium. Mix gently.

C. Combine the diluted RNAi duplex with the diluted Lipofectamine™ RNAiMAX. Mix gently and incubate for 10-20 min at room temperature.

3. Add the RNAi duplex-Lipofectamine® RNAiMAX complexes to each well containing cells. This gives a final volume of 600 µL and a final RNA concentration of 10 nM. Mix gently by rocking the plate back and forth.

4. Incubate the cells 6-12 h at 37°C in a CO_2 incubator until you are ready to assay for gene knockdown. Medium may be changed after 4-6 h.

5. Perform qRT-PCR to detect transfection efficiency.

Appendix 10

Telomerase Activity

Extract Preparation

1. Pellet the cells or tissue, wash once with PBS, repellet, and carefully remove all PBS.

2. Resuspend the cell pellet in 200 µL of CHAPS lysis buffer/10^5-10^6 cells.

3. Incubate the suspension on ice for 30 min.

4. Spin the sample in a microcentrifuge at 12,000 x g for 20 min at 4°C.

5. Transfer 160 µL of the supernatant into a fresh tube and determine the protein concentration. For cell extract concentration should be 10-750 ng/µL.

6. Aliquot and quick-freeze the remaining extract on dry ice, and store at -80°C.

Required Controls and Samples:

5X TRAPEZE® RT Reaction Mix*	5.0 µL
Taq Polymerase (5 units/µL)	0.4 µL (2 Units)
Nuclease Free Water	17.6 µL
Samples:	2.0 µL

(TSR8 dilutions, positive extract control, telomerase negative, NTC, experimental samples +/- heat treatment)

TOTAL VOLUME 25.0 µL

PCR Amplification

1. Set-up the real-time experiment to include the following PCR parameters.

30°C 30 min 1 cycle

95°C 2.0 min 1 cycle

94°C 15

59 °C 60 sec } × 45

*45°C 10 sec

* Temperature and stage where the Real-time fluorescent data should be collected.

Appendix 11

Genotyping and DNA Electrophoresis

DNA Extraction from Tail Biopsy

1) Cut 0.5 cm tail from each mouse at 3 week-old age.

2) Transfer tail biopsy to 150 µL lysis solution 1 (500 mL: 1.25 mL 10 M NaOH; 2 mL 0.5 M EDTA; 496.75 mL ddH_2O). Incubate samples in 90°C heater block for 45 min.

3) Centrifuge briefly and add 150 µL Solution 2 (pH 7.4, 40 mM Tris). Vortex briefly.

Genotyping:

1. Primers: Serpina3c-A1Loxp-F, Serpina3c-A1Loxp-R; Seripina3c-Frt-F, Seripina3c-Frt-R; Cre-F, Cre-R; LRL-040-A1 Loxp-F, LRL-040-A1 Loxp-R.

2. Prepare a PCR reaction mix in a PCR tube (per 25 µL reaction):

Component	Volume per 25 µL Sample (µL)
AmpliTaq Gold 360 master mix	12.5
Forward Primer	1.0
Reverse Primer	1.0
DNA	2.0
Water	8.5
Total Volume	25.0

3. PCR cycling parameters as below:

95 °C 2 min

95 °C 30 sec
63 °C 30 sec
72 °C 25 sec
} X 35

72 °C 10 min

4°C Finished

DNA Electrophoresis

1. Prepare 3% agarose gel (3 g in 100 mL 1 X Tris-acetate-EDTA buffer, heated in microwave for 1-2 min).

2. Cool down the agarose solution to around 60 °C, add a final concentration of 5 µg/mL ethidium bromide and mix well.

3. Place comb into casting tray and pour the solution to casting tray.

4. Let casting tray sit for 5 min at 4°C or 30 min at room temperature.

5. Add 2 µL 10 X DNA loading buffer to each sample.

6. Set up gel electrophoresis unit. Fill gel box with 1 X TAE until complete covered.

7. Load molecular weight marker and samples into gel wells.

8. Run gel at 130 V for 40 min.

9. Visualize DNA products with UV light.

Appendix 12

Isolation of Mouse Lung Endothelial Cells

Digestion Lung Samples

1. Remove whole lungs of the mouse. Wash whole lungs with serum-free basal-DMEM. Chop the lung tissue using sterile, disposable blades to very small pieces.

2. Transfer the pieces into a 15-mL centrifuge tube containing 1 X working dilution of collagenase digestive solution (7–10 mL per 0.5 g of wet tissue).

3. Digest the lung at 37°C for 45 min under continuous horizontal shaking (300 r.p.m.). Quench the lung-digestive solution mixture with an equal volume of complete-DMEM.

4. Strain the lung digest through the 70-mm cell strainers by releasing the lung digest on the cell strainer using a 5-mL pipette.

5. Restrain cell suspension through a 40-μm cell strainer into a 50-mL centrifuge tube.

6. Centrifuge the 50-mL tube at 300 X g at 4°C for 10 min.

7. Decant the supernatant and resuspend the cell pellet in 10 mL of complete-DMEM.

8. Centrifuge the 50-mL tube at 300 X g at 4°C for 10 min.

9. Decant the supernatant and resuspend the cell pellet in 5 mL of MACS buffer (0.5 % BSA, 2 mM EDTA in PBS). Determine cell number.

Magnetic Labeling

10. Add 90 μL of buffer per 10^7 total cells to the cell pellet. Add 10 μL of CD31 microbeads per 10^7 total cells. Mix well and incubate for 15 min in the refrigerator.

11. Wash cells by adding 1−2 mL of buffer per 10^7 cells and centrifuge at 300 X g for 10 min. Aspirate supernatant completely.

12. Resuspend up to 10^8 cells in 500 μL of buffer.

Magnetic Separation

13. Prepare column by rinsing with 3 mL MACS buffer for each LS column.

14. Apply cell suspension onto the column. Collect flow-through containing unlabeled cells.

15. Wash column with 3 × 3 mL MACS buffer. Collect unlabeled cells that pass through and combine with the flow-through from step 3.

16. Remove column from the separator and place it on a suitable collection tube.

17. Pipette 5 mL MACS buffer onto the column. Immediately flush out the magnetically labeled cells by firmly pushing the plunger into the column.

18. Centrifuge for 5 min. Resuspend cells with EBM-2 media and culture cells in gelatin-coated dishes.

19. After 10 days' culture, digest cells and repeat steps 10-19 for second round of CD31 immunoselection.

Appendix 13

Immunocytochemistry

1. Aspirate the culture media of cells grown in 6- or 12-well plates, then cover cells with 4% formaldehyde diluted in 1 × PBS.

2. Allow cells to fix for 15 min at room temperature.

3. Aspirate fixative, rinse 3 times in 1 × PBS for 5 min each.

4. Block specimen in blocking buffer (1 × PBS / 3% BSA / 0.2% Triton X-100) for 60 min.

5. Aspirate blocking buffer, apply diluted primary antibody in antibody dilution buffer (1 ×PBS / 1% BSA / 0.3% Triton X-100) and incubate overnight at 4°C.

6. Rinse 3 times in 1 × PBS for 5 min each.

7. Incubate specimen in fluorochrome-conjugated secondary antibody diluted in antibody dilution buffer for 1-2 h at room temperature in the dark.

8. Rinse 3 times in 1 × PBS for 5 min each.

9. Counterstain the nuclei with Hoechst 33343 (5 µg/mL in PBS) for 5 min.

10. Rinse 3 times in 1 × PBS for 5 min each and mount.

Appendix 14

Picosirius Red Staining

Solutions:

0.2% Phosphomolybdic Acid (PMA): 0.2 g PMA in 100 mL ddH_2O.

1% aqueous solution Sirius red: 0.5 g in 50 mL ddH_2O.

Sirius red in picric acid: 10 mL of 1% aqueous solution, 90 mL saturated picric acid, pH 2.0. Let the solution sit for 24 h at room temperature.

Procedure

1. Deparaffinize and rehydrate paraffin-embedded sections to water.
2. Incubate slides in 0.2% PMA for 5 min.
3. Rinse briefly in distilled water.
4. Stain in picosirius red solution (pH 2.0) for 90 min.
5. Rinse in 0.01 N HCl, change solution in jars for 3 or 4 times.
6. Dehydrate and mount.

Appendix 15

SA-β-gal Staining

Solutions

Staining solution: 40 mM citric acid/sodium phosphate (pH 6.0), 0.15 M NaCl, 2 mM $MgCl_2$.

100 × Staining solution supplement A: 500 mM potassium ferrocyanide.

100 × Staining solution supplement B: 500 mM potassium ferricyanide.

Fixative solution: 2% formaldehyde, 0.2% glutaraldehyde in 1 × PBS

β-gal staining solution: For each 35 mm well to be stained, add 930 µL staining solution, 10 µL staining supplement A, 10 µL staining supplement B, 50 µL 20 mg/mL X-gal in DMF into a polypropylene container. Adjust pH to 5.9-6.1.

Procedure

1. Rinse the cell culture plate one time with 1 × PBS (2 mL for a 35 mm well).

2. Add 1 mL of fixative solution to each 35 mm well. Allow cells to fix for 10-15 min at room temperature.

3. Rinse the plate two times with 1 × PBS.

4. Add 1 mL of the β-gal staining solution to each 35 mm well. Incubate the plate at 37°C overnight in a dry incubator (no CO_2).

5. Check the cells under a microscope (200 × magnification) for the development of blue color.

6. For long-term shortage of the plates, remove the β-gal staining solution and overlay the cells with 70% glycerol. Store at 4°C.

REFERENCES:

Adhikari N, Basi DL, Townsend D, Rusch M, Mariash A, Mullegama S, Watson A, Larson J, Tan S, Lerman B, Esko JD, Selleck SB, Hall JL. Heparan sulfate Ndst1 regulates vascular smooth muscle cell proliferation, vessel size and vascular remodeling. J Mol Cell Cardiol. 2010; 49: 287-293.

Agarwal S, Loder S, Cholok D, Peterson J, Li J, Fireman D, Breuler C, Hsieh HS, Ranganathan K, Hwang C, Drake J, Li S, Chan CK, Longaker MT, Levi B. Local and Circulating Endothelial Cells Undergo Endothelial to Mesenchymal Transition (EndMT) in Response to Musculoskeletal Injury. Sci Rep. 2016; 6: 32514.

Alcendor RR, Gao S, Zhai P, Zablocki D, Holle E, Yu X, Tian B, Wagner T, Vatner SF, Sadoshima J. Sirt1 regulates aging and resistance to oxidative stress in the heart. Circ Res. 2007; 100: 1512-1521.

Alphonse RS, Vadivel A, Zhong S, McConaghy S, Ohls R, Yoder MC, Thebaud B. The isolation and culture of endothelial colony-forming cells from human and rat lungs. Nat Protoc. 2015; 10: 1697-1708.

Arciniegas E, Sutton AB, Allen TD, and Schor AM. Transforming growth factor beta 1 promotes the differentiation of endo- thelial cells into smooth muscle-like cells in vitro. J Cell Sci. 1992; 103: 521–529.

Asahara T, Murohara T, Sullivan A, Silver M, van der Zee R, Li T, Witzenbichler B, Schatteman G, Isner JM. Isolation of putative progenitor endothelial cells for angiogenesis. Science. 1997; 275: 964-967.

Baker JB, Low DA, Simmer RL, Cunningham DD. Protease-nexin: a cellular component that links thrombin and plasminogen activator and mediates their binding to cells. Cell. 1980; 21: 37-45.

Bennett MR. Apoptosis in the cardiovascular system. Heart. 2002; 87: 480-487.

Bhayadia R, Schmidt BM, Melk A, Homme M. Senescence-Induced Oxidative Stress Causes Endothelial Dysfunction. J Gerontol A Biol Sci Med Sci. 2016; 71: 161-169.

Bhoola KD, Figueroa CD, Worthy K. Bioregulation of kinins: kallikreins, kininogens, and kininases. Pharmacol Rev. 1992; 44: 1-80.

Billingsley GD, Walter MA, Hammond GL, Cox DW. Physical mapping of four serpin genes: alpha 1-antitrypsin, alpha 1-antichymotrypsin, corticosteroid-binding globulin, and protein C inhibitor, within a 280-kb region on chromosome l4q32.1. Am J Hum Genet. 1993; 52: 343-353.

Braitsch CM, Kanisicak O, van Berlo JH, Molkentin JD, Yutzey KE. Differential expression of embryonic epicardial progenitor markers and localization of cardiac fibrosis in adult ischemic injury and hypertensive heart disease. J Mol Cell Cardiol. 2013; 65: 108-119.

Brunet A, Sweeney LB, Sturgill JF, Chua KF, Greer PL, Lin Y, Tran H, Ross SE, Mostoslavsky R, Cohen HY, Hu LS, Cheng HL, Jedrychowski MP, Gygi SP, Sinclair DA, Alt FW, Greenberg ME. Stress-dependent regulation of FOXO transcription factors by the SIRT1 deacetylase. Science. 2004; 303: 2011-2015.

Cavallaro U, Castelli V, Del Monte U, Soria MR. Phenotypic alterations in senescent large-vessel and microvascular endothelial cells. Mol Cell Biol Res Commun. 2000; 4: 117-121.

Chai KX, Chen LM, Chao J, Chao L. Kallistatin: a novel human serine proteinase inhibitor. Molecular cloning, tissue distribution, and expression in Escherichia coli. J Biol Chem. 1993; 268: 24498-24505.

Chai KX, Ward DC, Chao J, Chao L. Molecular cloning, sequence analysis, and chromosomal localization of the human protease inhibitor 4 (kallistatin) gene. Genomics. 1994; 23: 370-378.

Chao J, Bledsoe G, Chao L. Protective Role of Kallistatin in Vascular and Organ Injury. Hypertension. 2016; 68: 533-541.

Chao J, Chai KX, Chen LM, Xiong W, Chao S, Woodley-Miller C, Wang LX, Lu HS, Chao L. Tissue kallikrein-binding protein is a serpin. I. Purification, characterization, and distribution in normotensive and spontaneously hypertensive rats. J Biol Chem. 1990; 265: 16394-16401.

Chao J, Chao L. A major difference of kallikrein-binding protein in spontaneously hypertensive versus normotensive rats. J Hypertens. 1988; 6: 551-557.

Chao J, Chao L. Biochemistry, regulation and potential function of kallistatin. Biol Chem Hoppe Seyler. 1995; 376: 705-713.

Chao J, Schmaier A, Chen LM, Yang Z, Chao L. Kallistatin, a novel human tissue kallikrein inhibitor: levels in body fluids, blood cells, and tissues in health and disease. J Lab Clin Med. 1996; 127: 612-620.

Chao J, Stallone JN, Liang YM, Chen LM, Wang DZ, Chao L. Kallistatin is a potent new vasodilator. J Clin Invest. 1997; 100: 11-17.

Chao J, Tillman DM, Wang MY, Margolius HS, Chao L. Identification of a new tissue-kallikrein-binding protein. Biochem J. 1986; 239: 325-331.

Chao J, Yin H, Yao YY, Shen B, Smith RS, Jr., Chao L. Novel role of kallistatin in protection against myocardial ischemia-reperfusion injury by preventing apoptosis and inflammation. Hum Gene Ther. 2006; 17: 1201-1213.

Chen JH, Ozanne SE, Hales CN. Methods of cellular senescence induction using oxidative stress. Methods Mol Biol. 2007; 371: 179-189.

Chen LM, Chao L, Chao J. Beneficial effects of kallikrein-binding protein in transgenic mice during endotoxic shock. Life Sci. 1997; 60: 1431-1435.

Chen LM, Ma J, Liang YM, Chao L, Chao J. Tissue kallikrein-binding protein reduces blood pressure in transgenic mice. J Biol Chem. 1996; 271: 27590-27594.

Chen VC, Chao L, Chao J. A positively charged loop on the surface of kallistatin functions to enhance tissue kallikrein inhibition by acting as a secondary binding site for kallikrein. J Biol Chem. 2000; 275: 40371-40377.

Chen VC, Chao L, Chao J. Reactive-site specificity of human kallistatin toward tissue kallikrein probed by site-directed mutagenesis. Biochim Biophys Acta. 2000; 1479: 237-246.

Chen VC, Chao L, Chao J. Roles of the P1, P2, and P3 residues in determining inhibitory specificity of kallistatin toward human tissue kallikrein. J Biol Chem. 2000; 275: 38457-38466.

Chen VC, Chao L, Pimenta DC, Bledsoe G, Juliano L, Chao J. Identification of a major heparin-binding site in kallistatin. J Biol Chem. 2001; 276: 1276-1284.

Chen X, Andresen BT, Hill M, Zhang J, Booth F, Zhang C. Role of Reactive Oxygen Species in Tumor Necrosis Factor-alpha Induced Endothelial Dysfunction. Curr Hypertens Rev. 2008; 4: 245-255.

Chen Z, Peng IC, Cui X, Li YS, Chien S, Shyy JY. Shear stress, SIRT1, and vascular homeostasis. Proc Natl Acad Sci U S A. 2010; 107: 10268-10273.

Cheng JC, Chang HM, Leung PC. Transforming growth factor-beta1 inhibits trophoblast cell invasion by inducing Snail-mediated downregulation of vascular endothelial-cadherin protein. J Biol Chem. 2013; 288: 33181-33192.

Clancy RM, Leszczynska-Piziak J, Abramson SB. Nitric oxide, an endothelial cell relaxation factor, inhibits neutrophil superoxide anion production via a direct action on the NADPH oxidase. J Clin Invest. 1992; 90: 1116-1121.

Clements ME, Chaber CJ, Ledbetter SR, Zuk A. Increased cellular senescence and vascular rarefaction exacerbate the progression of kidney fibrosis in aged mice following transient ischemic injury. PLoS One. 2013; 8: e70464.

Ehrlich HJ, Keijer J, Preissner KT, Gebbink RK, Pannekoek H. Functional interaction of plasminogen activator inhibitor type 1 (PAI-1) and heparin. Biochemistry. 1991; 30: 1021-1028.

Erusalimsky JD. Vascular endothelial senescence: from mechanisms to pathophysiology. J Appl Physiol (1985). 2009; 106: 326-332.

Foreman KE, Tang J. Molecular mechanisms of replicative senescence in endothelial cells. Exp Gerontol. 2003; 38: 1251-1257.

Forstermann U, Munzel T. Endothelial nitric oxide synthase in vascular disease: from marvel to menace. Circulation. 2006; 113: 1708-1714.

Forstermann U, Sessa WC. Nitric oxide synthases: regulation and function. Eur Heart J. 2012; 33: 829-837, 837a-837d.

Freund A, Orjalo AV, Desprez PY, Campisi J. Inflammatory networks during cellular senescence: causes and consequences. Trends Mol Med. 2010; 16: 238-246.

Frippiat C, Chen QM, Zdanov S, Magalhaes JP, Remacle J, Toussaint O. Subcytotoxic H2O2 stress triggers a release of transforming growth factor-beta 1, which induces biomarkers of cellular senescence of human diploid fibroblasts. J Biol Chem. 2001; 276: 2531-2537.

Fujii H, Ichimori K, Hoshiai K, Nakazawa H. Nitric oxide inactivates NADPH oxidase in pig neutrophils by inhibiting its assembling process. J Biol Chem. 1997; 272: 32773-32778.

Gao L, Li P, Zhang J, Hagiwara M, Shen B, Bledsoe G, Chang E, Chao L, Chao J. Novel role of kallistatin in vascular repair by promoting mobility, viability, and function of endothelial progenitor cells. J Am Heart Assoc. 2014; 3: e001194.

Gao L, Yin H, S. Smith R J, Chao L, Chao J. Role of kallistatin in prevention of cardiac remodeling after chronic myocardial infarction. Lab Invest. 2008; 88: 1157-1166.

Gorgoulis VG, Pratsinis H, Zacharatos P, Demoliou C, Sigala F, Asimacopoulos PJ, Papavassiliou AG, Kletsas D. p53-dependent ICAM-1 overexpression in senescent human cells identified in atherosclerotic lesions. Lab Invest. 2005; 85: 502-511.

Guo Y, Li P, Bledsoe G, Yang ZR, Chao L, Chao J. Kallistatin inhibits TGF-beta-induced endothelial-mesenchymal transition by differential regulation of microRNA-21 and eNOS expression. Exp Cell Res. 2015; 337: 103-110.

Guo Y, Li P, Gao L, Zhang J, Yang Z, Bledsoe G, Chang E, Chao L, Chao J. Kallistatin reduces vascular senescence and aging by regulating microRNA-34a-SIRT1 pathway. Aging Cell. 2017; 16: 837-846.

Guzik TJ, Touyz RM. Oxidative Stress, Inflammation, and Vascular Aging in Hypertension. Hypertension. 2017; 70: 660-667.

Hashimoto N, Phan SH, Imaizumi K, Matsuo M, Nakashima H, Kawabe T, Shimokata K, Hasegawa Y. Endothelial-mesenchymal transition in bleomycin-induced pulmonary fibrosis. Am J Respir Cell Mol Biol. 2010; 43: 161-172.

Hatcher HC, Ma JX, Chao J, Chao L, Ottlecz A. Kallikrein-binding protein levels are reduced in the retinas of streptozotocin-induced diabetic rats. Invest Ophthalmol Vis Sci. 1997; 38: 658-664.

Heiss C, Keymel S, Niesler U, Ziemann J, Kelm M, Kalka C. Impaired progenitor cell activity in age-related endothelial dysfunction. J Am Coll Cardiol. 2005; 45: 1441-1448.

Hornsby PJ. Telomerase and the aging process. Exp Gerontol. 2007; 42: 575-581.

Huang X, Wang X, Lv Y, Xu L, Lin J, Diao Y. Protection effect of kallistatin on carbon tetrachloride-induced liver fibrosis in rats via antioxidative stress. PLoS One. 2014; 9: e88498.

Huber MA, Azoitei N, Baumann B, Grunert S, Sommer A, Pehamberger H, Kraut N, Beug H, Wirth T. NF-kappaB is essential for epithelial-mesenchymal transition and

metastasis in a model of breast cancer progression. J Clin Invest. 2004; 114: 569-581.

Imanishi T, Tsujioka H, Akasaka T. Endothelial progenitor cells dysfunction and senescence: contribution to oxidative stress. Curr Cardiol Rev. 2008; 4: 275-286.

Ito T, Yagi S, Yamakuchi M. MicroRNA-34a regulation of endothelial senescence. Biochem Biophys Res Commun. 2010; 398: 735-740.

Jiang Y, Chen X, Tian W, Yin X, Wang J, Yang H. The role of TGF-beta1-miR-21-ROS pathway in bystander responses induced by irradiated non-small-cell lung cancer cells. Br J Cancer. 2014; 111: 772-780.

Jimenez SA. Role of endothelial to mesenchymal transition in the pathogenesis of the vascular alterations in systemic sclerosis. ISRN Rheumatol. 2013; 2013: 835948.

Julien S, Puig I, Caretti E, Bonaventure J, Nelles L, van Roy F, Dargemont C, de Herreros AG, Bellacosa A, Larue L. Activation of NF-kappaB by Akt upregulates Snail expression and induces epithelium mesenchyme transition. Oncogene. 2007; 26: 7445-7456.

Kitada M, Ogura Y, Koya D. The protective role of Sirt1 in vascular tissue: its relationship to vascular aging and atherosclerosis. Aging (Albany NY). 2016; 8: 2290-2307.

Kong P, Christia P, Frangogiannis NG. The pathogenesis of cardiac fibrosis. Cell Mol Life Sci. 2014; 71: 549-574.

Kumarswamy R, Volkmann I, Jazbutyte V, Dangwal S, Park DH, Thum T. Transforming growth factor-beta-induced endothelial-to-mesenchymal transition is partly mediated by microRNA-21. Arterioscler Thromb Vasc Biol. 2012; 32: 361-369.

Kumarswamy R, Volkmann I, Thum T. Regulation and function of miRNA-21 in health and disease. RNA Biol. 2011; 8: 706-713.

Kurz DJ, Decary S, Hong Y, Trivier E, Akhmedov A, Erusalimsky JD. Chronic oxidative stress compromises telomere integrity and accelerates the onset of senescence in human endothelial cells. J Cell Sci. 2004; 117: 2417-2426.

Lakatta EG. Age-associated cardiovascular changes in health: impact on cardiovascular disease in older persons. Heart Fail Rev. 2002; 7: 29-49.

Lawrence T. The nuclear factor NF-kappaB pathway in inflammation. Cold Spring Harb Perspect Biol. 2009; 1: a001651.

Li P, Bledsoe G, Yang ZR, Fan H, Chao L, Chao J. Human kallistatin administration reduces organ injury and improves survival in a mouse model of polymicrobial sepsis. Immunology. 2014; 142: 216-226.

Li P, Guo Y, Bledsoe G, Yang Z, Chao L, Chao J. Kallistatin induces breast cancer cell apoptosis and autophagy by modulating Wnt signaling and microRNA synthesis. Exp Cell Res. 2016; 340: 305-314.

Li P, Guo Y, Bledsoe G, Yang ZR, Fan H, Chao L, Chao J. Kallistatin treatment attenuates lethality and organ injury in mouse models of established sepsis. Crit Care. 2015; 19: 200.

Li RL, Lu ZY, Huang JJ, Qi J, Hu A, Su ZX, Zhang L, Li Y, Shi YQ, Hao CN, Duan JL. SRT1720, a SIRT1 specific activator, protected H2O2-induced senescent endothelium. Am J Transl Res. 2016; 8: 2876-2888.

Liao YC, Wang YS, Guo YC, Lin WL, Chang MH, Juo SH. Let-7g improves multiple endothelial functions through targeting transforming growth factor-beta and SIRT-1 signaling. J Am Coll Cardiol. 2014; 63: 1685-1694.

Lin F, Wang N, Zhang TC. The role of endothelial-mesenchymal transition in development and pathological process. IUBMB Life. 2012; 64: 717-723.

Lin WC, Chen CW, Huang YW, Chao L, Chao J, Lin YS, Lin CF. Kallistatin protects against sepsis-related acute lung injury via inhibiting inflammation and apoptosis. Sci Rep. 2015; 5: 12463.

Lin WC, Lu SL, Lin CF, Chen CW, Chao L, Chao J, Lin YS. Plasma kallistatin levels in patients with severe community-acquired pneumonia. Crit Care. 2013; 17: R27.

Lin Y, Weisdorf DJ, Solovey A, Hebbel RP. Origins of circulating endothelial cells and endothelial outgrowth from blood. J Clin Invest. 2000; 105: 71-77.

Ling M, Li Y, Xu Y, Pang Y, Shen L, Jiang R, Zhao Y, Yang X, Zhang J, Zhou J, Wang X, Liu Q. Regulation of miRNA-21 by reactive oxygen species-activated ERK/NF-kappaB in arsenite-induced cell transformation. Free Radic Biol Med. 2012; 52: 1508-1518.

Liu DH, Chen YM, Liu Y, Hao BS, Zhou B, Wu L, Wang M, Chen L, Wu WK, Qian XX. Ginsenoside Rb1 reverses H2O2-induced senescence in human umbilical endothelial cells: involvement of eNOS pathway. J Cardiovasc Pharmacol. 2012; 59: 222-230.

Liu M, Tao G, Liu Q, Liu K, Yang X. MicroRNA let-7g alleviates atherosclerosis via the targeting of LOX-1 in vitro and in vivo. Int J Mol Med. 2017; 40: 57-64.

Liu Y, Bledsoe G, Hagiwara M, Shen B, Chao L, Chao J. Depletion of endogenous kallistatin exacerbates renal and cardiovascular oxidative stress, inflammation, and organ remodeling. Am J Physiol Renal Physiol. 2012; 303: F1230-1238.

Loomans CJ, de Koning EJ, Staal FJ, Rookmaaker MB, Verseyden C, de Boer HC, Verhaar MC, Braam B, Rabelink TJ, van Zonneveld AJ. Endothelial progenitor cell dysfunction: a novel concept in the pathogenesis of vascular complications of type 1 diabetes. Diabetes. 2004; 53: 195-199.

Luo F, Ji J, Liu Y, Xu Y, Zheng G, Jing J, Wang B, Xu W, Shi L, Lu X, Liu Q. MicroRNA-21, upregulated by arsenite, directs the epithelial-mesenchymal transition and

enhances the invasive potential of transformed human bronchial epithelial cells by targeting PDCD4. Toxicol Lett. 2015; 232: 301-309.

Ma JX, King LP, Yang Z, Crouch RK, Chao L, Chao J. Kallistatin in human ocular tissues: reduced levels in vitreous fluids from patients with diabetic retinopathy. Curr Eye Res. 1996; 15: 1117-1123.

Mattagajasingh I, Kim CS, Naqvi A, Yamamori T, Hoffman TA, Jung SB, DeRicco J, Kasuno K, Irani K. SIRT1 promotes endothelium-dependent vascular relaxation by activating endothelial nitric oxide synthase. Proc Natl Acad Sci U S A. 2007; 104: 14855-14860.

Matthews JR, Botting CH, Panico M, Morris HR, Hay RT. Inhibition of NF-kappaB DNA binding by nitric oxide. Nucleic Acids Res. 1996; 24: 2236-2242.

Meadows KN, Iyer S, Stevens MV, Wang D, Shechter S, Perruzzi C, Camenisch TD, Benjamin LE. Akt promotes endocardial-mesenchyme transition. J Angiogenes Res. 2009; 1: 2.

Miao RQ, Agata J, Chao L, Chao J. Kallistatin is a new inhibitor of angiogenesis and tumor growth. Blood. 2002; 100: 3245-3252.

Miao RQ, Chen V, Chao L, Chao J. Structural elements of kallistatin required for inhibition of angiogenesis. Am J Physiol Cell Physiol. 2003; 284: C1604-1613.

Minamino T, Komuro I. Vascular cell senescence: contribution to atherosclerosis. Circ Res. 2007; 100: 15-26.

Minamino T, Miyauchi H, Yoshida T, Tateno K, Kunieda T, Komuro I. Vascular cell senescence and vascular aging. J Mol Cell Cardiol. 2004; 36: 175-183.

Nicolosi PA, Tombetti E, Maugeri N, Rovere-Querini P, Brunelli S, Manfredi AA. Vascular Remodelling and Mesenchymal Transition in Systemic Sclerosis. Stem Cells Int. 2016; 2016: 4636859.

Olmos Y, Sanchez-Gomez FJ, Wild B, Garcia-Quintans N, Cabezudo S, Lamas S, Monsalve M. SirT1 regulation of antioxidant genes is dependent on the formation of a FoxO3a/PGC-1alpha complex. Antioxid Redox Signal. 2013; 19: 1507-1521.

Ota H, Eto M, Kano MR, Kahyo T, Setou M, Ogawa S, Iijima K, Akishita M, Ouchi Y. Induction of endothelial nitric oxide synthase, SIRT1, and catalase by statins inhibits endothelial senescence through the Akt pathway. Arterioscler Thromb Vasc Biol. 2010; 30: 2205-2211.

Ota H, Eto M, Ogawa S, Iijima K, Akishita M, Ouchi Y. SIRT1/eNOS axis as a potential target against vascular senescence, dysfunction and atherosclerosis. J Atheroscler Thromb. 2010; 17: 431-435.

Peinado H, Quintanilla M, Cano A. Transforming growth factor beta-1 induces snail transcription factor in epithelial cell lines: mechanisms for epithelial mesenchymal transitions. J Biol Chem. 2003; 278: 21113-21123.

Potenta S, Zeisberg E, Kalluri R. The role of endothelial-to-mesenchymal transition in cancer progression. Br J Cancer. 2008; 99: 1375-1379.

Potente M, Dimmeler S. NO targets SIRT1: a novel signaling network in endothelial senescence. Arterioscler Thromb Vasc Biol. 2008; 28: 1577-1579.

Potente M, Ghaeni L, Baldessari D, Mostoslavsky R, Rossig L, Dequiedt F, Haendeler J, Mione M, Dejana E, Alt FW, Zeiher AM, Dimmeler S. SIRT1 controls endothelial angiogenic functions during vascular growth. Genes Dev. 2007; 21: 2644-2658.

Powter EE, Coleman PR, Tran MH, Lay AJ, Bertolino P, Parton RG, Vadas MA, Gamble JR. Caveolae control the anti-inflammatory phenotype of senescent endothelial cells. Aging Cell. 2015; 14: 102-111.

Regoli D, Rhaleb NE, Drapeau G, Dion S. Kinin receptor subtypes. J Cardiovasc Pharmacol. 1990; 15 Suppl 6: S30-38.

Reyes M, Dudek A, Jahagirdar B, Koodie L, Marker PH, Verfaillie CM. Origin of endothelial progenitors in human postnatal bone marrow. J Clin Invest. 2002; 109: 337-346.

Rodriguez M, Snoek LB, De Bono M, Kammenga JE. Worms under stress: C. elegans stress response and its relevance to complex human disease and aging. Trends Genet. 2013; 29: 367-374.

Rosenberg RD, Damus PS. The purification and mechanism of action of human antithrombin-heparin cofactor. J Biol Chem. 1973; 248: 6490-6505.

Rumpold H, Wolf D, Koeck R, Gunsilius E. Endothelial progenitor cells: a source for therapeutic vasculogenesis? J Cell Mol Med. 2004; 8: 509-518.

Salminen A, Kauppinen A, Kaarniranta K. Emerging role of NF-kappaB signaling in the induction of senescence-associated secretory phenotype (SASP). Cell Signal. 2012; 24: 835-845.

Sarrazin S, Lamanna WC, Esko JD. Heparan sulfate proteoglycans. Cold Spring Harb Perspect Biol. 2011; 3.

Selemidis S, Dusting GJ, Peshavariya H, Kemp-Harper BK, Drummond GR. Nitric oxide suppresses NADPH oxidase-dependent superoxide production by S-nitrosylation in human endothelial cells. Cardiovasc Res. 2007; 75: 349-358.

Shammas MA. Telomeres, lifestyle, cancer, and aging. Curr Opin Clin Nutr Metab Care. 2011; 14: 28-34.

Shen B, Chao L, Chao J. Pivotal role of JNK-dependent FOXO1 activation in downregulation of kallistatin expression by oxidative stress. Am J Physiol Heart Circ Physiol. 2010; 298: H1048-1054.

Shen B, Gao L, Hsu YT, Bledsoe G, Hagiwara M, Chao L, Chao J. Kallistatin attenuates endothelial apoptosis through inhibition of oxidative stress and activation of Akt-eNOS signaling. Am J Physiol Heart Circ Physiol. 2010; 299: H1419-1427.

Shen B, Hagiwara M, Yao YY, Chao L, Chao J. Salutary effect of kallistatin in salt-induced renal injury, inflammation, and fibrosis via antioxidative stress. Hypertension. 2008; 51: 1358-1365.

Shen B, Smith RS, Jr., Hsu YT, Chao L, Chao J. Kruppel-like factor 4 is a novel mediator of Kallistatin in inhibiting endothelial inflammation via increased endothelial nitric-oxide synthase expression. J Biol Chem. 2009; 284: 35471-35478.

Stadnicki A, Mazurek U, Plewka D, Wilczok T. Intestinal tissue kallikrein-kallistatin profile in inflammatory bowel disease. Int Immunopharmacol. 2003; 3: 939-944.

Storz P. Forkhead homeobox type O transcription factors in the responses to oxidative stress. Antioxid Redox Signal. 2011; 14: 593-605.

Strait JB, Lakatta EG. Aging-associated cardiovascular changes and their relationship to heart failure. Heart Fail Clin. 2012; 8: 143-164.

Tazawa H, Tsuchiya N, Izumiya M, Nakagama H. Tumor-suppressive miR-34a induces senescence-like growth arrest through modulation of the E2F pathway in human colon cancer cells. Proc Natl Acad Sci U S A. 2007; 104: 15472-15477.

Thum T, Gross C, Fiedler J, Fischer T, Kissler S, Bussen M, Galuppo P, Just S, Rottbauer W, Frantz S, Castoldi M, Soutschek J, Koteliansky V, Rosenwald A, Basson MA, Licht JD, Pena JT, Rouhanifard SH, Muckenthaler MU, Tuschl T, Martin GR, Bauersachs J, Engelhardt S. MicroRNA-21 contributes to myocardial disease by stimulating MAP kinase signalling in fibroblasts. Nature. 2008; 456: 980-984.

Tissenbaum HA, Guarente L. Increased dosage of a sir-2 gene extends lifespan in Caenorhabditis elegans. Nature. 2001; 410: 227-230.

van Meeteren LA, ten Dijke P. Regulation of endothelial cell plasticity by TGF-beta. Cell Tissue Res. 2012; 347: 177-186.

Velarde MC, Flynn JM, Day NU, Melov S, Campisi J. Mitochondrial oxidative stress caused by Sod2 deficiency promotes cellular senescence and aging phenotypes in the skin. Aging (Albany NY). 2012; 4: 3-12.

Wassmann S, Wassmann K, Nickenig G. Modulation of oxidant and antioxidant enzyme expression and function in vascular cells. Hypertension. 2004; 44: 381-386.

Williamson K, Stringer SE, Alexander MY. Endothelial progenitor cells enter the aging arena. Front Physiol. 2012; 3: 30.

Wolf WC, Harley RA, Sluce D, Chao L, Chao J. Localization and expression of tissue kallikrein and kallistatin in human blood vessels. J Histochem Cytochem. 1999; 47: 221-228.

Wynn TA. Cellular and molecular mechanisms of fibrosis. J Pathol. 2008; 214: 199-210.

Xia N, Strand S, Schlufter F, Siuda D, Reifenberg G, Kleinert H, Forstermann U, Li H. Role of SIRT1 and FOXO factors in eNOS transcriptional activation by resveratrol. Nitric Oxide. 2013; 32: 29-35.

Yan C, Boyd DD. Regulation of matrix metalloproteinase gene expression. J Cell Physiol. 2007; 211: 19-26.

Yan F, Wang Y, Wu X, Peshavariya HM, Dusting GJ, Zhang M, Jiang F. Nox4 and redox signaling mediate TGF-beta-induced endothelial cell apoptosis and phenotypic switch. Cell Death Dis. 2014; 5: e1010.

Yang J, Chen D, He Y, Melendez A, Feng Z, Hong Q, Bai X, Li Q, Cai G, Wang J, Chen X. MiR-34 modulates Caenorhabditis elegans lifespan via repressing the autophagy gene atg9. Age (Dordr). 2013; 35: 11-22.

Yin H, Gao L, Shen B, Chao L, Chao J. Kallistatin inhibits vascular inflammation by antagonizing tumor necrosis factor-alpha-induced nuclear factor kappaB activation. Hypertension. 2010; 56: 260-267.

Yiu WH, Wong DW, Wu HJ, Li RX, Yam I, Chan LY, Leung JC, Lan HY, Lai KN, Tang SC. Kallistatin protects against diabetic nephropathy in db/db mice by suppressing AGE-RAGE-induced oxidative stress. Kidney Int. 2016; 89: 386-398.

Yoder MC. Human endothelial progenitor cells. Cold Spring Harb Perspect Med. 2012; 2: a006692.

Yoshida LS, Tsunawaki S. Expression of NADPH oxidases and enhanced H(2)O(2)-generating activity in human coronary artery endothelial cells upon induction with tumor necrosis factor-alpha. Int Immunopharmacol. 2008; 8: 1377-1385.

Yoshimatsu Y, Watabe T. Roles of TGF-beta signals in endothelial-mesenchymal transition during cardiac fibrosis. Int J Inflam. 2011; 2011: 724080.

Zeisberg EM, Potenta SE, Sugimoto H, Zeisberg M, Kalluri R. Fibroblasts in kidney fibrosis emerge via endothelial-to-mesenchymal transition. J Am Soc Nephrol. 2008; 19: 2282-2287.

Zhang X, Ng WL, Wang P, Tian L, Werner E, Wang H, Doetsch P, Wang Y. MicroRNA-21 modulates the levels of reactive oxygen species by targeting SOD3 and TNFalpha. Cancer Res. 2012; 72: 4707-4713.

Zhang Y, Chen N, Zhang J, Tong Y. Hsa-let-7g miRNA targets caspase-3 and inhibits the apoptosis induced by ox-LDL in endothelial cells. Int J Mol Sci. 2013; 14: 22708-22720.

Zhang Y, Unnikrishnan A, Deepa SS, Liu Y, Li Y, Ikeno Y, Sosnowska D, Van Remmen H, Richardson A. A new role for oxidative stress in aging: The accelerated aging phenotype in Sod1(-/)(-) mice is correlated to increased cellular senescence. Redox Biol. 2017; 11: 30-37.

Zhao T, Li J, Chen AF. MicroRNA-34a induces endothelial progenitor cell senescence and impedes its angiogenesis via suppressing silent information regulator 1. Am J Physiol Endocrinol Metab. 2010; 299: E110-116.

Zhi X, Lin L, Yang S, Bhuvaneshwar K, Wang H, Gusev Y, Lee M, Kallakury B, Shivapurkar N, Cahn K, Tian X, Marshall J, Byers S, He A. betaII-Spectrin suppresses progression of hepatocellular carcinoma and Wnt signaling by regulation of Wnt inhibitor kallistatin. Hepatology. 2015; 61: 598-612.

Zhou GX, Chao L, Chao J. Kallistatin: a novel human tissue kallikrein inhibitor. Purification, characterization, and reactive center sequence. J Biol Chem. 1992; 267: 25873-25880.

Zhou KI, Pincus Z, Slack FJ. Longevity and stress in Caenorhabditis elegans. Aging (Albany NY). 2011; 3: 733-753.

Zhou S, Sun Y, Zhuang Y, Zhao W, Chen Y, Jiang B, Guo C, Zhang Z, Peng H, Chen Y. Effects of kallistatin on oxidative stress and inflammation on renal ischemia-reperfusion injury in mice. Curr Vasc Pharmacol. 2015; 13: 265-273.

Zhu H, Chao J, Kotak I, Guo D, Parikh SJ, Bhagatwala J, Dong Y, Patel SY, Houk C, Chao L, Dong Y. Plasma kallistatin is associated with adiposity and cardiometabolic risk in apparently healthy African American adolescents. Metabolism. 2013; 62: 642-646.

Zhu S, Deng S, Ma Q, Zhang T, Jia C, Zhuo D, Yang F, Wei J, Wang L, Dykxhoorn DM, Hare JM, Goldschmidt-Clermont PJ, Dong C. MicroRNA-10A* and MicroRNA-21 modulate endothelial progenitor cell senescence via suppressing high-mobility group A2. Circ Res. 2013; 112: 152-164.

Zhu H, Chao J, Raed A, Huang Y, Bhagatwala J, Parikh S, Dong Y. Plasma Kallistatin is Associated with Leukocyte Telomere Length in Young African Americans. FASEB J. 2016; 30: 625.1.